VORTEX SHEDDING FROM SINGLE AND TANDEM FINNED CYLINDERS

VORTEX SHEDDING FROM SINGLE AND TANDEM FINNED CYLINDERS

By

Mohammed Hosny Eid

A Thesis
Submitted to the School of Graduate Studies
in Partial Fulfillment of the Requirements
for the Degree

Master of Applied Science

McMaster University

MASTER OF APPLIED SCIENCE (2004) McMaster University
(Mechanical Engineering) Hamilton, Ontario

TITLE: Vortex shedding From Single and Tandem Finned Cylinders

AUTHOR: Mohammed Hosny Eid, B.Sc. (Ain Shams University)

SUPERVISOR: Professor Samir Ziada

NUMBER OF PAGES: xviii, 131

Abstract

The effect of fins on vortex shedding and acoustic resonance in the case of single and tandem cylinders with spacing ratios of 1.5, 2 and 3 has been investigated in an open circuit wind tunnel at the Reynolds number range from 1.56×10^4 to 1.13×10^5. Sound pressure and velocity measurements were performed for finned cylinders with three different fin densities. Similar measurements were made on bare cylinders for the purpose of comparison. In the case of tandem bare cylinders, the first acoustic mode is excited over two different ranges of flow velocity. The first resonance range ends before the vortex shedding frequency approaches the acoustic resonance frequency and is therefore referred to as the pre-coincidence resonance. The other resonance range starts at the coincidence between the frequencies of vortex shedding and acoustic resonance and is referred to as the post-coincidence resonance. The fins in the case of single cylinders are found to reduce the strength of vortex shedding, increase the broadband turbulence level and decrease the sound pressure at the acoustic resonance. The lock-in range of acoustic resonance for the single cylinders is found to be generally smaller than that of the tandem cylinders. Before the onset of resonance, the fins cause the sound pressure to increase in the case of tandem finned cylinders with $S/D_e = 1.5$ and 2. Increasing the fin density promotes the onset of resonance, but reduces the sound pressure level at resonance for $S/D_e = 1.5$ and 2. The fins are observed to weaken the pre-coincidence resonance for $S/D_e = 2$ such that the sound pressure level is not sufficient to produce resonance. However, the fins increase the sound pressure at the pre-coincidence resonance range for $S/D_e = 3$, but decrease the sound pressure at the post-coincidence resonance range. Increasing the spacing ratio between the cylinders is found to generally reduce the sound pressure level at the post-

coincidence resonance, but decreases the sound pressure level at the pre-coincidence resonance range. The effect of fins is therefore rather complex and depends on the spacing ratio and the fin density.

Acknowledgments

The author would like to express his gratitude to Dr. S. Ziada for his advice, guidance and continuous support. The author would like also to express his gratitude to Dr. D. S. Weaver and all members of the FIV group for their help and support.

The author would like to extend his gratitude to all the staff, faculty, and technicians of the Department of Mechanical Engineering at McMaster University. The author would like also to thank Mr. Mahmoud Safar for his kind support.

The author would like to express his profound gratitude to his beloved mother and wife for whom he dedicates this thesis.

CONTENTS

LIST OF TABLES

LIST OF FIGURES

NOMENCLATURE

B	Duct width
B	Height of the test section
b	Distance between centers of fins
c	Speed of sound
C_L	Coefficient of oscillating lift
C'_L	Root mean squared lift coefficient
D	Bare cylinder diameter
D_e	Effective diameter
D_f	Fins diameter
f	Frequency
f_a	Natural acoustic frequency of the test section
f_v	Vortex shedding frequency
f_v	Vortex shedding frequency
H	Fin height
I_R	Sound intensity
k	Wave number
L	Cylinder length

L_c	Correlation length
M	Mach number
P	Sound pressure
P^*	Dimensionless sound pressure
P_r^*	Dimensionless sound pressure at the natural acoustic frequency
P_v	Sound pressure at vortex shedding frequency
P_v^*	Dimensionless pressure at vortex shedding frequency
Re	Reynolds Number
s	Distance between the fins
SPL	Sound pressure level
St	Strouhal number
T	Distance between side-by-side cylinders centerlines
t	Fin thickness
Tu_f	Turbulence intensity at the fundamental vortex shedding frequency
V	Free stream flow velocity
V_r	Reduced velocity
W	Sound power
x	Downstream distance
y	Transverse distance

$\overline{P^2}$ Mean squared sound pressure

ρ Fluid density

CHAPTER 1
Introduction

Heat exchangers are one of the most important engineering devices that exist in many engineering applications today. One of these applications, where heat exchangers are found in different configurations and capacities, is thermal power plants. Heat exchangers play a basic role in power generation. The increased demand on energy makes it necessary to increase the capacities of thermal power plants. This results in increasing the capacity of heat exchangers to be able to exchange more energy which leads to an increase in the flow rate through the heat exchangers.

The fluid flowing in heat exchangers interacts with the tubes and may cause flow induced vibrations and acoustic emissions. At certain conditions, the produced sound level becomes very high. This sound is capable of entraining the vortex shedding across the tube span. This increases the vortex shedding correlation length and causes excessive tube vibrations that may lead to tubes failure. Baird (1954) reported intense noise and severe vibrations observed in Estiwanda Steam Power Station. A high sound intensity of 126 dB was measured. Baird reported that the destructive effect of the noise and the vibrations in this case was higher than any previously observed case. Flow induced vibrations and acoustic resonance problems continue to be a major problem especially in nuclear power plants (Pettigrew *et al.*, 1998). It is therefore crucial to the future of power generation industry to investigate and understand the flow induced vibrations and aeroacoustics problems.

The need for increasing the capacity of power stations which is limited by the problems of flow induced vibrations and aeroacoustics motivates the research on the flow through tube bundles. All the different excitation mechanisms in the case of flow through tube bundles have been extensively studied. The flow over single and twin cylinders have been studied extensively as well. Beside the relevance of these simple configurations in many engineering applications, understanding the flow over single and twin cylinders are very important in understanding the more complex flow in the case of tube bundles of heat exchangers.

Finned tubes are used extensively in heat exchangers, basically to enhance the heat transfer by increasing the heat transfer area of the tubes. Similar problems to that of bare tubes have been observed in the case of finned tubes. Acoustic resonance takes place in the case of finned tube bundles and the overall sound pressure levels are generally higher than that for bare tubes (Nemoto *et al.*, 1997). Although much work has been performed on bare tubes, little work has been done on finned tubes. Many questions about the effect of fins on the flow, the fluid-structure interaction and the acoustic resonance in the case of finned tubes need to be answered.

In order to understand the flow and acoustic resonance in the case of finned tube bundles, it is necessary to understand the flow over a single finned cylinder and twin finned cylinders. Understanding of these relatively simpler configurations is crucial to the understanding of the finned tube bundles flow. Several investigations have been devoted to the flow over single finned cylinders. The effect of fins on the flow and vortex shedding has been investigated. However, no investigation has been made to the effect of fins on acoustic resonance in the case of single cylinders. Moreover, no work has been reported on the effect of fins on flow and acoustic resonance in the case of twin finned cylinders to the best knowledge of the author.

The purpose of this study is to investigate the vortex shedding and acoustic resonance mechanisms in the case of single and twin tandem finned cylinders. The effect of the fin density on vortex shedding and acoustic resonance will be investigated. The effect of the spacing between the cylinders on vortex shedding as well as on acoustic resonance for different fin densities will be investigated as well. For this purpose, measurements will be performed for spacing ratios 1.5, 2 and 3 based on the effective diameter of the finned cylinders as defined by Mair *et al.* (1975). The same measurements will be repeated for bare cylinders to provide a basis for comparison. These investigations are intended to improve our understanding of the vortex shedding and acoustic resonance in the case of single and tandem finned cylinders in order to achieve better understanding of the flow over finned tube bundles.

In Chapter 2 of this thesis, the research literature will be reviewed for the flow over single, twin and bundles of bare tubes as well as finned tubes. In Chapter 3, the experimental setup as well as the measurement procedure will be described. The results will be presented in detail in Chapter 4. Summary and conclusions of this work as well as the recommendations for future work will be presented in Chapter 5.

CHAPTER 2
Literature Survey

Flow over cylinders is one of the most important flow problems that received a lot of attention for more than a century. The importance of this kind of flow comes from its occurrence in many engineering applications. Understanding of the flow over single and tandem cylinders helps to understand the more complex problems involving tube bundles as in heat exchangers.

Despite the large amount of work that has been done on bare cylinders, relatively very little work has been done on finned cylinders. Finned cylinders are widely used now in heat exchangers. Understanding of the flow over single and tandem finned cylinders is very important in understanding the flow over finned tube bundles.

In this chapter, an overview of the work that has been conducted on bare and finned cylinders will be presented with an emphasis on the work related to the present study.

2.1 Single Cylinder Flow

When there is a cylinder exposed to cross-flow, the pressure increases as the fluid particles flow downstream and approach the cylinder, until it reaches the stagnation pressure just upstream the cylinder. The high pressure forces induce the fluid particles to move around the surface of the cylinder until the pressure

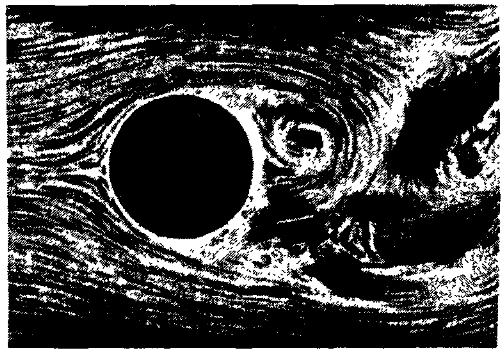

Figure 2.1: Vortex shedding from a single cylinder (Prandtl 1927).

becomes insufficient to maintain the boundary layer attached to cylinder surface. The boundary layer therefore separates from the cylinder to form two shear layers that confine the wake of the cylinder (Figure 2.1).

The innermost of the shear layer which was adjacent to the surface of the cylinder is slower than the outermost which is in contact with the free stream. So, the shear layer roll into the near wake and form the periodic vortices. The formation of these vortices in the wake of the cylinder is well known as vortex street. The point of separation and the pattern of vortices in the wake of the cylinder depend on Reynolds number.

2.1.1 Flow Regimes For A Single Cylinder

The flow regimes for different Reynolds numbers were summarized by Lienhard (1966) as shown in figure 2.2:

Re $<$ **5** : There is no boundary layer separation.

5 to 15 $<$ **Re** $<$ 40 : The boundary layer separates to form a pair of vortices in the near wake.

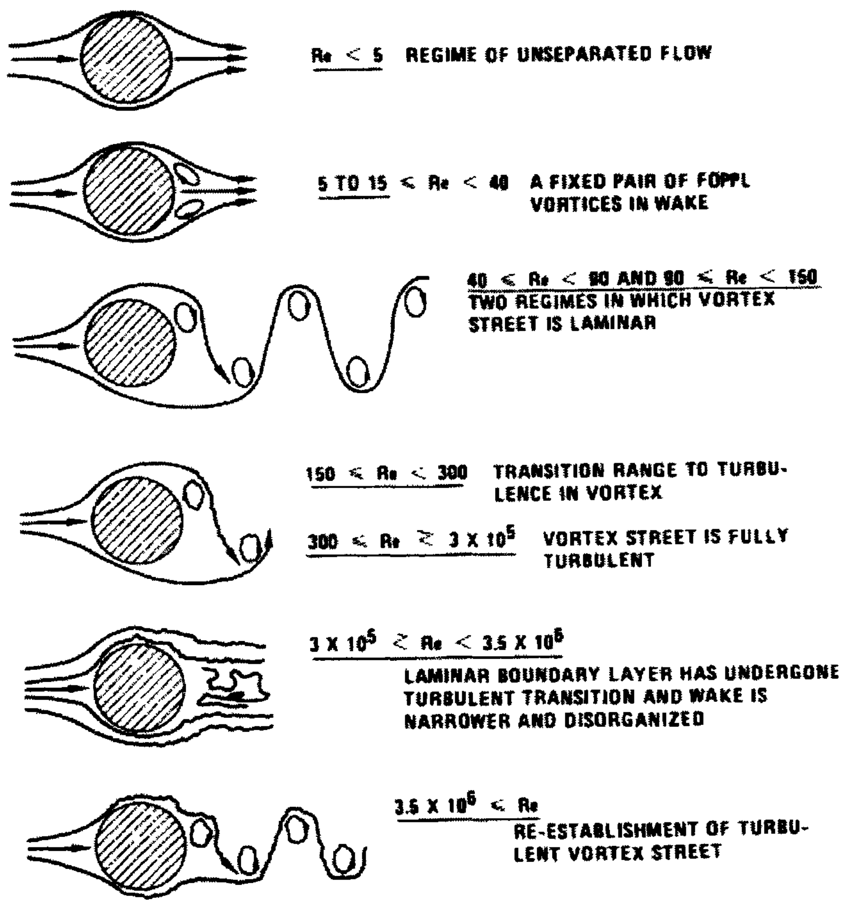

Figure 2.2: Regimes of fluid flow across smooth circular cylinders (Lienhard, 1966).

40 < Re < 150 : After the separation, the vortices break away alternatively to form two vortex streets. However, the vortex in this range is laminar.

150 < Re < 300 : The vortices that break away start to become turbulent. It becomes fully turbulent at Re = 300.

300 < Re < 1.5 $\times$ **10^5** : This is called the subcritical region. In this region the Strouhal number, which is the dimensionless proportionality constant between the frequency of the vortex shedding and the free stream velocity divided by the cylinder diameter, is constant. The vortices are turbulent but the boundary layer is still laminar. The boundary layer separates in this range at 80 degrees from the stagnation point.

$\mathbf{1.5 \times 10^5 < Re < 3.5 \times 10^6}$: This is the transition range where the boundary layer starts to become turbulent. Hence, the separation retarded until it reaches 140 degrees. There is no distinguished vortices in this range due to the three dimensional effects that disrupt the vortex shedding.

$\mathbf{Re > 3 \times 10^6}$: The supercritical Reynolds number range where the boundary layer is turbulent and the shed vortices, which start to be distinguished again, are turbulent also. The vortex shedding persists to very high Reynolds number as it was found in the satellite photo of wind driven clouds (Griffen, 1982).

The vortex shedding, as explained above, starts with the boundary layer separation from the sides of the cylinder in an alternating manner. This separation causes the surface pressure of the cylinder to oscillate. This oscillation of the surface pressure is responsible for the the vibration and the sound generated (Figure 2.3).

The extent of the subcritical regime depends on the flow conditions. Norberg *et al.*(1987) have investigated the effect of the free stream turbulence on the flow and the fluid forces on a single bare cylinder. It was observed that increasing the turbulence intensity results in increasing the pressure forces on the cylinder in the subcritical regime until $Re = 10^5$. For higher Reynolds numbers, the opposite effect has been observed.

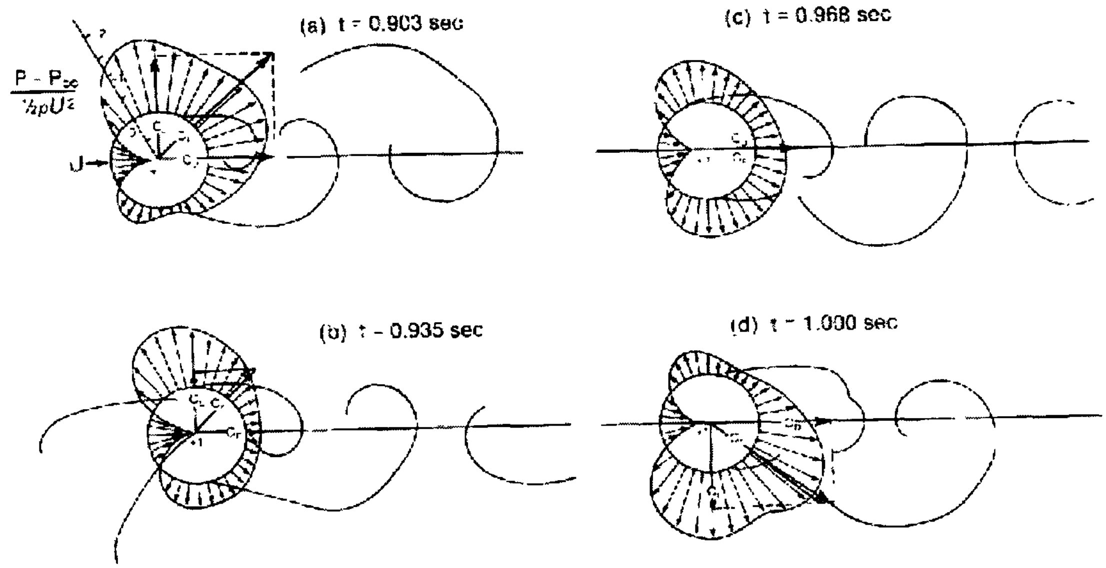

Figure 2.3: A sequence of simultaneous surface pressure fields and wake forms at $Re = 112000$ for approximately one-third of one cycle of vortex shedding (Drescher, 1956).

2.1.2 Strouhal Number

Strouhal number is the dimensionless proportionality constant between the predominant frequency of vortex shedding f_s and the free stream velocity divided by the cylinder diameter (D) (Blevins, 1990)

$$St = \frac{f_v D}{V} \tag{2.1}$$

The Strouhal number is a very important dimensionless parameter in dealing with bluff body flows. It depends mainly on the Reynolds number and shows small dependence on surface roughness and free stream turbulence (figure 2.4). But in the end of the subcritical and in the transitional region, the Strouhal number shows

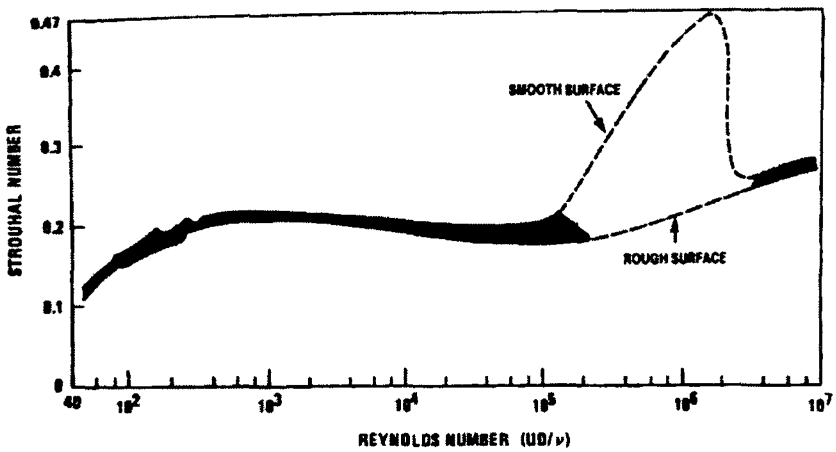

Figure 2.4: Strouhal number-Reynolds number relationship for circular cylinders (Lienhard, 1966).

dependence on the surface roughness as observed by Achenbach and Heinecke (1981).

The vortex shedding process from cylinders is not a two dimensional phenomenon. The three dimensionality of the vortex shedding is characterized by a spanwise correlation length. The correlation length indicates how the vortex shedding process is correlated along the cylinder span.

The vortex shedding does not have a constant amplitude and does not occur at a constant distinct frequency. It changes its value over a narrow band of frequencies. This narrow band decreases when there is an acoustic resonance or sound field applied (Blevins, 1990).

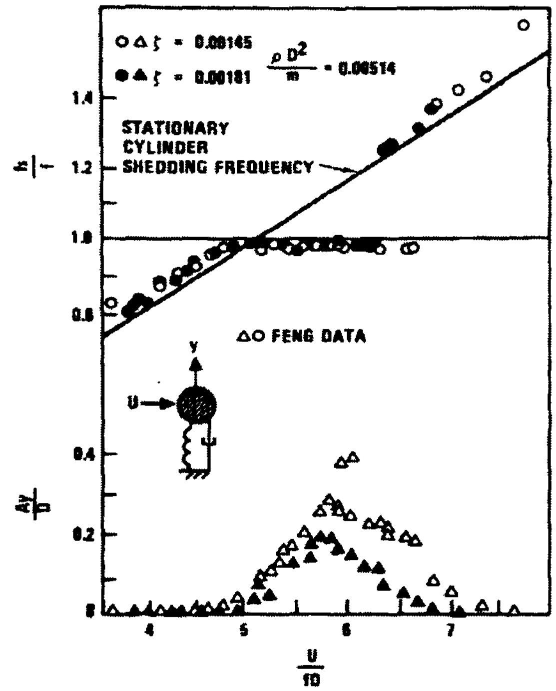

Figure 2.5: Vortex-induced vibration of a spring-supported, damped circular cylinder. f is the natural frequency of the cylinder (Feng, 1968).

2.1.3 Single Cylinder Vibration

As the flow velocity increases, the vortex shedding frequency increases until it becomes approximately equal to the natural frequency of the cylinder. The cylinder starts to vibrate with a frequency equal or nearly equal to the natural frequency of the cylinder and the vortex shedding frequency changes to lock into the same frequency. As the fluid velocity increases, the vortex shedding frequency remains equal to the natural frequency of the cylinder. The vibration amplitude increases until it reaches its maximum in the middle of the synchronization range (Figure 2.5).

The extent of the synchronization range depends on the maximum amplitude of oscillation, relative mass ratio and its damping characteristics. For a lightly damped cylinder in water, it can be as large as $4 < V_r < 10$ where V_r is the reduced velocity. The synchronization takes place in the streamwise direction also at low reduced velocity ($1 < V_r < 2$) (Zdravkovich,1988).

2.1.4 Sound Induced by Vortex Shedding

The vortex shedding from the cylinder is accompanied by sound generation. This happens because the cylinder acts on the fluid with a fluctuating force in reaction to the fluctuating fluid force acting on the cylinder.

Sound generation by vortex shedding received a lot of attention since the pioneering research of Strouhal in 1878, who made the first quantative measurement on the sound generated from the flow of air over wires stretched between radial arms from a rotating shaft. Strouhal found that the frequency of the sound produced is independent of the wire tension or length although the intensity increased with wire length and he was able to find the Strouhal number relation.

$$f = \frac{St\,V}{D} Hz \tag{2.2}$$

Strouhal explained the sound produced by the friction between the wires and the air (Blevins, 1990).

Von Karman *et al.* (1912) were able to observe the vortex street, known as Von Karman street, which led von Kruger *et al.* (1914) and Rayleigh (1915) to associate the sound produced with the periodic vortex shedding.

Several attempts have been made to find the relation between the sound power and the speed. Stowel *et al.* (1936) found that the sound power is proportional to the rod velocity to the power of 5.5 in the relation:

$$W \sim V^n L \tag{2.3}$$

The sound pressure around the rod falls in a double-lobed pattern, with the lobe axis normal to the flow direction. Different other attempts have been made to find the value of n. Philips shows a general agreement with the theoretical value of n = 6 (Blevins, 1990).

2.1.5 Sound Generated by Correlated Vortex Shedding

An expression for the sound radiated by correlated vortex shedding from the flow over the cylinder can be developed as explained by Blevins (1990). The total sound pressure is the sum of the sound pressure due to both of the horizontal and vertical fluctuating fluid forces and the cylinder vibration normal and parallel to the free stream (figure 2.6). Experimental measurements showed that the oscillating drag coefficient is approximately 5 % to 10 % of the oscillating lift coefficient. This agrees with the sound measurements which indicated that the sound produced by drag is much less than the sound produced from the lift, and therefore the cylinder can be considered as a dipole sound source.

Hence, the far field sound intensity radiated from a single cylinder is :

$$I_R = \frac{\overline{P^2}}{\rho c} = \frac{sin^2\theta cos^2\phi}{32c^3R^2}\rho V^6 L^2 C_L^2 St^2 \left(\frac{sin\eta}{\eta}\right)^2 \tag{2.4}$$

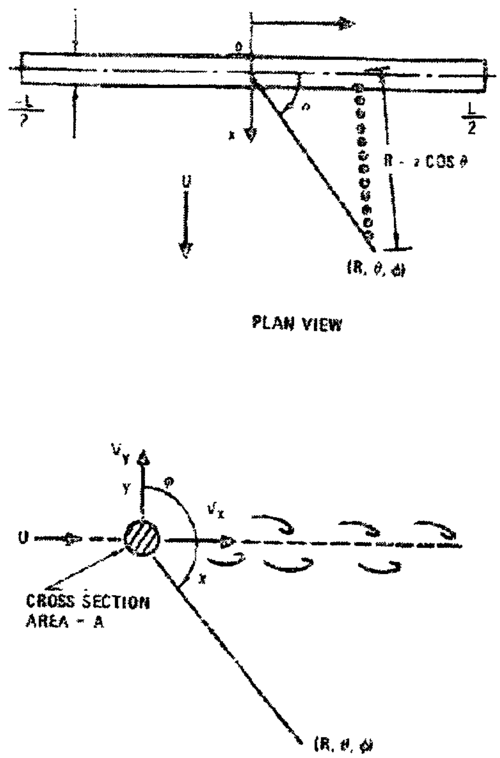

Figure 2.6: The coordinate system for the calculation of sound radiation (Blevins, 1990)

where,

I_R is the sound intensity

$\overline{P^2}$ is the mean squared sound pressure,

ρ is the fluid density,

c is the speed of sound,

C_L is the coefficient of oscillating lift,

$\eta = \frac{kL}{2} cos\theta = \frac{\pi L}{\lambda} cos\theta$, where k is the wave number (Blevins, 1990)

2.1.6 Sound Generated by Partially Correlated Vortex Shedding

The actual far field sound generated by the vortex shedding from a single cylinder can not be described by the above relation because the vortex shedding is not fully correlated along the span of the cylinder. At high Reynolds number, the vortex shedding becomes three dimensional and the frequency of vortex shedding wanders over a narrow band of frequencies (Blevins, 1990). The three dimensionality is characterized by the correlation length which shows the degree of the correlation between the vortex shedding along the cylinder span.

In case of laminar flow, the correlation length, L_c, is high, but it decreases with increasing Reynolds numbers ($L_c = 20D$ at $Re = 100$ and $L_c = 5D$ at $Re = 10^4$) (Friehe, 1980; King, 1977).

The sound intensity at far field for partially correlated vortex shedding can be given by the relation:

$$I_R = \frac{\overline{P^2}}{\rho c} = \frac{sin^2\theta\, cos^2\phi}{16c^3R^2}\rho V^6 L^2 \overline{C_L^2} St^2 L_c(L-\gamma), \tag{2.5}$$

where,

$$L_c = 2\int_0^L r(\xi)d\xi \quad , \quad \gamma = \frac{\int_0^L \xi r(\xi)d\xi}{\int_0^L r(\xi)d\xi}. \tag{2.6}$$

This relation shows that the sound intensity is a function of the correlation length, L_c. This makes it possible to obtain qualitative measurements for the correlation length of the vortex shedding by measuring the pressure of the sound radiating from the cylinder.

2.1.7 Acoustic Resonance

A synchronization can happen also when the vortex shedding frequency becomes close enough to the natural acoustic frequency of the enclosure in which the cylinder is fixed. When the sound pressure level is high enough, the synchronization takes place and the vortex shedding frequency locks-in with the acoustic natural frequency of the test section. The vortex shedding becomes more organized and correlated along the cylinder span. This produces not only high noise levels but also excessive vibrations, mainly because of the highly correlated vortex shedding.

Blevins (1993) has performed sixteen tests on single cylinders to characterize the effect of the duct geometry, Mach number and Reynolds number on the resonant sound levels. As the velocity was increased, the vortex shedding frequency was increased as well until it locked-in to the acoustic natural frequency of the test section (Figure 2.7). The velocity was then farther increased until the lock-in was broken and the sound level was reduced.

Blevins found that the Mach number is superior to Reynolds number in correlating the resonant sound pressure. He suggested an equation that can predict the maximum sound pressure levels with an absolute error of less than 26 % :

$$P_{rms,max} = (12.5\rho V^2/2)(V/c)(D/B) \tag{2.7}$$

where V is the flow velocity in the open duct, c is the speed of sound, D is the cylinder diameter, ρ is the fluid density and B is the duct width.

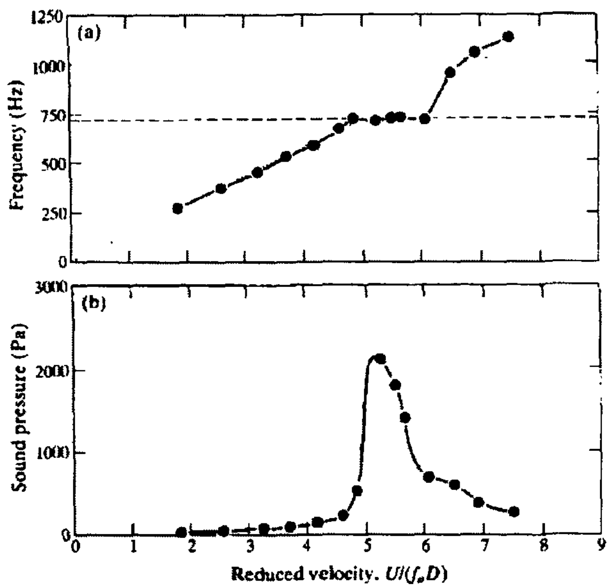

Figure 2.7: Sound pressure and frequency for a single 25.4 mm Diameter cylinder in 229 mm width duct: (a) frequency (first mode, $f_a = 720Hz$); (b) sound pressure (Blevins, 1993)

2.1.8 Vortex Shedding Suppression

It is always of interest to find methods for vortex shedding suppression to avoid the problems resulting from the vortex shedding process. Zdravkovich (1981) has reviewed the different method of vortex shedding suppressions. He divided these methods into three categories according to the way each method affects the vortex shedding:

1. Surface Protrusion: which attempts to suppress the vortex shedding through affecting the separation lines or the separated shear layer as in case of the helical strakes. Most means in this category are effective irrespective of flow direction (omnidirectioal).

2. Shrouds: which affects the entrainment layers as in case of the axial rods. All the methods in this category are effective in one flow direction only (unidirectional).

3. Nearwake Stabilisers: Which is working through preventing the interaction of the entrainment layers as in case of the splitter plates.

2.2 Flow Over Two Cylinders

The flow in the case of two cylinders differs significantly from that of the single cylinder. The addition of another cylinder causes a change in the flow behavior and vortex shedding. Therefore, a change in the forces affecting the cylinders takes place also.

Zdravkovich (1985) divided the possible regions where a second cylinder can be placed in the wake of another cylinder into four regions according to the nature of the flow interference that takes place due to the position of the second cylinder in this region (figure 2.8).

- The proximity interference region: Where the two cylinders are near each other that both of them are affected by the existence of the other cylinder.

- The wake interference region: Where the upstream cylinder in not affected by the existence of the other cylinder. The downstream cylinder is in the wake of the upstream cylinder.

- The wake and proximity interference region: where the downstream cylinder in the wake of the upper stream cylinder and in the same time close enough

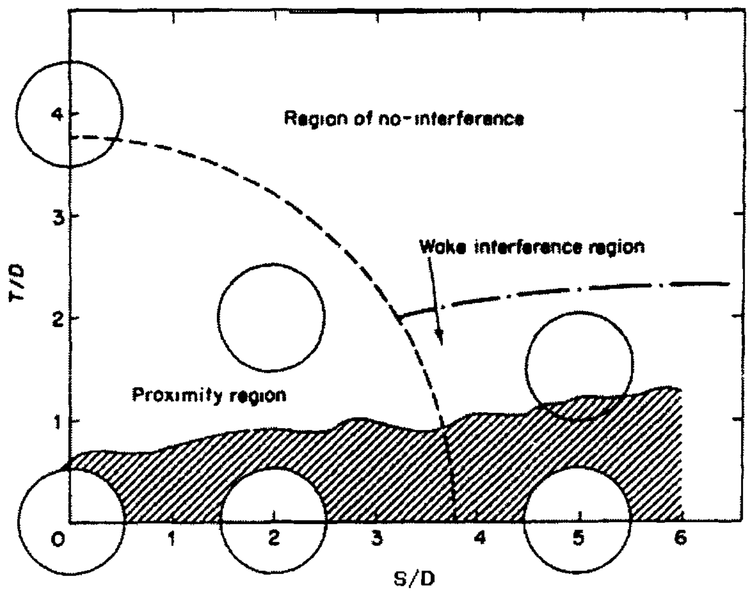

Figure 2.8: Classification of interference region (Zdravkovich, 1985).

to affect the flow over the upstream cylinder.

- The region of no interference: Where there is no interference between the flow over both of the cylinders.

2.2.1 Tandem Arrangement

In the tandem arrangement, the downstream cylinder is in the wake of the upstream one in such a way that the plane passing through the two cylinders centers is parallel to the mean stream velocity direction. As Zdravkovich (1985) and Igarashi (1981) explained, the flow interference can be divided according to the separation between the two cylinders as follows (figures 2.9 and 2.10):

1. **$S/D < 1.1 - 1.3$** : The two cylinders behave as a single body with high

Strouhal number until $S/D = 1.1$ *to* 1.3 depending on the Reynolds number. The flow in the gap between them is stagnant and the shear layers separated from the upstream cylinder do not reattach onto the downstream cylinder.

2. $\mathbf{1.1 - 1.3 < S/D < 1.6}$: An alternate reattachment of the shear layer separated from the front cylinder takes place on the front side of the rear cylinder in the rhythm of vortex shedding.

3. $\mathbf{1.6 < S/D <\sim 2.4}$: Quasi-steady reattachment of the separated shear layer is observed on the rear cylinder. Quasi-stationary vortices are formed between the cylinders.

4. $\mathbf{\sim 2.4 < S/D > 3.5 - 3.8}$: One of the reattachments is disrupted occasionally but still no regular vortex shedding behind the front cylinder. A bistable flow was observed where the vortex shedding behind the front cylinder persists for some time and then is intermittently suppressed and replaced by the reattachment flow regime.

5. $\mathbf{3.8 < S/D < 5 - 6}$: Two vortex streets synchronized in phase and frequency behind the two cylinders.

6. $\mathbf{S/D > 5 - 6}$: Two different vortex streets.

From the above, there is a critical spacing ($S/D = 3.5 - 3.8$). Within this critical spacing, there is no vortex shedding behind the upstream cylinder. However, at larger spacing, there is a vortex shedding as explained above.

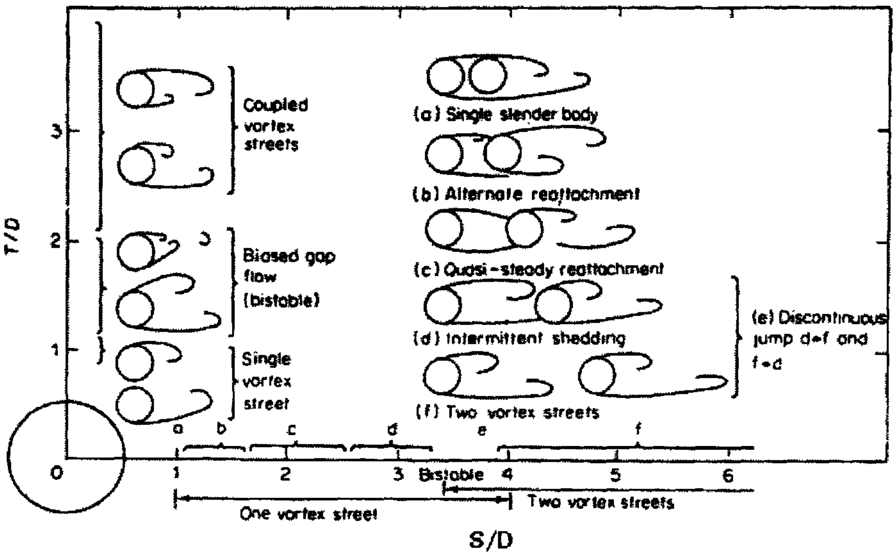

Figure 2.9: Classification of flow regimes in side-by-side and tandem arrangements for stationary cylinders (Zdravkovich, 1984).

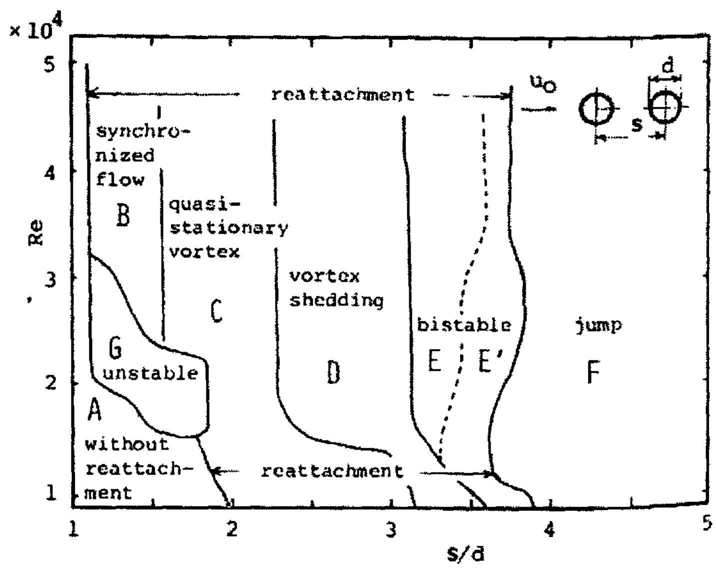

Figure 2.10: Classification of flow regimes in tandem arrangements for different Reynolds number and cylinders spacings (Igarashi, 1981).

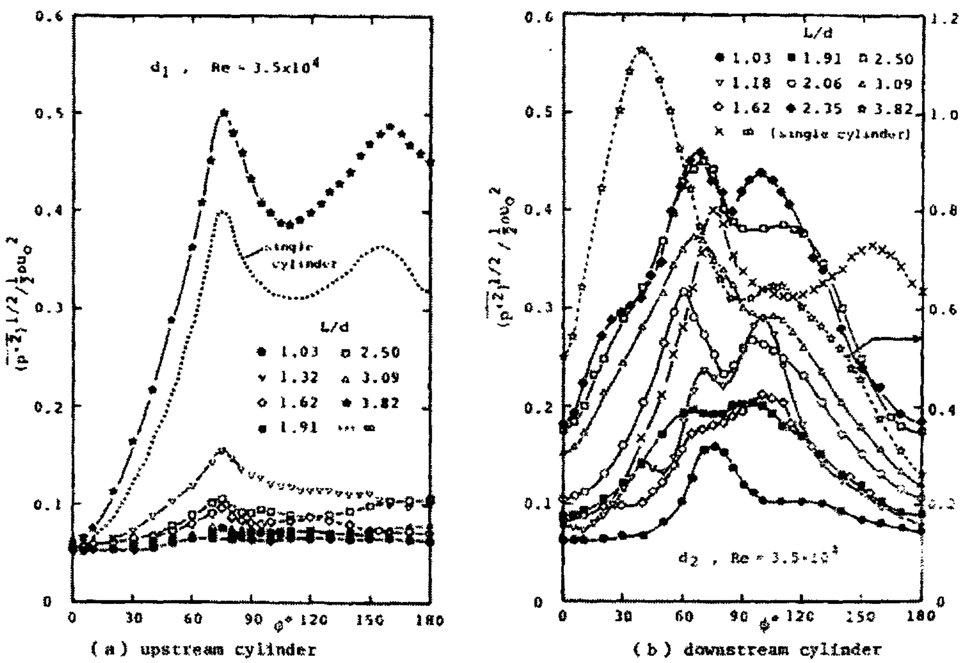

Figure 2.11: Effect of the distance between two cylinders in tandem on the distribution of R.M.S. pressure fluctuation around the two cylinders (Igarashi, 1981).

Igarashi (1981) made a detailed study to the flow characteristics for tandem cylinders. The mean pressure distribution measurements show dependence on the Reynolds number and the spacing between the cylinders as well. The root mean square of the pressure fluctuations increase as the Reynolds number and the spacing between the cylinders are increased as shown in figures (2.11) and (2.12). The flow visualization performed by Igarashi (figure 2.13) agrees with Zdravkovich classification. It was found that the Strouhal number is dependent on the spacing between the tandem cylinders and Reynolds number as shown in figure (2.14).

Arie *et al.* (1983) argued that the spacing between the cylinders doesn't have a strong effect on the drag force on the cylinders which doesn't agree with Igarashi

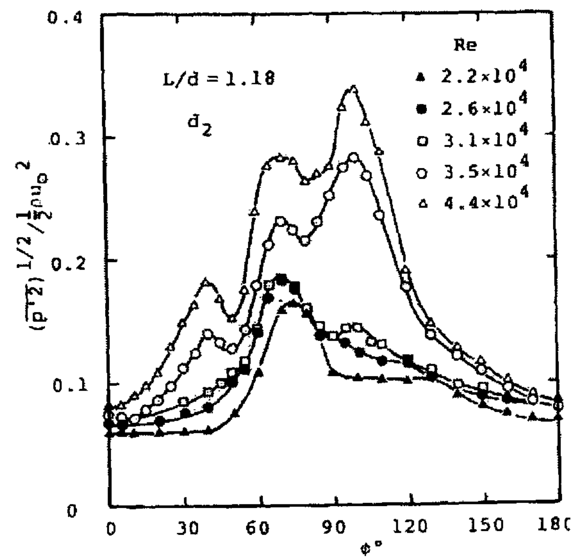

Figure 2.12: Effect of Reynolds number on the distribution of R.M.S. pressure fluctuation around the downstream cylinder of two cylinders in tandem (Igarashi, 1981).

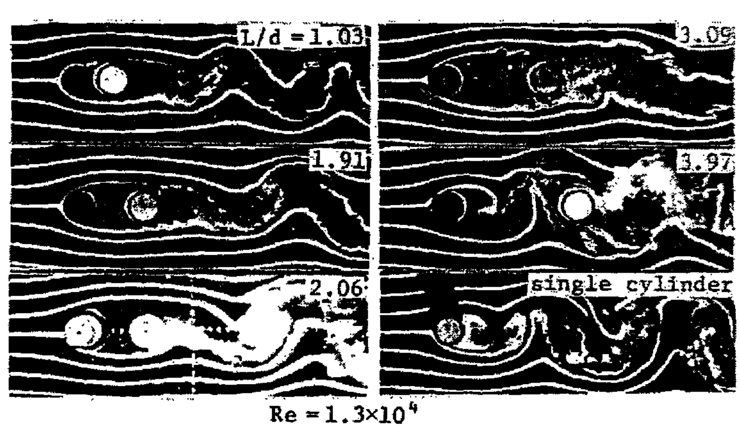

Figure 2.13: Flow visualization by smoke wind tunnel (Igarashi, 1981).

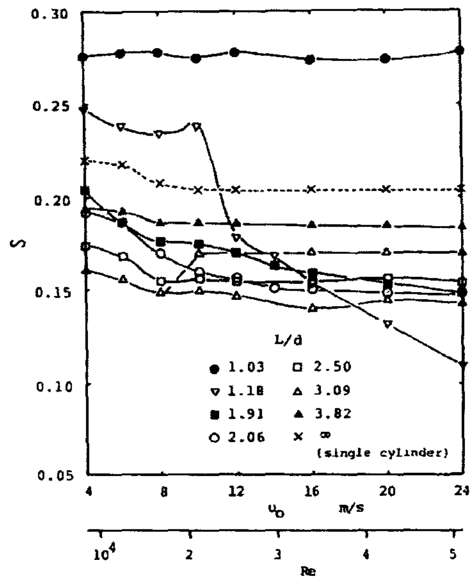

Figure 2.14: Effects of Reynolds number and spacing between two tandem cylinders on Strouhal number (Igarashi, 1981).

observations. However, Lin *et al.* (2002) and Mahbub Alam *et al.* (2003) have shown the strong dependence of the drag and lift force on the spacing between the cylinders, especially before the critical spacing, which agrees with the observations of Igarashi. Mahbub Alam *et al.* have found also that the separated shear layer reattachment position is changing with the change in the distance between the two cylinders (figure 2.15) and also that the value of the fluctuating lift and drag forces acting on the downstram cylinder is increasing as the reattachment position moves forward and decreasing when it moves back.

Lin *et al.* (2002) have used high-density particle image velocimetry to study the gap and near wake flow of two cylinders in tandem at Re = 10000. They were able to show clearly the small scale Kelvin-Helmholtz vortices in the unstable

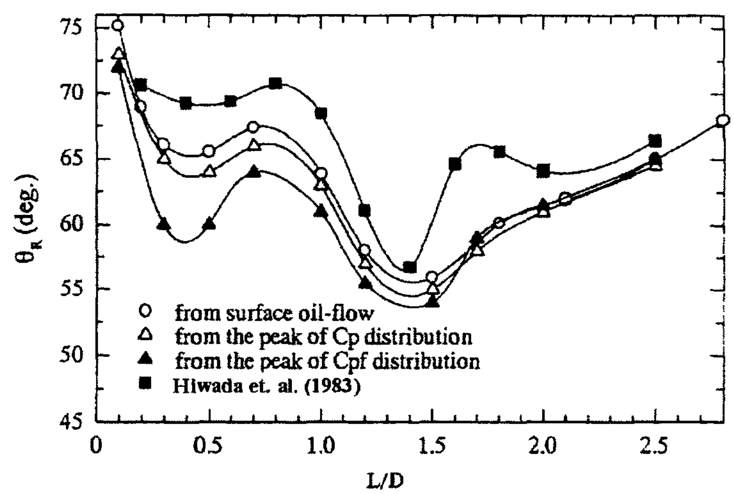

Figure 2.15: Variation in reattachment position with the increase in the spacing ratio for two cylinders in tandem (Mahbub Alam, 2003).

shear layers in the gap between the cylinders. These vortices are enhanced with the increase in Reynolds number and the increase in the turbulence level. The scale of the Kelvin-Helmholtz vortices is a function of the the spacing ratio as well. This makes the level of Reynolds stress and the significant extension of the Reynolds stress upstream the downstream cylinder, which results from the impingement of the vortices on the downstream cylinder, increase with the spacing ratio.

For small spacing up to S/D = 2.0, The Karman-like vortices formed behind the downstream cylinder are elongated with a tendency not to cut the separated shear layer of the other side.

The phase between the fluctuating lift forces on the two cylinders is affecting the fluctuating lift force on the upstream cylinder which becomes maximum when the flow patterns of the two cylinders are in phase and vice versa.

The free stream turbulence has a significant effect on the flow over tandem cylinders. Ljungkrona *et al.* (1991) have investigated the effect of the free stream turbulence on the flow over two cylinders in tandem. They have observed that the effect of the turbulence on the flow pattern is similar to the effect of increasing Reynolds number. A considerable decrease in Strouhal number has been observed in case of high turbulence intensity for the smallest spacings $S/D = 1.25$ and 1.5. The flow pattern was also affected as well and became the same for all the Reynolds numbers. The flow pattern showed a reattachment of the shear layer onto the downstream cylinder synchronized with vortex formation and vortex shedding in the near wake of the downstream cylinder.

For the spacing ratio $S/D = 2$, the turbulence intensity was observed to have a little effect because of the relatively stable flow at this spacing. The only effects that have been observed are a small increase in the Strouhal number and an increase in the drag coefficient on both the upstream and the downstream cylinders.

For the spacing ratios $S/D = 2.5$ and 3, the drag coefficient was observed to increase on the downstream cylinder from a negative to a positive value with the increase in the turbulence intensity. Vortex formation was observed in the front of the downstream cylinder which is similar to the flow for the non-turbulent case with a spacing ratio $S/D \geq 3.5$.

Generally, Ljungkrona *et al.* have observed that increasing the turbulence intensity caused a decrease in the critical spacing ratio, while the root mean square pressure coefficient was observed to increase with the increase in the turbulence intensity.

2.2.2 Side-by-Side Arrangement

In side-by-side arrangement, The plane passing through the two cylinder centers is perpendicular to the mean stream velocity direction. The flow interference can be divided according to the separation between the two cylinders as follows:

1. $\mathbf{1 < T/D < 1.1 - 1.2}$: The spacing is small. A single vortex street is formed downstream and the two cylinders behave like a single bluff body with base bleed in the gap between them.

2. $\mathbf{1.1 - 1.2 < T/D < 2.2}$: Narrow and wide wake will form with bistable biased jet flow divides between them and hence, the wide and narrow wake can intermittently exchange between the two cylinders. The frequency of vortex shedding is different in the two wakes.

3. $\mathbf{2.2 < T/D < 4 - 5}$: When the spacing is further increased, the vortex shedding frequencies from the two cylinders become the same. Vortex streets are coupled in out of phase mode i.e. simultaneously shed on the gap side then on the outer sides. The coupling gradually decreases and finally disappears beyond T/D of about 4.

2.2.3 Staggered Arrangement

In Staggered Arrangement, two Flow regimes can exist:

1. The vortex streets are formed in the narrow wake behind the front cylinder and in the wide wake behind the downstream cylinder with high and low frequency of vortex shedding.

2. When the transverse spacing is sufficiently small, the vortex shedding behind the front cylinder is suppressed and a strong gap flow induces large transverse component of force on the two cylinders.

2.3 Multi Tube Arrays

Tube bundles have received a lot of attention due to the importance of understanding this kind of flow in improving design of the heat exchangers as well as avoiding the problems that may arise during the operation. There are numerous disturbance sources in such kind of flow. Parameters like free stream turbulence, spacing between the tubes, wake interference and tubes oscillation make the problem of multi-tube arrays quite complicated.

The tube arrays can be grouped into two main types based on the geometry and, consequently, the interstitial flow nature. The first type is the in-line category where the flow is mostly straight through the tubes. The second type is the staggered tube array which may be normal triangle, rotated square, or parallel triangle arrays with wavy flow paths (Zdravkovich, 2003).

Structural failures of heat exchanger due to the flow excitation started to appear in the literature in 1950's. It became well known now that the flow excitation for heat exchanger tube arrays can be categorized as turbulence buffeting, vortex shedding, fluidelastic instability, and acoustic resonance (Weaver, 2000).

Baird reported in 1954 that an intense sound and vibration were observed in the heat exchanger of Estiwanda steam power station. The noise was very loud that "it could easily be heard in the concrete control room some distance away".

Typical value for sound pressure level of acoustic resonance in tube arrays are 160-176 dB and approximately 20-40 dB lower outside the heat exchanger shell.

Acoustic resonance is associated with an acoustic mode that is transverse to the tube and the flow. The sound waves generated at resonance are reflected at the ducting containing the tube to create a pattern of a standing wave depending on the geometry of the ducting. Blevins (1985) showed that it is the particle velocity and not the sound pressure that entrain the vortex shedding. and the greater the transverse velocity the greater the entrainment.

Acoustic resonance has been observed for many types of tube arrays. The excitation mechanism of staggered and in-line tube bundles are different. The excitation mechanism in staggered tube arrays is mainly due to vortex shedding while it is not necessarily related to vortex shedding in case of in line tube array. This makes it difficult for the case of in-line tube array to predict the onset of acoustic resonance from Strouhal number data. Therefore, the critical velocity for acoustic resonance onset must be calculated from acoustic resonance data available in the literature taking into account the level of the excitation energy which should be high enough to entrain the vortex shedding and produce high sound pressure level (Weaver, 2000).

Eisinger and Sullivan (1993) discussed the development and suppression methods of acoustic resonance. They have attributed the excitation of the acoustic modes to the flow turbulence and for the process of vortex shedding. They argued that the vortex shedding can not be alone the source of acoustic excitation considering the difference between the calculated vortex shedding frequency and

Figure 2.16: Flow visualization photos showing (a) symmetric vortex formation in a flow lane and (b) antisymmetric vortex formation in a tube wake (Ziada, 1990).

the frequency of the acoustic mode which has been excited in their study.

Ziada and Oengören (1990) made a series of studies on the acoustic resonance in different types of the tube bundles. They conducted a flow visualization for in-line tube bundles and were able to show the pattern of symmetric vortex formation in the flow lane and antisymmetric vortex formation in the tube wake (figure 2.16).

There are two kinds of flow instability in case of in-line tube arrays. The jet instability which is the dominant mode at non-resonance conditions and the shear layer instability which becomes dominant in case of resonance. Ziada and Oengören (1992) have described the transition mechanism as well as the condition for mode switching.

The acoustical response of the staggered tube arrays is very different from that of the in-line tube arrays because of the difference in geometry which makes

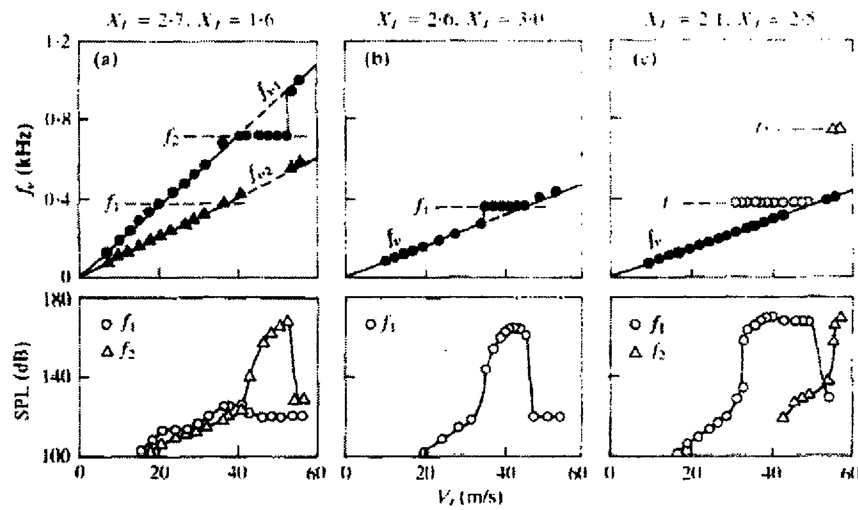

Figure 2.17: Frequency of vorticity shedding, f_v, and sound pressure level, SPL, at the resonance frequencies, f_1 and f_2, as functions of the gap flow velocity (a) Staggered array (Ziada *et al.* 1989); (b) In-line array (Ziada and Oengören, 1990)

the flow different as well. There are two vortex shedding frequencies in staggered arrays. As shown in figure (2.17), the first mode was not excited but the second mode is excited when the first vortex shedding frequency becomes close to the frequency of the second mode and a lock-in takes place. In the case of in-line tube arrays, there is only one dominant vortex shedding frequency. The acoustic resonance takes place much earlier than that in the case of staggered tube arrays (Oengören and Ziada, 1992). The lock-in range ends for in-line tube arrays when the frequency of vortex shedding is coincident with the acoustic natural frequency. Similar results are observed with present experiment on tandem cylinders.

The mechanism of acoustic resonance has been studied also for normal triangle tube arrays with different spacings . The relative importance of each vortex shedding component is found to be dependent on the number of tube rows and the number of tubes in each row in addition to the Reynolds number. Flow visualization studies show the formation of vortex shedding even in case of small spacings. The normal triangle arrays are dominated by the wake instability which is the case for the rotated square arrays as well. (Oengören and Ziada, 1998).

Fundamental differences have been found between the parallel triangle and normal triangle tube bundles. Ziada and Oengören (2000) have attributed these differences to the variation in the layout pattern of the tubes. It was found that for small spacings, the acoustic resonance could not be attributed to flow periodicities (Tanaka, 1998, and Ziada, 2000). It was found as well that the acoustic resonance seems to be similar to that of in-line arrays.

2.4 Finned Tube Arrays

Finned tubes are commonly used in heat exchangers. The fins enhance the heat transfer by increasing the area of the tubes. The use of the fins becomes very important when the stream to be used on the outside of the tubes is a gas of low heat transfer coefficient.

There are a lot of fins types used in the industry. The segmented fins usage in heat exchangers increased recently because it have several advantages as explained by Reid *et al.* (1994):

1. easier to manufacture.
2. the segmentation of the fins results in higher turbulence and improved gas penetration to the fins root area, thus equalizing the flow over the fin height

which results in a higher heat transfer coefficient than for plain fins by as much as 20%.

3. The ease of manufacturing makes it possible to increase the height of the fins and hence, makes it more efficient.

4. And as a consequence of all the previous, the heat exchangers become lighter and of lower cost.

The research on finned tube bundles received more attention recently because of the wide usage of finned tubes in heat exchangers.

Kouba (1986) has measured the velocity and pressure fluctuations for three different types of finned tube bundles. The velocity measurements shows the existence of vortex shedding in case of the finned tube bundles. Kouba argued that the behavior of the flow for the finned tubes are the same as the bare tubes which contradicts with the measurements by Nemoto *et al.* (1992).

Nemoto and Yamada (1992) have measured the sound pressure level generated from staggered arrays of finned tubes at the duct wall as well as the velocity profile downstream the tube array. They have found that finned tube arrays were not able to excite all of the modes that were excited in the case of bare tubes. They have explained this phenomenon later (1994) by the effect of fins that cause the generation of more broad band noise and sound which is not strong enough to excite the higher modes. Their velocity measurements at resonance downstream the tube array showed that the velocity is minimum at the antinodes and maximum at nodes.

Nemoto and Yamada showed that using baffle plates are effective in preventing the resonance for a single tube bank. The baffles have to protrude outside the tube banks, in case of multibank tubes, for more than double the tube pitch in the direction of flow in order to be effective.

Nemoto *et al.* (1997) compared between the total sound pressure level on the duct wall for three different types of finned tubes and bare tubes of the same bare diameter. The overall sound pressure level in the case of the bare tubes were less than that in case of all of other types of the finned tubes. The sound pressure level for serrated finned tubes were higher than the solid finned tubes as shown in figure (2.18). They have explained that by the higher flow velocity due to the larger contraction flow ratio causes the sound generating energy to be larger. However, they were not able to explain the difference between the solid and serrated finned tubes when both of them have the same flow contraction ratio.

Fan (2002) has studied the effect of fins on vortex shedding and acoustic resonance for staggered arrays of twisted serrated finned tubes. Vortex shedding has been observed. Acoustic resonance has been excited either by turbulence buffeting or by vortex shedding. The vortex shedding was observed to enhance or suppress the acoustic resonance when the vortex shedding frequency coincides with the resonance frequency. The small fins was observed to excite a stronger resonance than the longer fins.

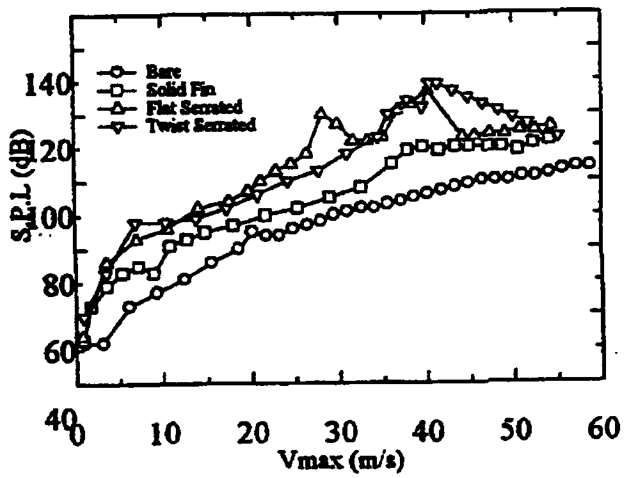

Figure 2.18: Sound pressure level vs flow velocity on duct wall surface of different types of finned tubing (Nemoto *et al.* 1997)

2.5 Single Finned Cylinders

Brevoort and Rollin (1937) have studied the characteristics of air flow across finned cylinders by measuring the average velocity using pitot tubes for a smooth and finned tubes of different fin densities and fin widths. They found that the fin density is a very important parameter in determining flow characteristics while the fins width is not so critical in determining the characteristics of the flow.

Carvajal-Mariscal *et al.* (2001) have studied the flow dynamics between the inclined fins of a finned tube and they found an increase in the drag coefficient by 50 % over that in case of the bare tube. A secondary flow is formed between the fins and the flow separates on the fins nearly at the same point as in case of the bare tube.

Hamakawa *et al.* (2001) have investigated the effect of the fin density and the

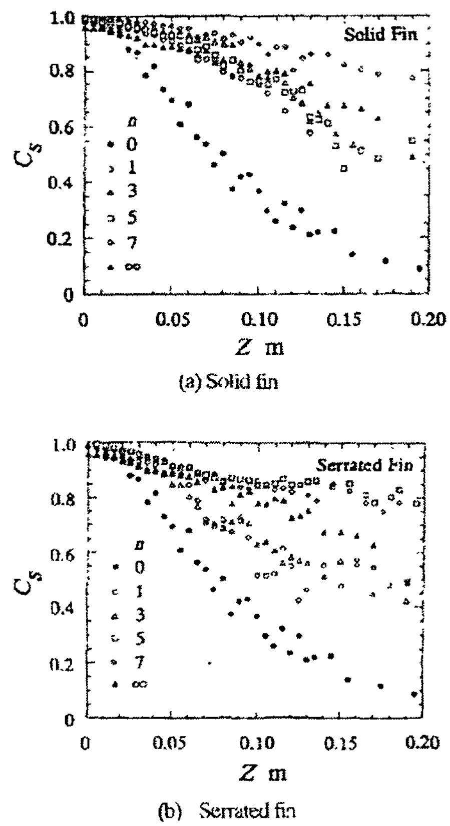

Figure 2.19: Spanwise distribution of the coherence function at vortex shedding frequency along the span of finned cylinders of different fin densities (Hamakawa *et al.*, 2001)

shape of the fins on the vortex shedding from a single finned cylinder for Reynolds number between 1.1×10^4 and 1.1×10^5. They found that the maximum value of turbulent intensity in case of the finned tubes is less than that in case of bare tube. However, the spanwise scale of the vortex was larger in case of finned tubes and it was increasing as the number of fins was increasing (figure 2.19). It was found also that the spanwise scale is considerably larger than the pitch of the fins.

Mair *et al.* (1975) have investigated the frequency of vortex shedding behind finned cylinders. He found that the use of an effective diameter, defined as the frontal area per unit length, was able to collapse the results of the bare and the finned tubes.

Ryu *et al.* (2003) have investigated the characteristics of the near wake flow behind a single circular cylinder with serrated fins. They make use of serrated finned tubes of different fin densities and heights. A hotwire anemometer was used to measure the velocity profile downstream of the cylinders in addition to measuring the through velocity profile between the fins. They have found that decreasing the pitch between the fins while increasing the fin height has changed the velocity near the roots of the fins significantly. Increasing densities accelerate the flow but in the same time increases the resistance to the flow. So, for low fin density and fin height, the flow was accelerating on the top of the cylinder and the speed reaches to a value higher than it is for bare cylinders. But with other models of higher fin density and height, the resistance was very high that the flow was decelerated.

A very strong velocity gradient on the surface has been observed for the case of high density finned cylinders. The formation length was measured as well. They have found that the formation length is increasing as the fins density and height are increasing while it is decreasing with increasing the flow velocity.

Jebodhsingh (2002) has studied the effect of fins on vortex shedding from single serrated finned cylinders in the subcritical range. His velocity measurements show larger velocity deficit in the case of finned cylinders and a decrease in the width of the wake which is opposite to the bare tubes case. Jebodhsingh has observed also that the turbulence intensity associated with the fundamental vortex shedding frequency is increasing with the increase in the fin density. The number of harmonic peaks increases as well with the increase in fin density.

The vibration of the finned tubes has been studied by Sviadosch *et al.* (1990). they have investigated the effect of the turbulence on the vortex shedding vibration of a single finned cylinder at different turbulence levels from 1% up to 12% and Reynolds numbers varying from 10^4 to 2×10^4. Vortex shedding was observed in all the cases they investigated. However, it was observed that increasing the turbulence level slightly reduces the the vortex-shedding vibration but increases the level of vibrations due to turbulence buffeting.

2.6 Discussion

A huge amount of work has been performed on single bare cylinders. The two cylinders flow as well as the tube bundles has received a lot of attention as well. However, no parallel work has been devoted to finned cylinders. Understanding the basic flow over single and two tandem finned cylinders is believed to be a basic step in understanding the flow in case of finned tube bundles. The work that has been completed to date on finned cylinders shows that they have their unique features which need to be investigated carefully. Investigation of the flow over single finned cylinder helps in understanding how the fins affect the flow behavior, flow induced vibrations and acoustic resonance. Investigating the case of two finned cylinders is also very important as it may clarify the effect of fins on the two tandem cylinders flow, and how the existence of another finned cylinder would modify the flow and the acoustic resonance mechanism. Understanding of these relatively simple flow configurations is crucial to understanding the flow behavior in finned tube bundles.

The research that exists in the literature on single finned cylinders is still not enough to fully understand the effect of fins on vortex shedding from single cylinders. Despite the large amount of work devoted to the case of tandem bare cylinders, there is no work investigating the effect of fins in the case of tandem finned cylinders to the best knowledge of the author.

The purpose of this study is to improve our understanding of the flow behavior and acoustic resonance in the case of finned tube bundles by looking into the effect of fins on vortex shedding and acoustic resonance for single and two tandem finned cylinders. It is hoped that the results of this study will lead to more understanding of the flow over the finned tube bundles.

CHAPTER 3
Experimental Setup

A group of experiments were performed in an open circuit wind tunnel equipped with variable speed blower to change the flow velocity during the test. The objective is to investigate the effect of fins on vortex shedding in the cases of single and two tandem cylinders. The experiments were carried out on cylinders with three different fin densities in addition to bare cylinders of the same effective diameter for purpose of comparison. The experiments included extensive measurements using a microphone and a hotwire anemometer.

3.1 The Cylinders

Cylinders with three different fin densities have been selected for this study. One of the cylinders has been designed to model one of the commercially widely available finned tubes. The dimensions of the other two cylinders are the same except that the fin density has been changed to investigate its effect on the vortex shedding from finned cylinders.

The commercially manufactured tubes are found to have an imperfect fins pattern along the span due to the manufacturing inaccuracies which can be accepted commercially but can not be accepted for fundamental studies. These imperfections add new uncontrolled parameters to the complex problem of finned tubes. Jebodhsingh (2002) observed that the results of the correlation length mea-

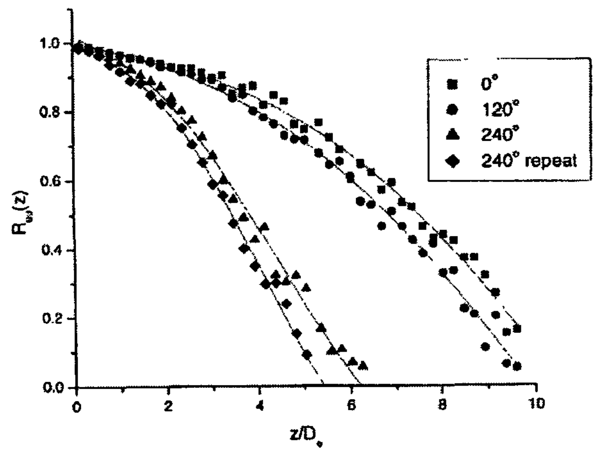

Figure 3.1: Correlation coefficient measurements along the span of the same finned tube at $x/D_e = 2.5$, $Re = 2.61 \times 10^4$ and at different tube angular positions (Jebodhsingh, 2002).

surements for the finned tubes are dependent on the orientation of the tubes as shown in figure (3.1).

The finned tubes used in this study were manufactured in the machine shop of the Mechanical Engineering Department. Care has been taken to be sure of the accuracy of the dimensions and the symmetry of the tubes with respect to its centreline to ensure that the measurements do not depend on the tubes orientation.

The finned tubes were made of precision ground cylinders on which discs and spacers have been fitted tightly. The fin density has been changed by changing the width of the spacers (Figure 3.2).

The diameter of the bare tubes used in this study is the same as the effective diameter of the finned tubes as defined by Mair *et al.*(1975):

$$D_e = \frac{1}{b}\left[(b-t)D + t\,D_f\right] \tag{3.1}$$

Where,

D_e is the effective diameter,

b is the distance between centers of fins,

t is the fin thickness,

D_f is the fins diameter.

Single finned cylinders are found to have the same vortex shedding frequency as single bare cylinders of the same effective diameter (Mair 1974 and Jebhodsingh 2002). This makes the coincidence of the vortex shedding frequency, from either the bare or the finned tubes, occur at the same velocity and hence at the same energy input to the system, which is necessary for comparison. All the dimensions of the cylinders are shown in table 3.1.

Table 3.1: The dimensions of the tubes

	Finned Tubes			Bare Tubes	
	Type 1	Type 2	Type 3	Type 1	Type 2
Fin density, (Fins/inch)	5.3	9.8	18.2	—	
Fin Spacing, s (mm.)	4.4	2.2	1.016	—	
D_e, (mm.)	16.3	15.7	17.5	16	17.5
Root Diameter, D (mm.)	15			16	17.5
D_f, (mm.)	24			—	
Fin Thickness, t (mm.)	0.381			—	
Fin Height, H (mm.)	4.5			—	
Length, L (mm.)	76				

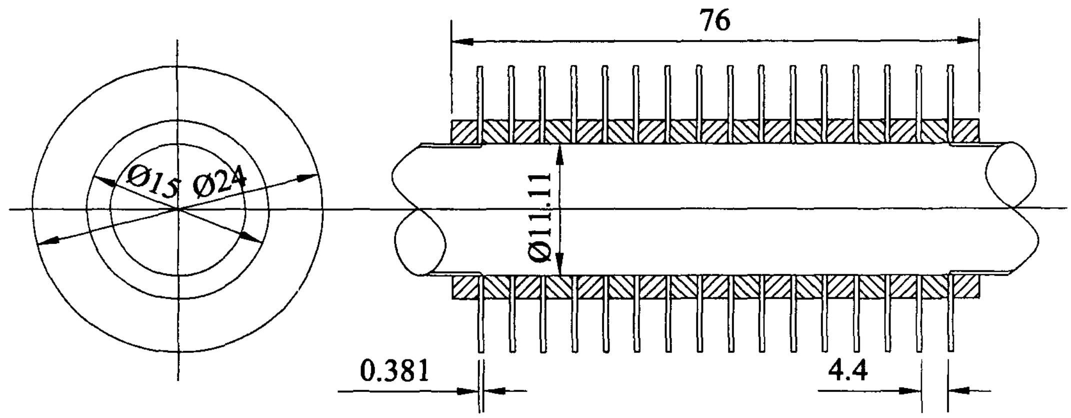

Figure 3.2: Geometry of the finned cylinders used in the present study (All dimensions in mm).

3.2 The Test Section

The experiments have been conducted in an open circuit, low speed wind tunnel. A sheltons industrial type centrifugal blower is used along with Toshiba TOSVERT 3-phase industrial type frequency inverter to control the speed. The motor-blower assembly was bolted firmly to the floor by using anchoring bolts.

The dimensions of the test section were carefully chosen so that the maximum vortex shedding frequency is coincident with the acoustic natural frequency of the test section well below the maximum attainable velocity of the wind tunnel. This makes it possible to get out of the lock-in range before reaching the maximum flow velocity. This gives the opportunity to investigate the effect of fins on vortex shedding at resonance and non-resonance conditions.

It is not enough to have the coincidence between the vortex shedding and the acoustic natural frequency to have resonance. It is very important as well to have a strong vortex shedding so that the lock-in can take place and the resonance can

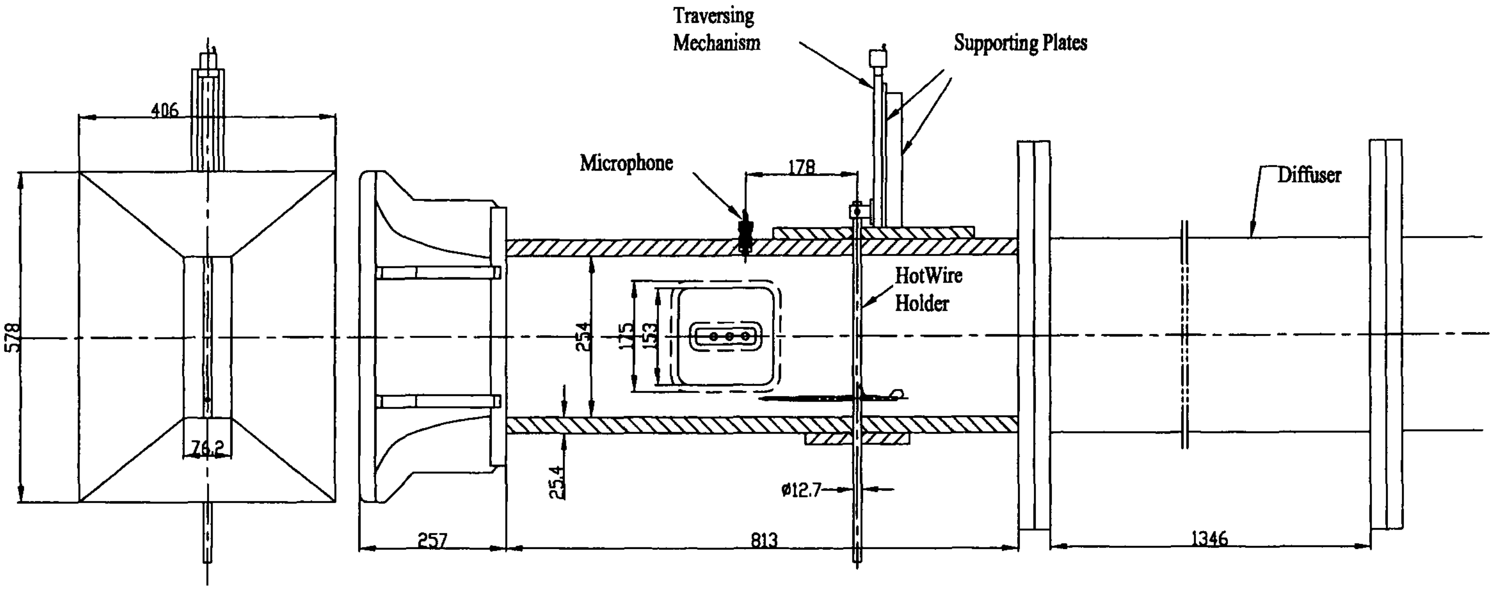

Figure 3.3: The Test Section (All dimensions in mm).

be achieved. This necessitates that the coincidence should happen at the highest possible speed by increasing the diameter of the cylinder within the acceptable limits of the blockage ratio. Taking all of the previous constraints into consideration, the test section dimensions were chosen to be as shown in figure (3.3). The blockage ratio varies between 6.3 % and 6.9 %.

To achieve a uniform velocity profile with as small as possible boundary layer thickness, a contraction designed by Macleod (1995) has been used. The details of the design as well as the velocity profiles in the test section with the contraction can be found in the master thesis of Macleod (1995).

A diffuser has been used between the test section and the blower as a transition section to allow the flow to gradually expand from the smaller area of the test section exit to the inlet area of the blower with minimum losses in the dynamic head. The diffuser was designed by She (2000). The diffuser is made of plywood of 12.7 mm thickness with the interior surface polished and lacquered to provide a smooth surface to reduce the friction losses. More details about the diffuser can be found in She (2000).

The test section is made of Acrylic with a thickness of 1". It has two side windows in order to access inside the test section with a small insert in each window. The inserts have holes at the center of the test section height used to fix the test cylinders. The exact distances required between the cylinders was achieved by making holes in the inserts with the exact required distance between them. Seals were put between the different wind-tunnel sections to avoid leakage.

It was important to avoid the vibration of the cylinders as it may affect the vortex shedding and acoustic resonance. The cylinders were rigidly fixed at the sides of the test section and the holes were made such that the cylinders tightly fit into them to minimize the cylinders vibrations as much as possible.

The Downstream cylinder position was the same for all of the cases investigated while the upstream cylinder position was changed to obtain the desired spacing ratio.

3.2.1 Acoustic Modes of The Test Section

The test section can be modelled as a rectangular volume open at both ends. The volume of the cylinders is small with respect to the volume of the test section. Hence, their effect can be neglected and the natural frequency of the transverse acoustic mode can be calculated from the relation:

$$f_a = \frac{ic}{2B}, \quad i = 1, \ 2, \ 3, 4, ... \tag{3.2}$$

Where c is the speed of sound in the air and B is the height of the test section.

The natural frequency of the first mode for the test section ($i = 1$) is calculated to be $f_a = 681\,Hz$. The measurements show that the acoustic natural frequency of the test section is 686 Hz. This small difference is due to the effect of the cylinder volume which increases the acoustic natural frequency of the test section.

3.3 The Hotwire Anemometry

A hotwire anemometry system has been used to measure the mean and the fluctuating flow velocity. A DANTEC hot-wire probe type 55P11 mounted on DANTEC hot-wire holder type 55H1 have been used in conjunction with DISA hot-wire bridge type 56M01.

A manual traversing mechanism has been used to traverse the hotwire probe vertically across the test section. The mechanism can traverse the hotwire vertically for 200 mm with a precision of 0.01 mm. The traversing mechanism was fixed and supported rigidly by means of three perpendicular plates at the top of the test section as shown in figure (3.3).

The hotwire holder has been designed to have the same blockage ratio at all traversing positions in the test section so that the flow conditions doesn't change during the test. The diameter of the holder (12.7 mm.) has been selected so as to have a vortex shedding frequency at the maximum flow velocity lower than the acoustic natural frequency of the test section. This ensures that no resonance would take place due to the vortex shedding from the holder which would affect the flow over the upstream cylinders . The holder was removed from the test section during the sound pressure measurements.

3.4 The Microphone

A G.R.A.S. 1/4" pressure microphone of type 40BP has been used to measure the sound pressure at the top wall of the test section. The microphone has a flat constant frequency response over the range from 10 Hz to 25 kHz within ± 1 dB. A

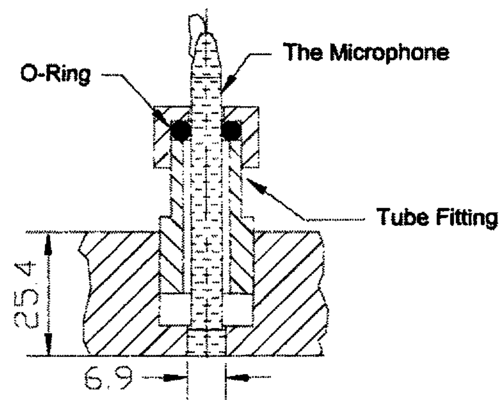

Figure 3.4: The details of the microphone fixation (All dimensions in mm).

preamplifier of type 26AC was used in conjunction with a dual-channel G.R.A.S. power module of type 12AA for microphone signal conditioning.

The microphone was flush mounted with the internal top surface of the test section so that it does not disturb the flow (Figure 3.4). All the microphone measurements have been taken above the downstream cylinder.

3.5 The Measurements

Measurements were performed on single finned cylinders with three different fin spacings as shown in table (3.1) to study the effect of fin spacing on the vortex shedding. The measurements on finned cylinders I and II were compared with measurements on a bare cylinder with a diameter that is within 2% of their effective diameter. The finned cylinder III has been compared with bare cylinder II with the same effective diameter.

Measurements were carried out on tandem cylinders as well. The distance between the cylinders have been chosen to fall within three different flow regimes. The values of the spacing ratio have been chosen to be 1.5, 2, and 3. As in the case of single cylinders, the flow over the three types of the finned cylinders was investigated and compared with the bare cylinders in the same way as in the case of single cylinders.

A national instrument 16 bit 4-channel card type PCI-4452 has been used for data acquisition. The card is equipped with an anti-aliasing filter. An existing Labview program has been used to process the signal and calculate the spectra.

The sound pressure measured at the top wall of the test section is a function of the strength of the vortex shedding and the correlation length as shown in equation (2.5). Thus, the sound measurements were used to investigate the effect of the fins on the vortex shedding strength and its correlation length as well.

The measurements were performed for a Reynolds number range of 1.56×10^4 to 1.13×10^5, which is well inside the subcritical regime (figure 2.2). By investigating within this range, it was possible to get the required information before the onset of resonance as well as during the resonance for the subcritical regime. More details of the flow have been acquired using hotwire anemometry system for specific cases of interest.

CHAPTER 4
Results and Discussion

This chapter presents in detail the results of the measurements that have been done on the single cylinders as well as the tandem bare and finned cylinders. The measurements were made in the Reynolds number range from 1.56×10^4 to 1.13×10^5. Sound pressure was measured using a microphone. Hotwire measurements were also performed at specific points of interest.

The change in the sound pressure at vortex shedding frequency with the velocity was obtained for each case. The results for different cases will be compared and discussed in this chapter. The results of the measurements on the bare cylinders will be presented first then the measurements on the finned cylinders will be presented and compared to the bare cylinders results. A discussion of all the results will be presented at the end of this chapter.

4.1 Bare Cylinders

In order to investigate the effect of fins on vortex shedding from cylinders, it was necessary to make similar measurements on bare cylinders first to provide a basis for the comparison. Measurements were made on single bare cylinders and tandem bare cylinders. The spacing ratio has been changed in case of the tandem cylinders to investigate the effect of the spacing ratio on the vortex shedding and acoustic resonance. The measurements made on the single bare cylinder will be

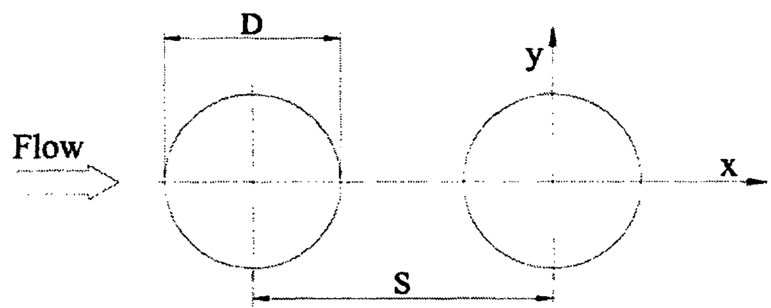

Figure 4.1: The cylinders configuration and the frame of reference

presented first then the measurements made on the tandem bare cylinders will be presented in details. A comparison between the results of different cases will be given at the end of this section.

Figure (4.1) shows the frame of reference for the present study. The upstream cylinder was taken out during the single cylinder measurements. For the tandem cylinders, the downstream cylinder position was fixed while the upstream cylinder position was changed to get the desired spacing ratio.

4.1.1 Single Bare Cylinder

The sound pressure has been measured using a microphone above the cylinder at different flow velocities. The spectra of the pressure have been calculated for all of the different cases. The frequency of the vortex shedding as well as the sound pressure amplitude at the vortex shedding frequency for each case have been determined from the pressure spectra.

The results are presented in terms of the vortex shedding frequency (f_v), nondimensionalized by the acoustic natural frequency of the test section (f_a), and the reduced velocity (V_r), which is defined by:

$$V_r = \frac{V}{Df_a} \tag{4.1}$$

where,

V is the free stream velocity,

D is the cylinder diameter,

f_a is the acoustic natural frequency of the test section.

The non-dimensionalized pressure at vortex shedding frequency P_v^* was used also to present the results where:

$$P_v^* = \frac{P_v}{\frac{1}{2}\rho V^2 M} \tag{4.2}$$

where,

P_v is the rms amplitude of sound pressure at vortex shedding frequency obtained from the pressure spectra,

ρ is the density of the air ,

M is the Mach number.

P_v^* is nondimensionalized in this way using equation (2.5) in an attempt to show the effect of the change in the correlation coefficient and the lift force while reducing the effect of Mach number and the change in the velocity head.

For a far-field, starting from equation (2.5):

$$\frac{\overline{P^2}}{\rho c} = \frac{sin^2\theta\, cos^2\phi}{16c^3R^2}\rho V^6 L^2 \overline{C_L^2} St^2 L_c(L-\gamma), \tag{4.3}$$

Hence,

$$\sqrt{\frac{\overline{P^2}c^2}{\frac{1}{4}\rho^2 V^6}} = \sqrt{\frac{sin^2\theta\, cos^2\phi}{4R^2} L^2 \overline{C_L^2} St^2 L_c(L-\gamma)}, \tag{4.4}$$

Which leads us to the expression,

$$P_v^* = \frac{sin\theta\, cos\phi}{2R} L St C_L^{'} \sqrt{\rho L_c(L-\gamma)}, \tag{4.5}$$

So, from this equation, it can be concluded that P_v^* in this study is basically a function of the root mean squared lift coefficient, $C_L^{'}$, and the correlation length, L_c.

Figure (4.2) shows the change in f_v/f_a and P_v^* as a function of the reduced velocity for a single bare cylinder. The figure shows a linear increase in the vortex shedding frequency with the increase in the velocity before and after the acoustic resonance. However, it is observed that the vortex shedding frequency at high Reynolds numbers after the lock-in becomes spread over a wider frequency range.

It is observed also that P_v^* is decreasing with the increase in the reduced velocity before and after the lock-in region. This can be explained by a decrease in the correlation length with the increase in the velocity. This doesn't apply to the lock-in velocity range because of the effect of sound which becomes very intense at resonance. This sound is strong enough to organize the flow and concentrate the vortex shedding energy at the resonance frequency.

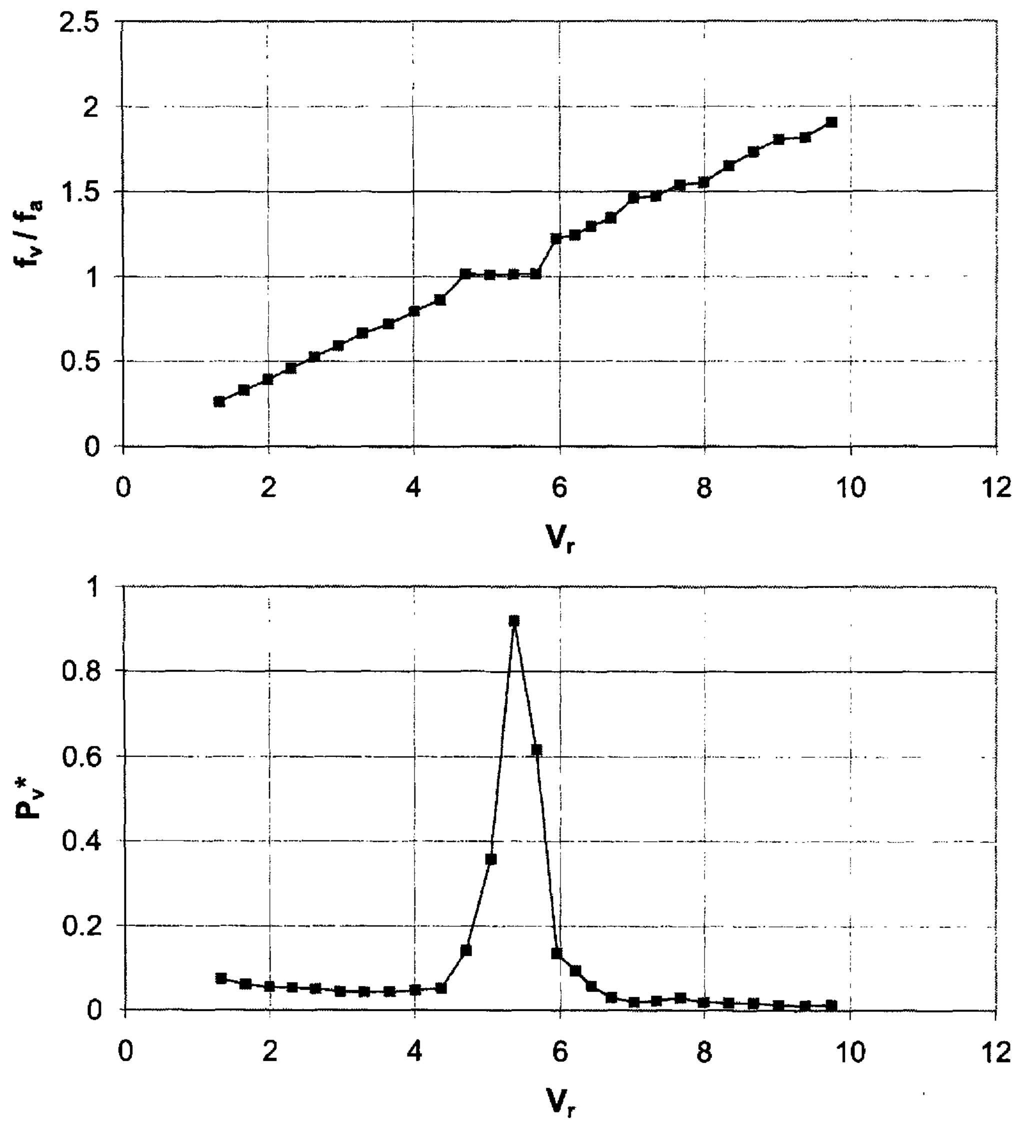

Figure 4.2: Variation of f_v/f_a and P_v^* as functions of V_r for a single bare cylinder of type I.

The frequency of the vortex shedding locks in to the acoustic natural frequency in the range of $V_r = 4.7$ to 5.7. The highest values for P_v^* have been observed at the lock-in region because of the feedback effect described earlier. The maximum value of P_v^* is measured near the coincidence of the frequency of vortex shedding with the acoustic natural frequency of the test section.

These results compare generally well with the results of Blevins and Bressler (1993) as shown in figure (4.3). The lock-in starts and ends nearly at the same reduced velocity. The maximum sound pressure level was also observed near the point of frequency coincidence.

Blevins and Bressler (1993) have suggested an expression to correlate the maximum sound pressure levels for different bare cylinder diameters with an average absolute value of error 26%. Using this correlation with the results obtained from the measurements on single bare cylinders I and II, the maximum sound pressure values were obtained with an error of less than 11%.

4.1.2 Tandem Bare Cylinders

The flow regimes for tandem cylinders with different spacing ratios were described by Igarashi (1981) and Zdravkovich *et al.* (1985). A fair understanding to the flow in the gap between the cylinders and in their wake was obtained for low turbulence intensity case. For higher turbulence intensity, Ljungkrona (1991) showed that the flow behavior changes significantly. The critical spacing beyond which vortex shedding occurs in the gap becomes smaller. Although not enough information is available to be able to describe precisely the flow pattern in the gap

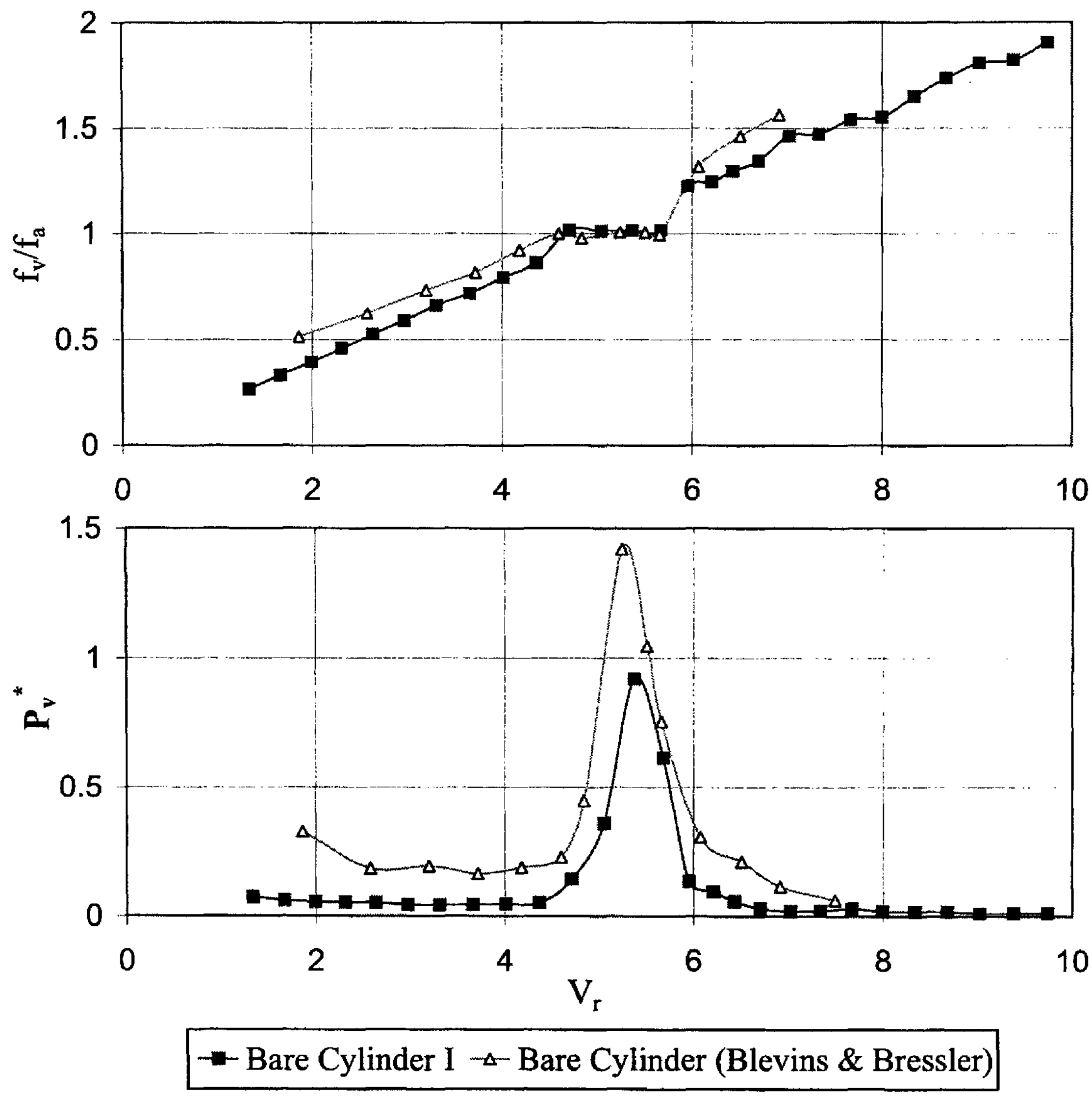

Figure 4.3: Comparison of the variation of f_v/f_a and P_v with V_r for single bare cylinder I with that of Blevins and Bressler (1993).

between the cylinders, an approximate prediction of the flow can be obtained from the pressure and the Strouhal number measurements when they are compared to the literature.

The same measurements as in case of the single cylinder have been performed for tandem bare cylinders with spacing ratios of $S/D = 1.5$, 2 and 3. The three spacings that have been chosen are expected to represent three different flow regimes. The sound pressure measurements were carried out using a microphone flush with the test section top wall, just above the downstream cylinder. The downstream cylinder position remained the same during all of the measurements while the position of the upstream cylinder was changed (figure 4.1).

4.1.2.1 Tandem Bare Cylinders with S/D = 1.5

For a low turbulence case, the flow regime that would be expected for $S/D = 1.5$ is flow with no reattachment on the downstream cylinder at a low Reynolds number and a synchronized flow regime at $Re > 3.3 \times 10^4$, where the shear layer separates from the upstream cylinder and reattaches to the downstream cylinder while the other shear layer is shed with no reattachment at the wake of the downstream cylinder (Igarashi, 1981). Between these two regimes there is an unstable region where the flow is alternating between the two regimes. Lin *et al.* (2002) have observed low-level concentrations of vorticity in the upper and lower side of the gap. These concentrations coalesce as they impinge on the downstream cylinder.

The relationship between f_v and V_r as well as P_v^* and V_r for $S/D = 1.5$ are illustrated in figure (4.4). It is observed that the vortex shedding frequency

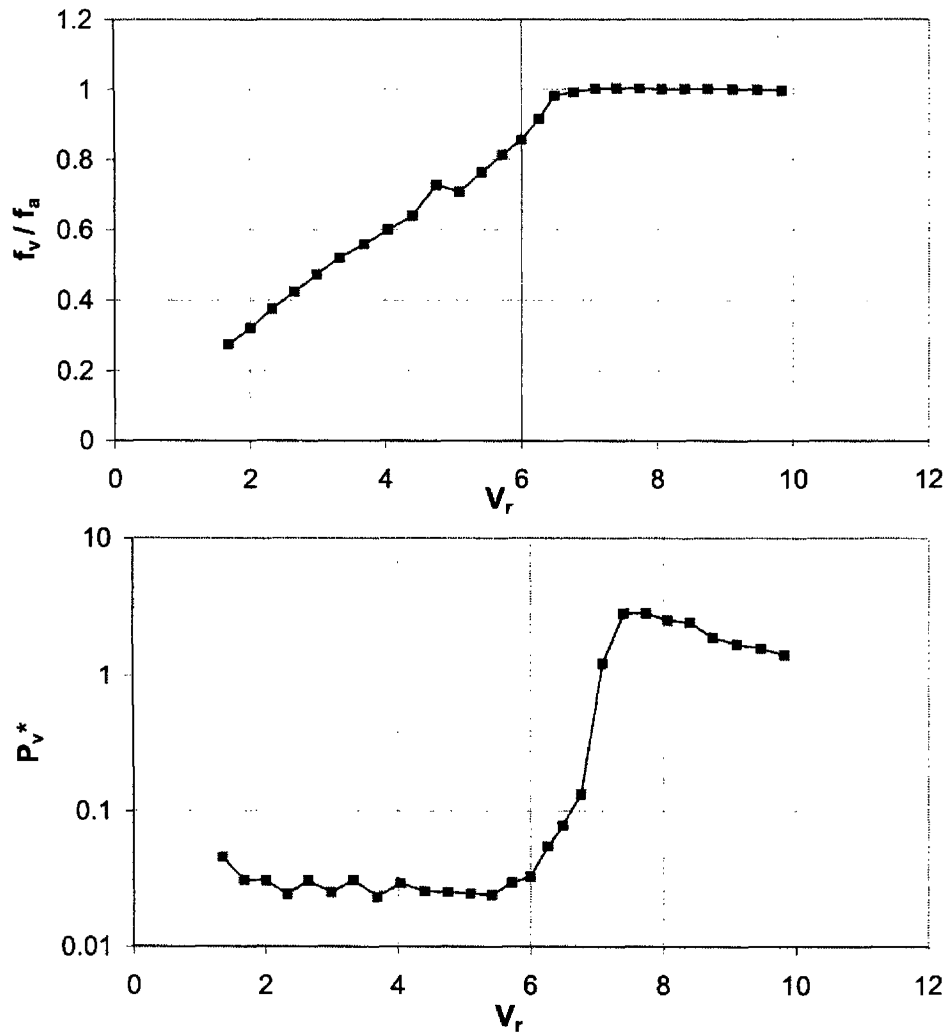

Figure 4.4: Variation of f_v/f_a and P_v^* as functions of V_r for a tandem bare cylinders of type I with a spacing ratio $S/D = 1.5$.

changes linearly with the velocity before the resonance. This observation means that the Strouhal number is constant which contradicts the observation of Igarashi (1981) who found the Strouhal number to be changing with Reynolds number in this case. This difference can be explained by the effect of the free stream high turbulence intensity which was measured to be 1.5%. This high turbulence intensity promotes the transition into the synchronized flow regime as explained by Ljungkrona (1991). This flow regime is more stable than the non-turbulent case which results in a nearly constant Strouhal number and hence a linear relation between the frequency and the velocity.

A very strong resonance has been observed in this case. The lock-in between the vortex shedding frequency and the acoustic natural frequency occurred at $V_r = 6.4$ which is later than the case of the single cylinder. This difference in the lock-in onset velocity can be explained by the difference in the Strouhal number. Strouhal number was determined from the microphone measurements to be 0.198 for the single bare cylinder and 0.15 for the tandem bare cylinders. This means that f_v will be equal to f_a for a single cylinder when $St = 0.198 = f_a D/V$, i.e. at $V_r = 1/0.198 = 5.05$ while this will happen in case of the tandem cylinders with $S/D = 1.5$ at $V_r = 1/0.15 = 6.67$. Hence, the higher Strouhal number resulted in earlier coincidence with the vortex shedding frequency and earlier lock-in onset.

As observed in figure (4.3), the lock-in is very strong and is maintained over a wide range of reduced velocity. Moreover, maximum sound pressure doesn't occur at the coincidence of f_v with f_a, at $V_r = 6.5$, but rather after the frequency coincidence at $V_r = 7.4$.

4.1.2.2 Tandem Bare Cylinders with S/D = 2

For the low turbulence level case, quasi-stationary vortices are expected to form between the two cylinders. The shear layers separated from the upstream cylinder will reattach alternatively to the downstream cylinder. Ljungkrona (1991) observed an increase in the Strouhal number with the increase in the turbulence intensity. But generally, this flow regime is relatively stable which reduces the effect of the turbulence intensity.

A strong resonance has been observed in this case as well (figure 4.4). The first mode was excited and the vortex shedding frequency locked in to the resonance frequency. The lock-in region can be divided into two ranges. The first range is the pre-coincidence resonance before the coincidence between the vortex shedding frequency and the acoustic natural frequency of the test section. The pre-coincidence resonance starts at $V_r \simeq 4$ which is less than that corresponding to the case of a single cylinder and the tandem cylinders with $S/D = 1.5$. The second range is the post-coincidence lock-in which starts afterwards at $V_r = 6.48$.

At the pre-coincidence lock-in range, P_v^* increases with the increase in the velocity until it reaches its maximum value at $V_r = 4.4$, then it decreases again. This maximum value of the sound pressure is higher than the maximum value exhibited in the post-coincidence resonance. Figure (4.6) shows the spectra of maximum sound pressure points in the pre-coincidence and post-coincidence ranges.

It is observed that the pre-coincidence resonance has been excited while the vortex shedding frequency was still far below the resonance frequency. This can be explained as the sum of two effects. The turbulence intensity, which covers a broad

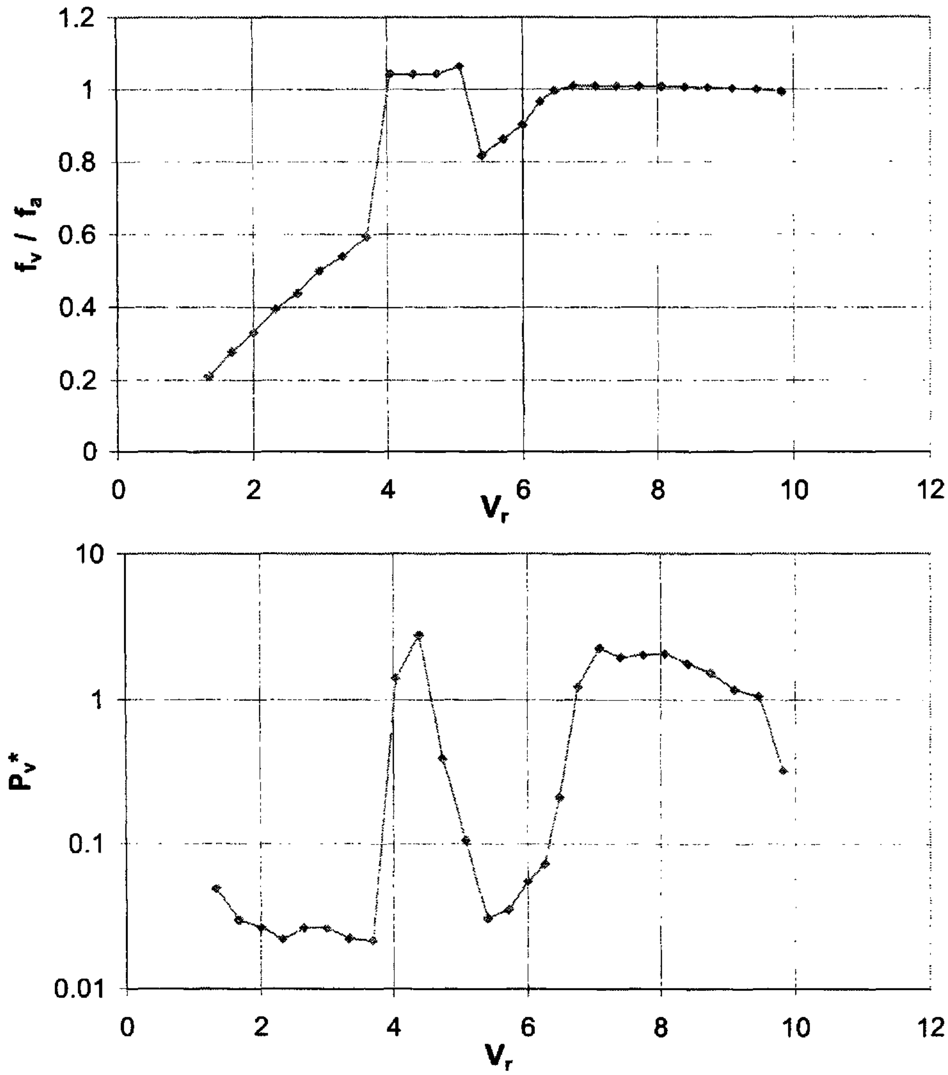

Figure 4.5: Variation of f_v/f_a and P_v^* as functions of V_r for a tandem bare cylinders of type I with a spacing ratio S/D = 2.

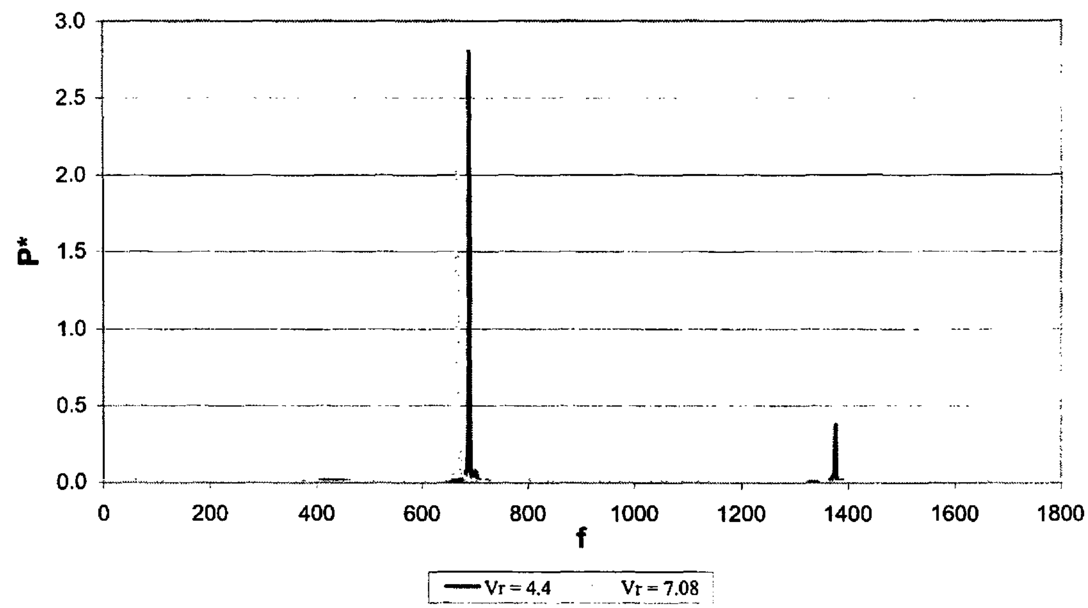

Figure 4.6: Dimensionless pressure spectra for maximum sound pressure points at the pre-coincidence and post-coincidence resonance ranges for tandem bare cylinders of type I with a spacing ratio $S/D = 2$.

band of frequencies including the first mode frequency, was high enough to excite the first mode. On the other hand, the vorticity concentrations that have been observed by Lin *et al.* (2002) at the sides of the gap may have the opportunity to grow larger because of the larger spacing ratio. These vorticity concentrations are buffeting the downstream cylinder at a frequency larger than the vortex shedding frequency. The sound generated by buffeting the downstream cylinder may be able to excite the first acoustic mode at a lower reduced velocity.

However, for the post-coincidence resonance, it seems that the sound pressure produced by vortex shedding from the downstream cylinder, becomes the main source which excites the first acoustic mode. This means that the excitation in the pre-coincidence and the post-coincidence lock-in probably results from two different mechanisms.

4.1.2.3 Tandem Bare Cylinders with S/D = 3

The flow regime for the low turbulence case is characterized by unstable vortices in the gap between the two cylinders with a reattachment of the shear layer onto the downstream cylinder. The vortex shedding in the gap between the cylinders is observed intermittently (Igarashi, 1981).

Because of the relatively high turbulence intensity in the test section, the unstable flow behavior is expected to change significantly as explained by Ljungkrona (1991). Ljungkrona observed that the drag coefficient for the downstream cylinder changes from a negative to a positive value which indicates a change in the flow pattern. Hence, it is expected that there will be vortex shedding in the front of the downstream cylinder.

Figure (4.7) shows the results of the case with $S/D = 3$. The frequency of the vortex shedding is increasing linearly with the velocity until $V_r = 4.4$. This means that the flow pattern probably was the same before resonance.

Resonance has been observed at this spacing as well. The first mode excitation and the lock-in starts early at $V_r = 4.7$. This early excitation can be initiated by the flow pattern in the gap between the cylinders. However, the pressure levels are different from the case of $S/D = 2$. This difference may result from the change in the size of vorticity concentrations which are allowed to grow larger due to the larger spacing ratio.

The lock-in range is divided by the coincidence point between f_v and f_a as in the case of $S/D = 2$. In the pre-coincidence range, the values of sound pressure are higher than those in the post-coincidence lock-in range. At frequency coincidence, the sound pressure drops to a relatively very low value and the lock-in no longer exists. Then, it increases again as the velocity increases. This drop may be caused by a change in the excitation mechanism. A similar feature was observed in the case of tandem plates (Stoneman, 1988) and in the case of tube bundles (Oengören, 1992). Figure (4.8) shows the non-dimensionalized pressure spectra (P^*) at the coincidence and just before it. The drop in P^* was more than 20 times as can be seen from the figure.

At $V_r = 8.4$, the third mode is excited and the vortex shedding frequency jumps from the lock-in with the first mode to the lock-in with the third mode. P_v^* is maximum at the onset of the third mode excitation then it decreases with an increase in the velocity.

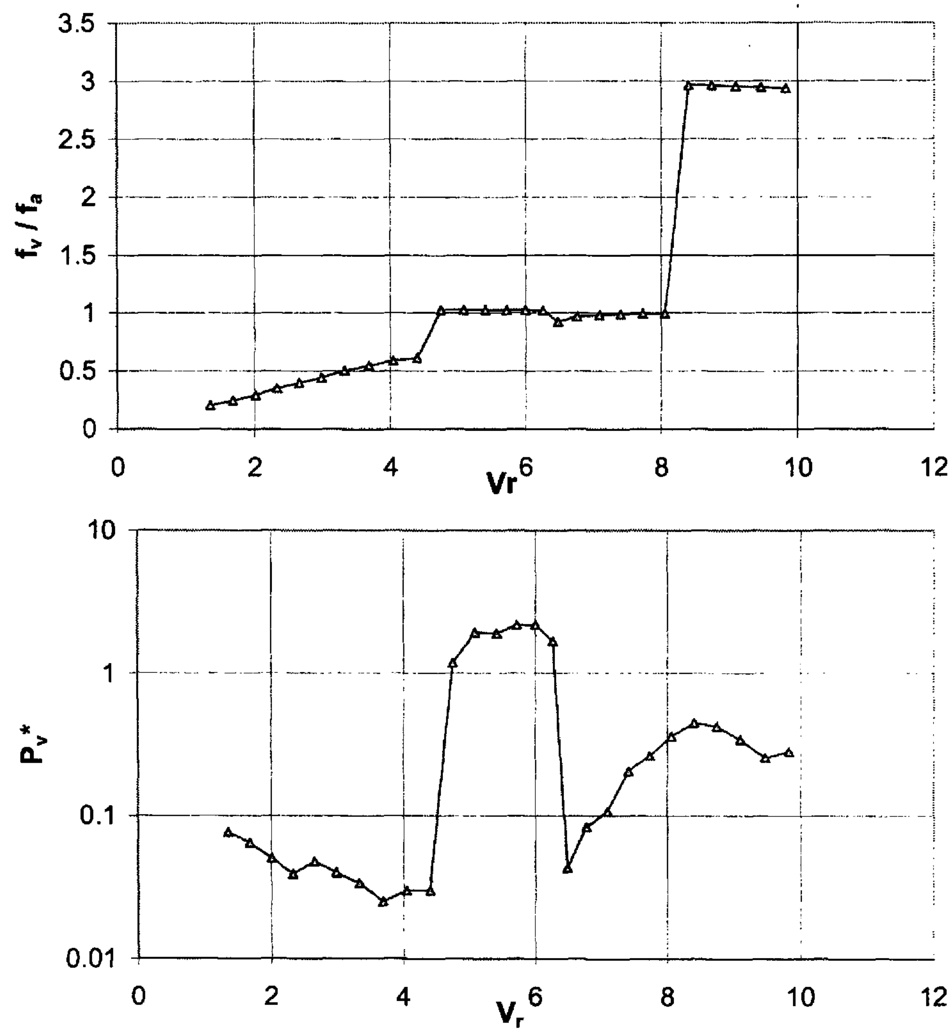

Figure 4.7: Variation in f_v/f_a and P^* as functions of V_r for a tandem bare cylinders of type I with a spacing ratio S/D = 3.

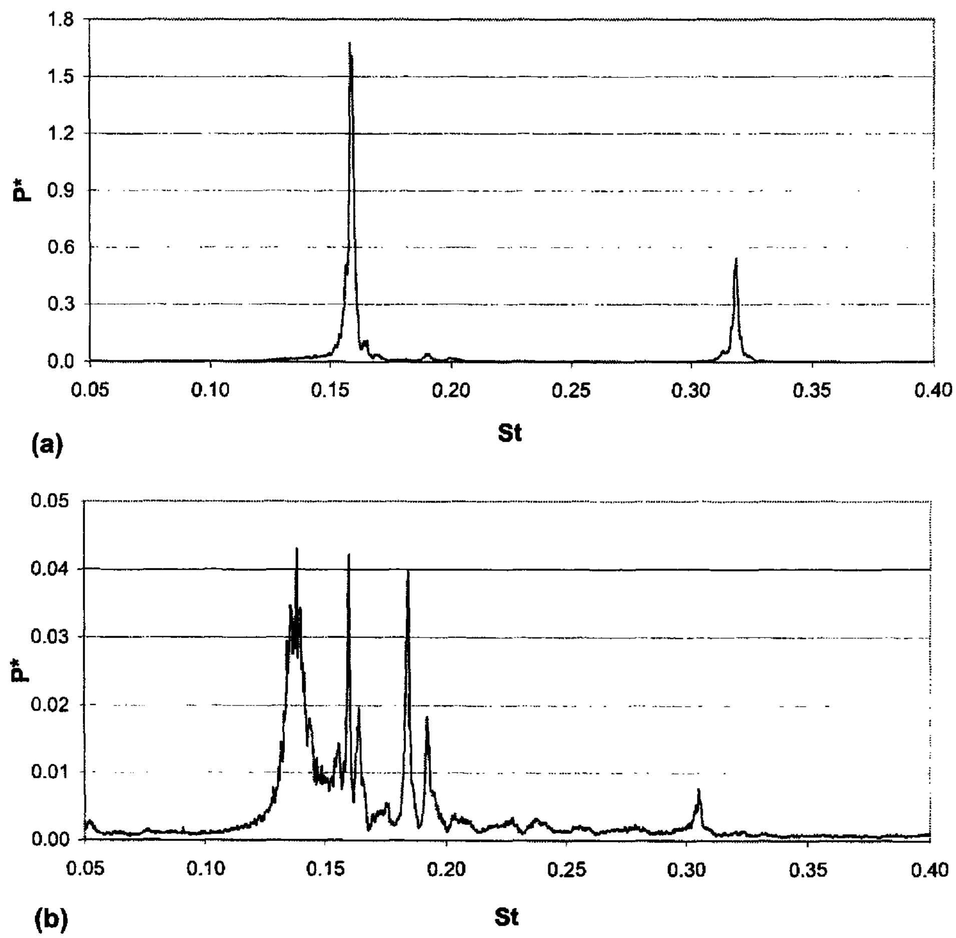

Figure 4.8: Dimensionless pressure spectra for tandem bare cylinders of type I with $S/D = 3$ (a) Just before frequency coincidence, $V_r = 6.26$; (b) At the frequency coincidence, $V_r = 6.48$.

4.1.3 Comparison

The results of single and tandem cylinders are compared in figure (4.9). It is observed that P_v^* for the tandem cylinders is higher than P_v^* in the case of a single cylinder at resonance. However, P_v^* before resonance is higher in the case of a single cylinder than it is in the case of tandem cylinders with $S/D = 1.5$ and $S/D = 2$. It is also higher than or equal to P_v^* for $S/D = 3$ before the resonance.

It is observed also that P_v^* is higher in case of $S/D = 3$ than in the other cases before resonance. This can be explained, as shown by Lin *et al.* (2002), by the increase in the Kelvin-Helmholtz vortices scale in the shear layer in the gap between the cylinders which eventually buffet the surface of the downstream cylinder. The scale of these vortices is increasing with the spacing ratio S/D between the cylinders. The loading due to buffeting increases with the increase in the scale of the vortices which increases the sound pressure as well.

The lock-in of the vortex shedding frequency to the acoustic natural frequency has different characteristics for each spacing. In the case of $S/D = 2$ and $S/D = 3$, The lock-in starts at $V_r = 4.4$ and $V_r = 4.7$ which is earlier than the lock-in in the case of the single cylinder and the tandem cylinders of $S/D = 1.5$ for which the resonance starts at $V_r = 6.4$. It is observed also that the third mode was excited in the case of $S/D = 3$ but it was not excited in the other cases.

Pre-coincidence lock-in range of the first mode resonance for $S/D = 3$ is wider and stronger than that for $S/D = 2$. Although the dimensionless pressure P_v^* reaches a higher maximum value in the case of $S/D = 2$, it raises to this maximum value in a slower rate than in the case of $S/D = 3$. The latter rises

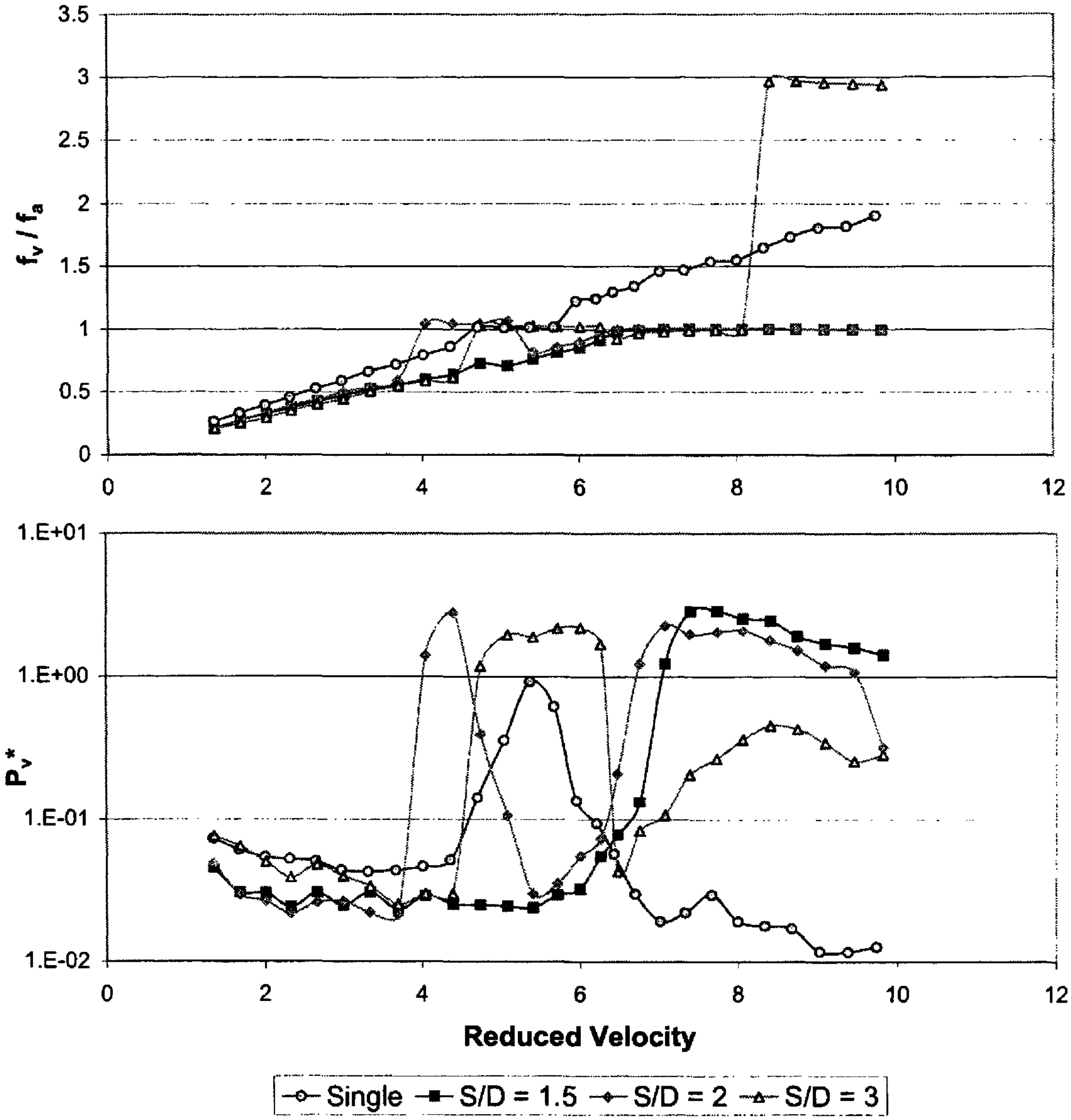

Figure 4.9: Comparison between the change in f_v/f_a and P_v^* as a function of V_r for single and tandem bare cylinders.

sharply at the beginning of the lock-in range to a high pressure value and maintains this high value until the coincidence between the vortex shedding frequency and the acoustic natural frequency, where it drops sharply to a small value. Thus, the wider pre-coincidence lock-in range in the case of $S/D = 3$ is caused by the high sound pressure level it generates which is capable of entraining the vortex shedding and thereby sustaining the resonance. It is observed also that the maximum value of the sound pressure at the pre-coincidence resonance ($V_r = 4.4$) is higher than the maximum sound pressure at any reduced velocity for the single and the tandem cylinders.

In the post-coincidence lock-in range, the sound pressure for $S/D = 3$ is much lower than the sound pressure for the other two tandem cylinders cases. The sound pressure at the third mode are also lower than the corresponding pressure at the same reduced velocity. It can be seen clearly that the low post-coincidence pressure makes it possible for the vortex shedding to get out of lock-in with the first mode and excite the third mode, while the first mode for the same reduced velocity range was still strong for the other cases.

The lock-in in the post-coincidence range is weaker in the case of $S/D = 2$ than in the case of $S/D = 1.5$. The values of the sound pressure are less than the corresponding values for $S/D = 1.5$. The sound pressure drops significantly at the end of the lock-in for $S/D = 2$ which gives an indication that it starts to come out of the lock-in. It is expected, if more data points were obtained at higher reduced velocities, that the vortex shedding would come out of resonance before this happens for $S/D = 1.5$.

Table 4.1: Strouhal number for the single and the tandem cylinders

	Single Cylinder	Tandem Cylinders		
		$S/D = 1.5$	$S/D = 2$	$S/D = 3$
Bare Cylinder Type I	0.198	0.15	0.162	0.145

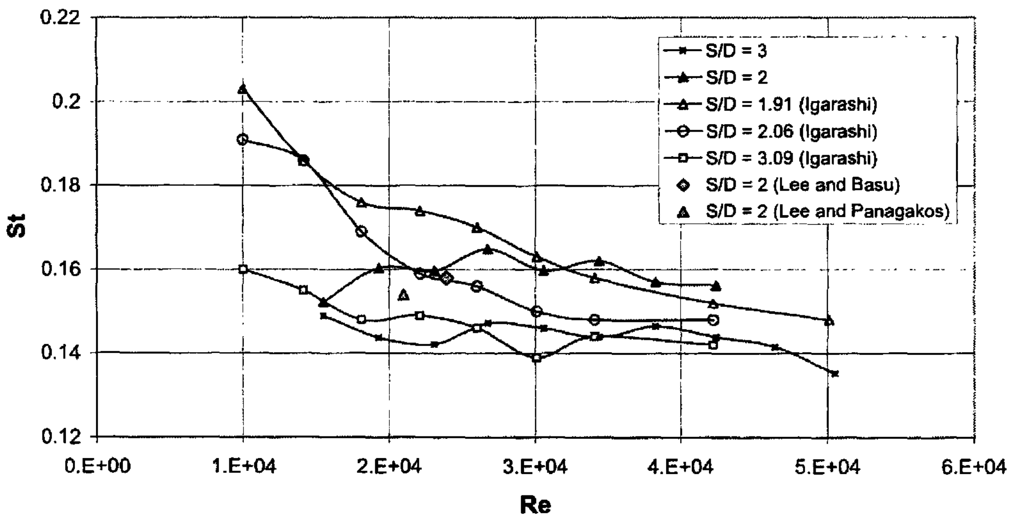

Figure 4.10: Comparison between the Strouhal number from the present study and the literature for tandem bare cylinders.

It is observed generally that the increase in the spacing ratio, reduces the sound pressures at the vortex shedding frequency inside the lock in region.

4.1.4 Strouhal Number for single and tandem bare cylinders

The values of the vortex shedding frequency have been determined from the spectra of the sound pressure measured by the microphone. The Strouhal number values were based on the values of vortex shedding frequencies measured outside the lock-in range. It has been observed that the relationship between the non-dimensionalized frequency (f_v/f_a) and the reduced velocity (V_r) is approximately linear. Hence, from the best-fit linear equation for each of the different cases investigated, the Strouhal number has been determined as shown in table (4.1).

The Strouhal number for the single bare cylinder generally agrees with the Strouhal number values in the literature (figure 2.4). The Strouhal number for the tandem bare cylinders also generally compares well with the Strouhal number in the literature as shown in figure (4.10).

The observed differences in the case of tandem cylinders are basically due to differences between the experimental conditions which have an effect on the Strouhal number as explained earlier. The most important parameters that may have significant effects are the turbulence intensity which was higher than for other cases shown in figure (4.10) and the aspect ratio which was different for each of the cases presented. Also, there are small differences between the spacing ratios.

The difference between the Strouhal number for $S/D = 2$ and that of Igarashi for $S/D = 1.91$ and $S/D = 2.06$ is not only because of the difference in the spacing ratio. The difference is most probably due to the higher turbulence intensity which affects the unstable flow regime at this spacing ratio. The high turbulence intensity makes the flow pattern the same for the range of Reynolds number of interest while the pattern is changing in the case of low turbulence with the increase in the Reynolds number as explained by Igarashi (1981).

4.2 Finned Cylinders

The measurements on the finned cylinders revealed significant effects of the fins on the vortex shedding and the behavior of the flow. In order to investigate these effects, measurements were done on cylinders with three different fin densities. The spacing ratio, based on the finned cylinders effective diameter, was changed to investigate the effect of the spacing on the vortex shedding and acoustic resonance. In this section, these measurements will be compared with those of the bare cylinders. Both the pressure measurements and the velocity measurements will be presented in detail.

4.2.1 Single Finned Cylinders

4.2.1.1 Pressure Measurements

Figure (4.11) shows the change in the non-dimensionalized vortex shedding frequency (f_v/f_a) and the non-dimensionalized sound pressure (P_v^*) at the vortex shedding frequency as functions of reduced velocity (V_r) for single bare and finned cylinders.

The sound pressure at vortex shedding frequency (P_v^*) before resonance is much higher for the bare cylinders than it is for the finned cylinders (figure 4.11). This is due to the fins that reduce the strength of the vortex shedding by disrupting the flow over the cylinder. This results in higher broadband turbulence levels in the case of finned cylinders than the bare cylinder as shown in figure (4.12).

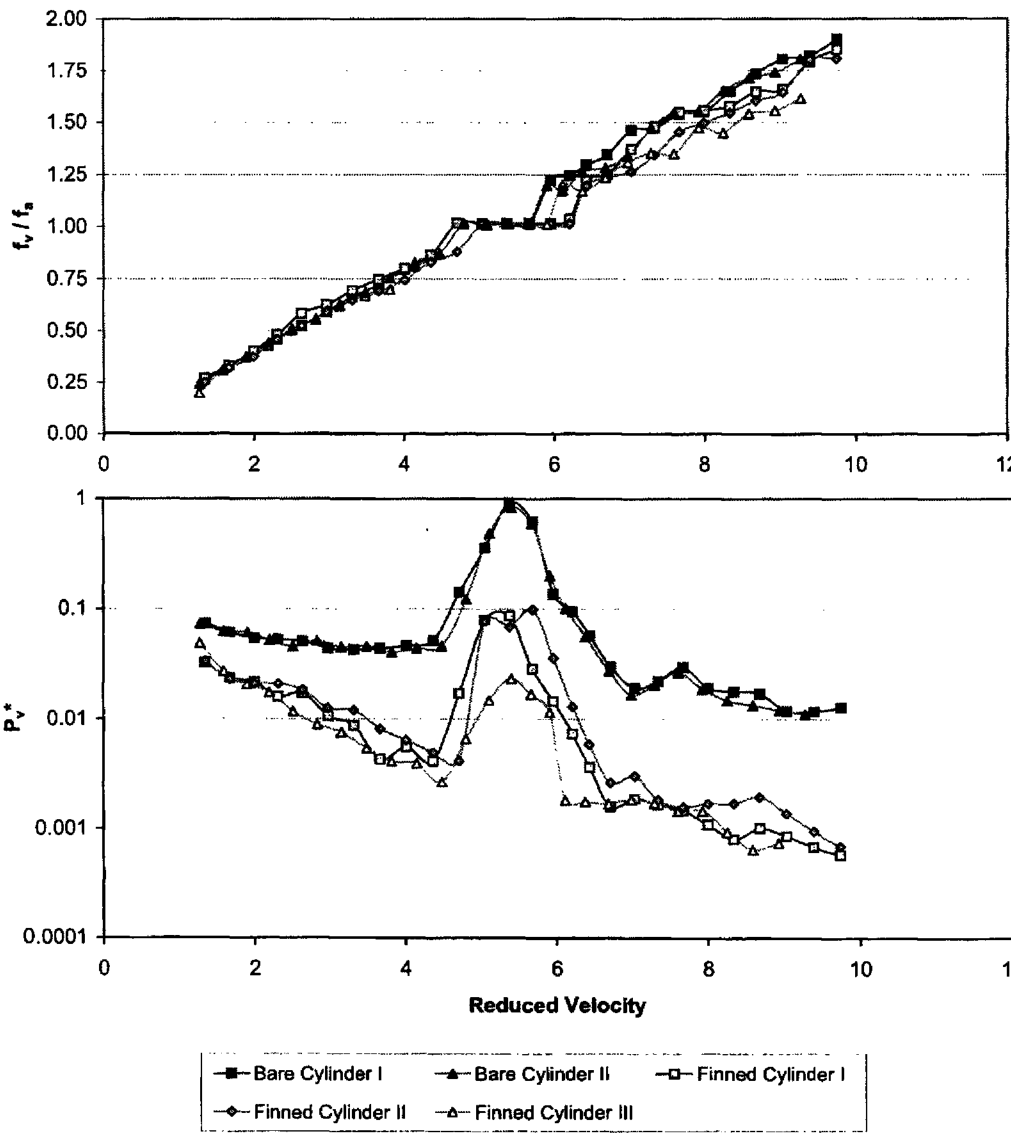

Figure 4.11: Variation of f_v/f_a and P_v^* with V_r for single cylinders.

The difference in the magnitude of the sound pressure P_v between the finned and the bare cylinders is increasing with the increase in the velocity before resonance which indicates that the effect of the fins on disrupting the flow becomes more significant with the increase in Reynolds number. It is observed also that the level of broadband pressure is increasing with the increase in the velocity as shown in figure (4.13).

No specific trend has been observed for the change in the sound pressure with the increase in the fin density before resonance. However, it is observed that the broadband fluctuating pressure measured by the microphone in the case of finned cylinder III is higher than the broad band pressure in all of the other cases as shown in figure (4.12). This confirms the effect of the fins on disorganizing the flow which becomes more pronounced for the highest fin density of finned cylinder III.

The sound pressure at resonance in the case of finned cylinders is less than that for the bare cylinders. There is no significant difference in the sound pressure levels between the finned cylinders I and II. However, there is a significant difference in the case of finned cylinders III. The sound pressure at resonance is significantly less than the other cases. This decrease in resonance intensity can be explained by the effect of the high density fins which disrupt the vortex shedding at resonance and hence, makes the resonance weaker (figure 4.14).

After resonance, P_v in the case of bare cylinders is higher than P_v for the finned cylinders. The difference between them doesn't change with the increase in the velocity. The level of broadband pressure fluctuations is still higher for finned

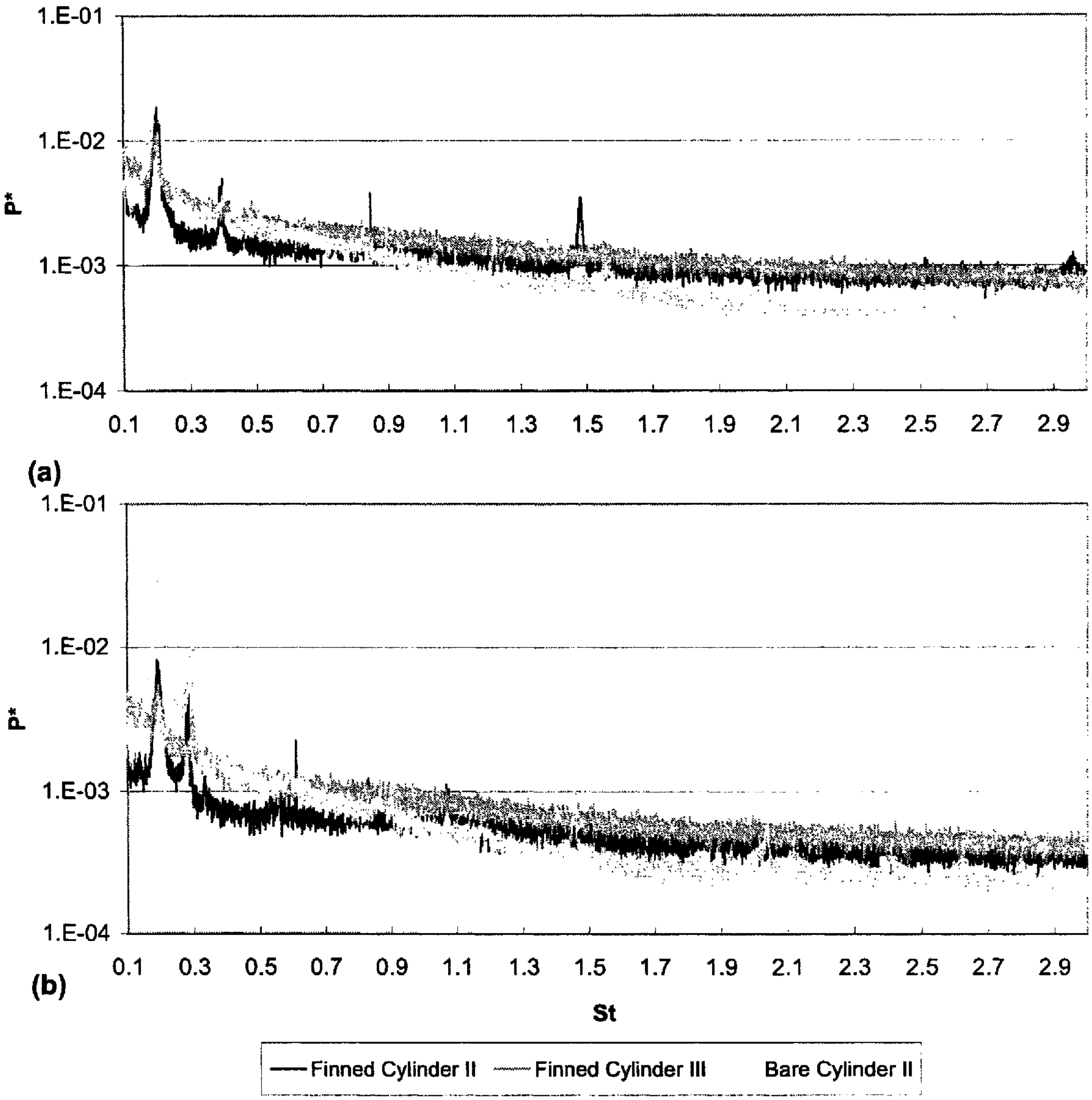

Figure 4.12: Typical pressure spectra for single cylinders: (a)$V_r = 2.51$ for the bare cylinder II and finned cylinder III; $V_r = 2.64$ for the finned cylinder II; (b)$V_r = 3.48$ for the bare cylinder II and finned cylinder III; $V_r = 3.66$ for the finned cylinder II.

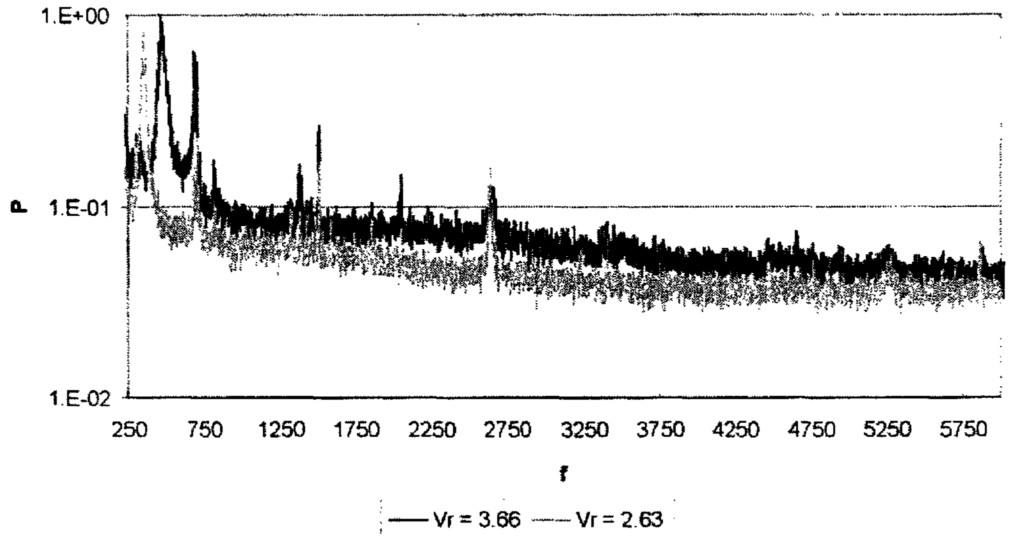

Figure 4.13: Pressure spectra for finned cylinder II at two different velocities before the onset of resonance.

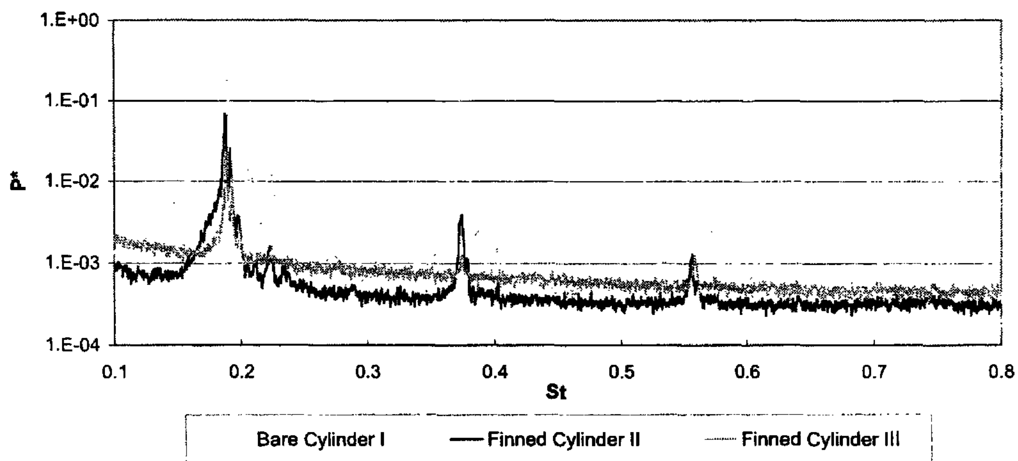

Figure 4.14: Dimensionless pressure spectra for single cylinders in case of resonance at $V_r = 5.4$.

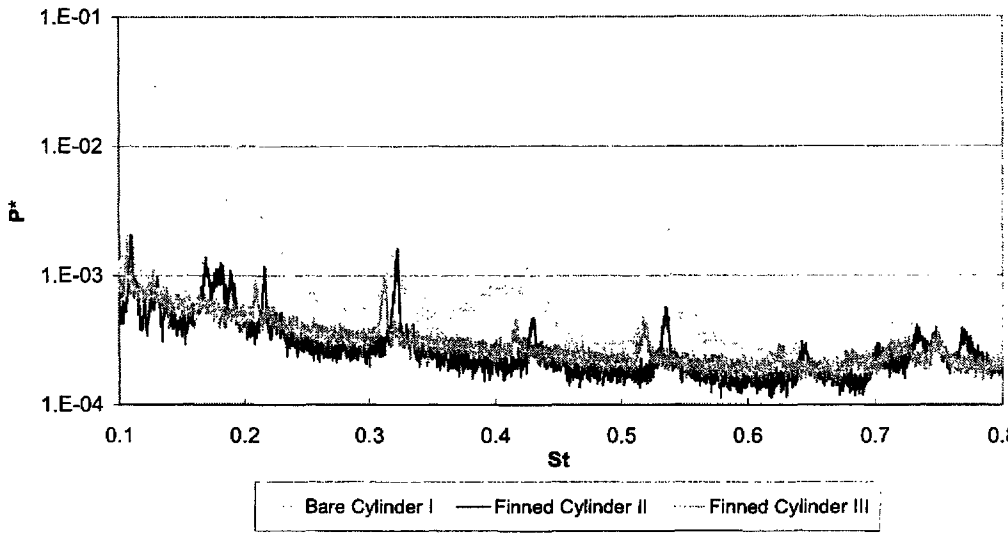

Figure 4.15: The dimensionless pressure spectrum for single cylinders after resonance; $V_r = 9.15$.

cylinder III than for the other finned cylinders, which confirms the effect of the higher fin density on increasing the broad band turbulence level (figure 4.15).

4.2.1.2 Velocity Measurements

To gain more understanding of the flow behavior over the single finned cylinders, hotwire measurements have been done at three different velocities before, during and after resonance. These measurements are intended to give more information about the effect of fins on the flow behavior. For this purpose, one finned cylinder only, of type II, has been selected as well as the bare cylinder I to compare between the flow in each case.

All velocity measurements were carried out at a distance $x/D_e = 2.5$ downstream of the cylinder. The mean velocity profile as well as the turbulence intensity

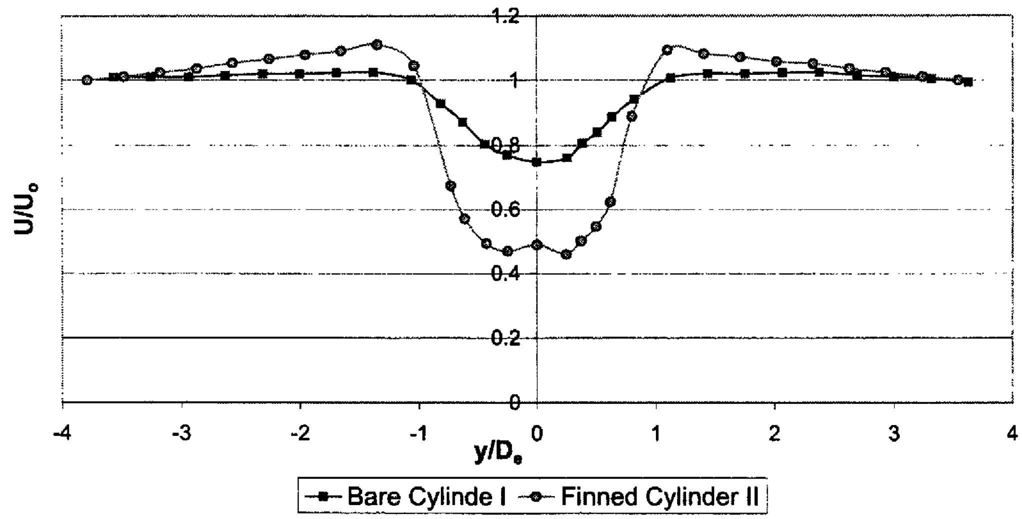

Figure 4.16: Dimensionless mean velocity profiles for single cylinders at $x/D_e = 2.5$ for $Re = 3.7 \times 10^4$ ($V_r = 3.2$).

profile have been obtained for each cylinder. From measurements of velocity spectra, the turbulence intensity due to the fundamental vortex shedding component has been determined. The results will be presented in detail in this section.

Velocity Profiles at $\mathbf{Re = 3.7 \times 10^4}$

Measurements were done at Reynolds number of 3.7×10^4 ($V_r = 3.2$) on the finned cylinder II as well as bare cylinder I at $x/D_e = 2.5$ downstream of the cylinders. Figure (4.16) shows the mean velocity, V, non-dimensionalized by the free stream velocity, V_o, against the transverse distance measured from the cylinder centerline, y, non-dimensionalized by the cylinder effective diameter, D_e.

As shown in figure (4.16), the mean velocity profiles show the quite significant effect that the fins have on the flow at this velocity. The mean velocity in the case of the finned cylinder is increasing with y/D_e until it reaches its maximum at

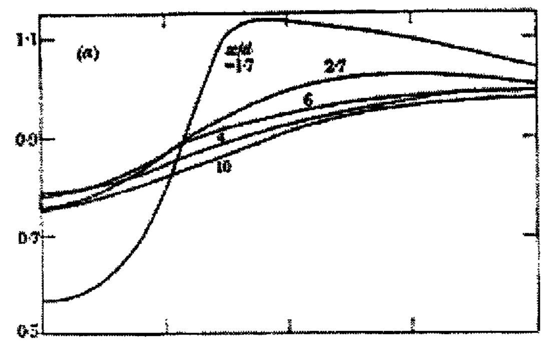

Figure 4.17: Dimensionless mean velocity profiles at different positions downstream of a single bare cylinder at $Re = 1.6 \times 10^4$ (Bloor and Gerrard, 1966).

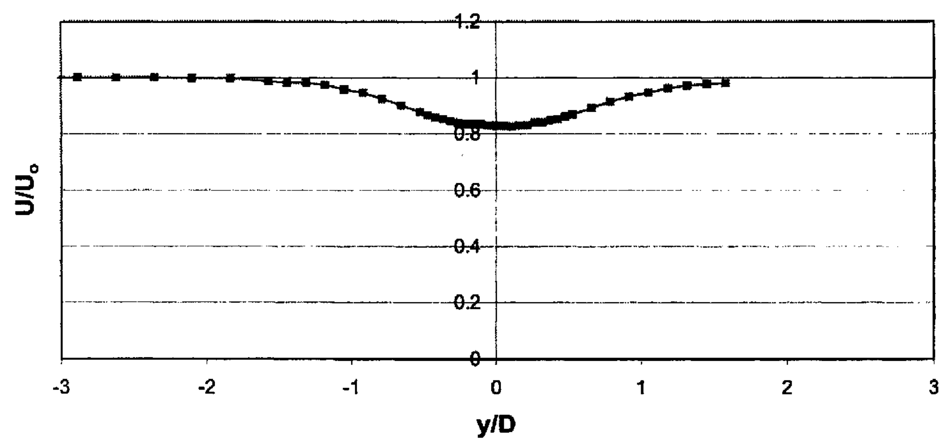

Figure 4.18: Dimensionless mean velocity profile for a single bare cylinder at $x/D_e = 2.5$ for $Re = 4.69 \times 10^4$ (Jebhodsingh, 2002).

$y/D_e = \pm 1.1$ and then decreasing again. A hump was also observed in the mean velocity profile of the bare cylinder which agrees with the observation of Bloor (1966) as shown in figure (4.17). However, the mean velocity increases 11% above the approach velocity in the case of the finned cylinder while it is less than 1.1% in the case of bare cylinder. This difference may be explained by the larger velocity deficit in case of the finned cylinders which results in increasing the flow velocity

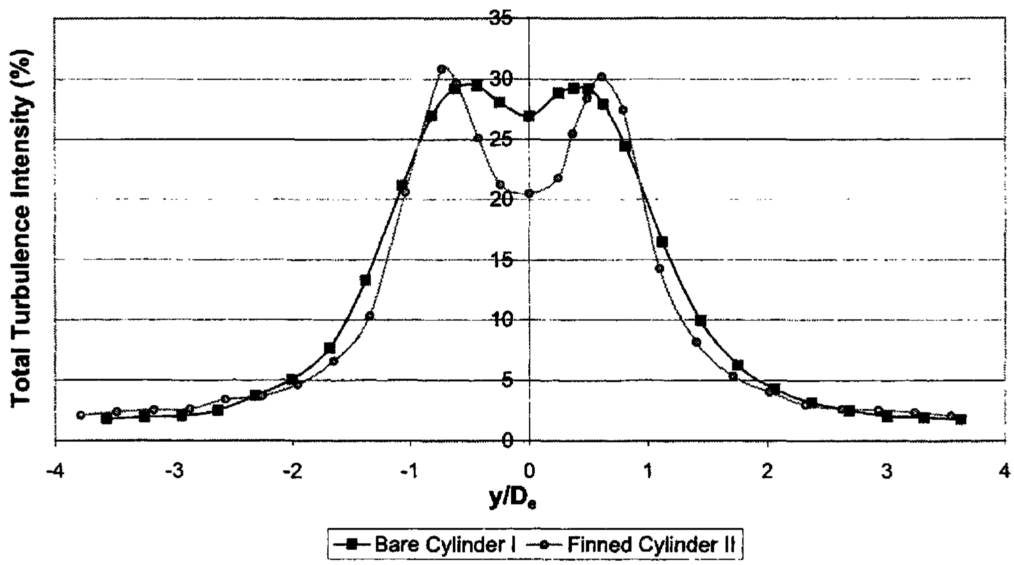

Figure 4.19: Total turbulence intensity profiles for single cylinders at $x/D_e = 2.5$ for $Re = 3.7 \times 10^4$ ($V_r = 3.2$).

more than the case of the bare cylinders at the location of the hump. The mean velocity profiles for the bare cylinder generally compare well with that of Bloor (1966) and Jebohdsingh (2002) (Figures 4.17 and 4.18).

The mean velocity decreases in the case of finned cylinder with a higher rate than the bare cylinder until it reaches its minimum. The minimum value for the mean velocity in the case of finned cylinder is $0.46\,V_o$ which is lower than the bare cylinder($0.75\,V_o$). The minimum value for the mean velocity in the case of bare cylinder is at the cylinder centerline plane while that for the finned is at ± 0.46. There is a slight increase in the mean velocity at $y/D_e = 0$ by nearly 2 % more than the value of the velocity minimum at $y/D_e = \pm 0.46$. This increase was not observed in case of the bare cylinder.

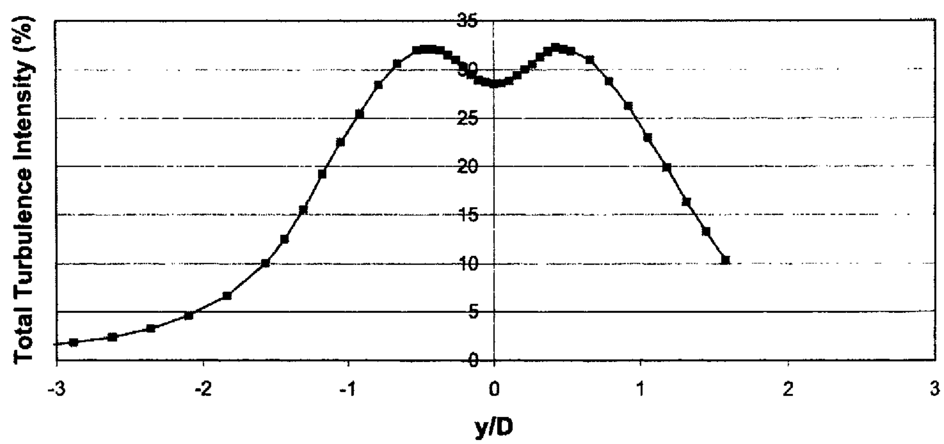

Figure 4.20: Total turbulence intensity profiles downstream of a single bare cylinder at $x/D = 2.5$ for $Re = 4.69 \times 10^4$ (Jebodhsingh, 2002).

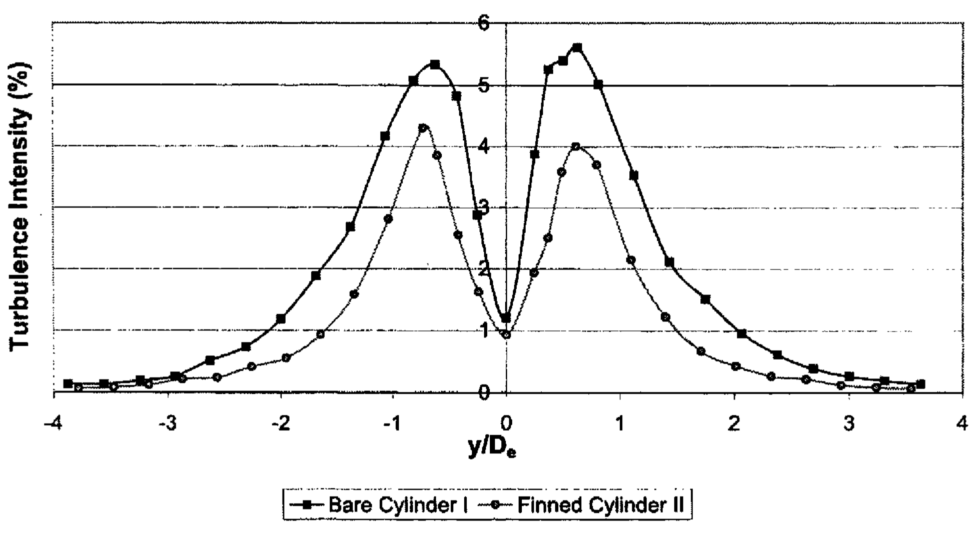

Figure 4.21: Turbulence intensity profiles of single cylinders due to fundamental vortex shedding component at $x/D_e = 2.5$ for $Re = 3.7 \times 10^4$ ($V_r = 3.2$).

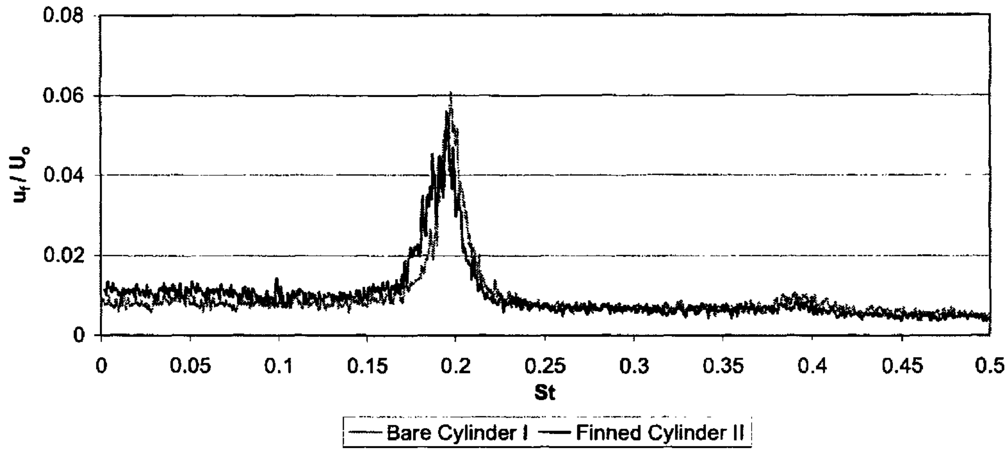

Figure 4.22: Dimensionless velocity spectra at the maximum turbulence intensity point at $x/D = 2.5$ for single bare and finned cylinders.

Figure (4.19) shows the total turbulence intensity profiles. The bare cylinder profile compares well with that of Jebohdsingh (2002) (figure 4.20). It is observed that the drop in the turbulence intensity level near the wake centerline plane was higher in the case of the finned cylinder.

Figure (4.21) shows the turbulence intensity due to the fundamental vortex shedding component (Tu_f) against y/D_e. It is observed that Tu_f in the case of the finned cylinder is less than Tu_f for the bare cylinder. This implies that the vortex strength in the case of the finned cylinder is less than the vortex strength in the case of the bare cylinder. This agrees with the higher sound pressure level measured in the case of bare cylinder which has a stronger vortex shedding and confirms the rule of the fins in disrupting the vortex shedding. Figure (4.22) shows typical velocity spectra at the maximum turbulence intensity point.

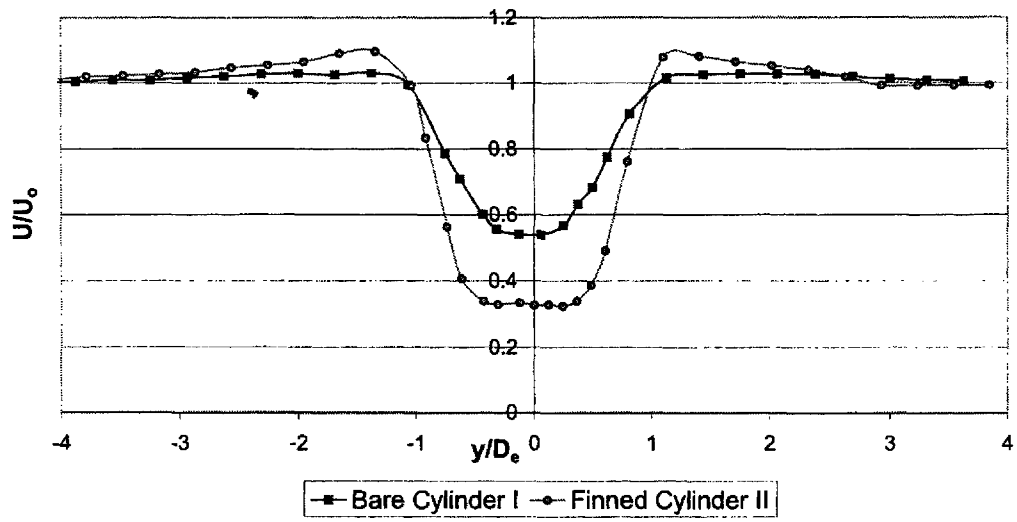

Figure 4.23: Dimensionless velocity profiles for single cylinders at $x/D_e = 2.5$ for $Re = 7.22 \times 10^4$ and $V_r = 6.2$ near the end of the lock-in range.

Velocity Profiles at Re $= 7.22 \times 10^4$

Measurements were performed at resonance, near the end of the lock-in range, for a Reynolds number of 7.22×10^4 ($V_r = 6.2$) to obtain more details about the effect of the fins on the vortex shedding at resonance.

A larger deficit in the mean velocity has been observed compared to the previous case as shown in Figure (4.23). The difference between the minimum value of the mean velocity for the bare and the finned cylinder, which is 20% of the mean velocity, is still the same as in the previous case. Also, the larger hump in case of the finned cylinder is still observed.

The mean velocity profile shows a different behavior for the finned cylinder (figure 4.23). The velocity deficit range for the finned cylinder shows a nearly constant velocity near the wake centerline over the range from $y/D_e = 0.4$ to

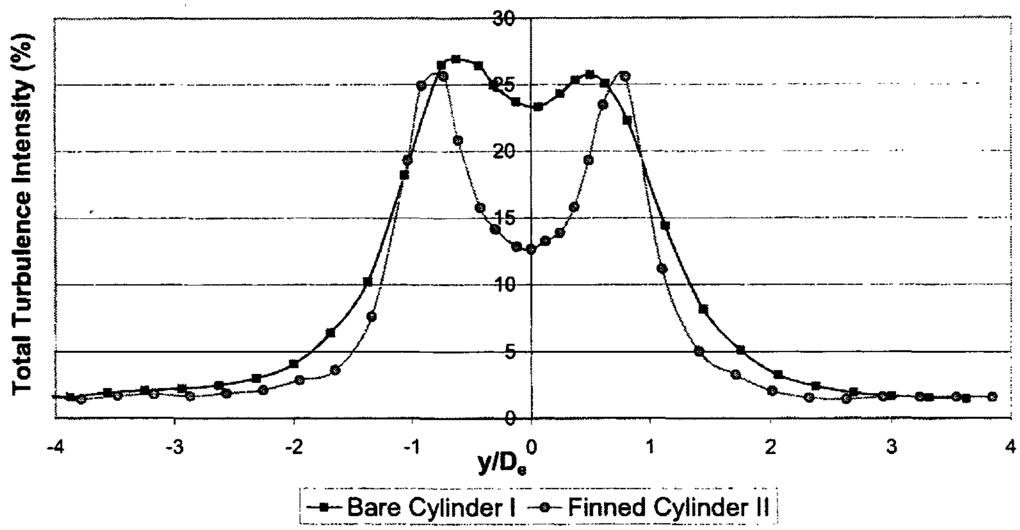

Figure 4.24: Total turbulence intensity profiles for single cylinders at $x/D_e = 2.5$ for $Re = 7.22 \times 10^4$ and $V_r = 6.3$ near the end of the lock in range.

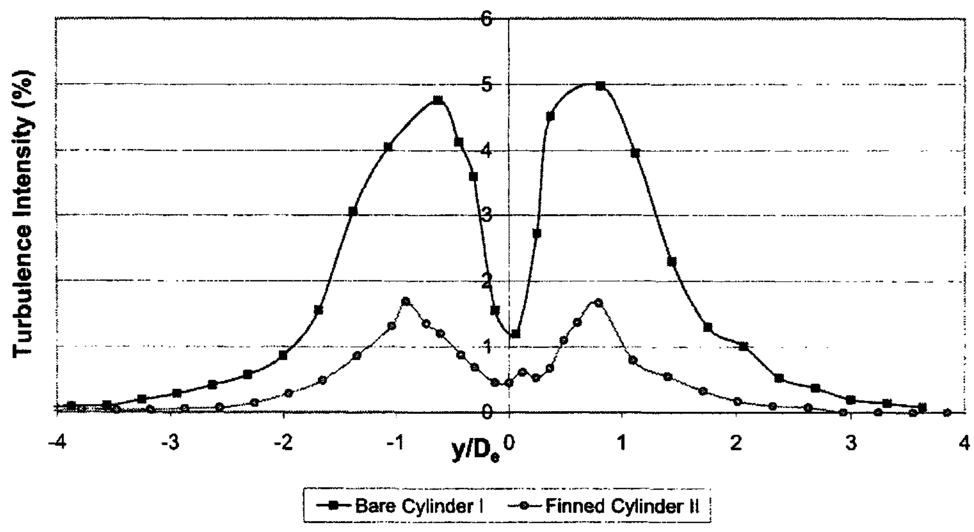

Figure 4.25: Turbulence intensity profiles for single cylinders at fundamental vortex shedding component at $x/D_e = 2.5$ for $Re = 7.22 \times 10^4$ and $V_r = 6.3$ near the end of the lock in range.

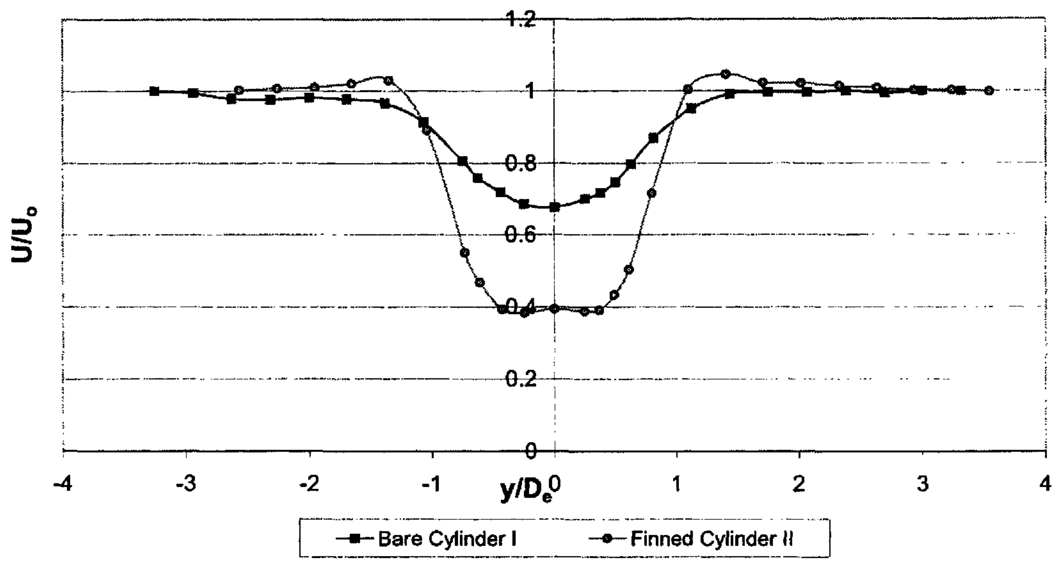

Figure 4.26: Dimensionless velocity profiles at $x/D_e = 2.5$ for $Re = 1.03 \times 10^5$ and $V_r = 9$.

$y/D_e = -0.4$. As shown in figure (4.24), the drop at the middle of the total turbulence intensity profile in the case of the finned cylinder is higher than the bare cylinder as was observed in the previous case.

The profile of the turbulence intensity due to the fundamental vortex shedding frequency (Tu_f) is shown in figure (4.25). It is observed that Tu_f in case of the finned cylinder is significantly less than Tu_f for the bare cylinder. This agrees with the microphone measurements which shows that the resonance in the case of the bare cylinder was much stronger than the resonance for the finned cylinder. The effect of fins on disrupting the flow seems to continue effective in the case of resonance.

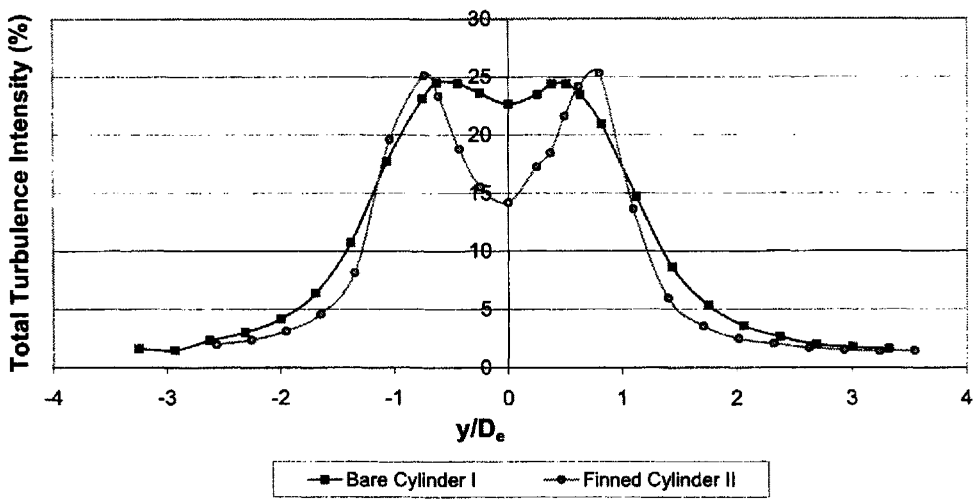

Figure 4.27: Total turbulence intensity profiles at $x/D_e = 2.5$ for $Re = 1.03 \times 10^5$ and $V_r = 9$.

Velocity Profiles at $\mathbf{Re = 1.03 \times 10^5}$

Measurements were also conducted using hotwire at a flow velocity beyond the lock-in range, $V_r = 9$. As shown in figure (4.26), the decrease in the mean velocity was less than the previous case at $V_r = 6.2$ but more than the case of $V_r = 3.23$. The deficit in the velocity profile in the wake of the cylinders becomes maximum at resonance. For all the cases, the deficit in the mean velocity was much more for the finned cylinder than that for the bare cylinder.

The hump in the case of the finned cylinder is still observed but it is much weaker than at lower V_r, while it completely disappears in the case of bare cylinder. The wake of the finned cylinder shows the same trends as in the previous case with the nearly constant velocity region near the wake centerline.

The total turbulence intensity profile was the same as in the previous cases

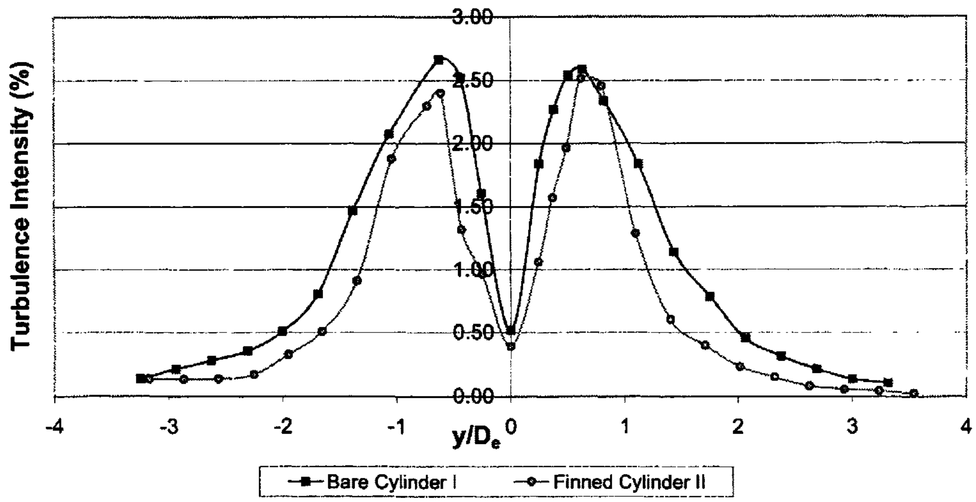

Figure 4.28: Turbulence intensity profiles due to fundamental vortex shedding component at $x/D_e = 2.5$ for $Re = 1.03 \times 10^5$ and $V_r = 9$.

with the same differences as before between the finned and the bare cylinder cases (figure 4.27).

Figure (4.28) shows that Tu_f is higher for the bare cylinder which again agrees with the measurements done using the microphone. The value of Tu_f is smaller in this case than the previous cases which means that the vortex shedding is more disrupted and becomes distributed over a wider frequency range at such high Reynolds numbers. The velocity fluctuations were more concentrated for the bare cylinder in the previous case because of the effect of the sound generated by resonance that organizes the vortex shedding and makes it more concentrated over a smaller frequency range. Figure (4.29) shows typical velocity spectra at the maximum turbulence intensity point.

There is no significant difference in the values of Tu_f for the finned cylinder

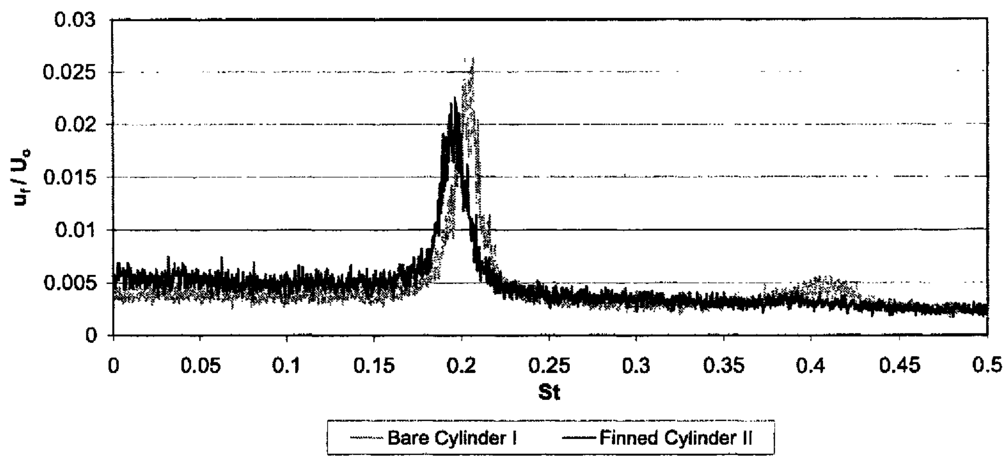

Figure 4.29: Dimensionless velocity spectra at the maximum turbulence intensity point at $x/D_e = 2.5$ for the single bare and finned cylinders at $Re = 1.03 \times 10^5$ and $V_r = 9$.

close to resonance at $V_r = 6.2$ and Tu_f at this case far after resonance. This may result from the very weak resonance in the case of finned cylinder which has a small effect on the vortex shedding process while the effect of the fins is dominant.

4.2.2 Tandem Finned Cylinders

The behavior of the flow over the tandem bare cylinders is quite different from flow over the single cylinder. It has been shown how the flow pattern is dependent on the spacing ratio and how the behavior of the flow for each flow pattern has different characteristics at resonance.

Rockwell (1998) shows the complexity of the problem of the normal vortex-body interaction when a vortex interacts normally with a thin body and gets distorted. This happens to the vortex shed from the upstream cylinder in case of the tandem finned cylinders, which is complicated initially by the effect of the fins in the upstream cylinder.

Although in the previous section, the fins are shown to weaken vortex shedding and acoustic resonance of single cylinders, these same fins seem to produce the opposite effect for tandem cylinders as will be shown in the following section. It is of interest in this section to have a general overview of how the fins affect the flow over tandem cylinders with different spacing ratios.

4.2.2.1 Tandem Cylinders With $\mathbf{S/D_e = 1.5}$

As explained earlier, the flow pattern for the tandem bare cylinders with a spacing ratio $S/D_e = 1.5$ is a synchronized flow pattern in which the vortex shed in the near wake of the downstream cylinder is synchronized with the reattachment of the other shear layer on the downstream cylinder. For the finned cylinders, there are some differences in the characteristics of the resonance between the finned and the bare cylinders which suggest that the flow pattern may have been altered by the fins. Figure (4.30) shows the change in the dimensionless frequency and the dimensionless sound pressure at vortex shedding frequency with the reduced velocity.

Before resonance, the frequency of vortex shedding is increasing linearly with the velocity for the all cases which indicates that the flow patterns probably don't change before resonance. It is observed that P_v^* is higher for the finned cylinders than that for the bare cylinders which is contrary to the case of single cylinders (figure 4.31 and 4.32). This may be due to the enhancement in the vortex shedding process due to a stronger feedback mechanism from the vortices interacting with the downstream cylinder.

It is observed that increasing the fin density has promoted the onset of resonance. Increasing the diameter also has the effect of promoting the onset of resonance which is the case for bare cylinder II. However, the fins have a more significant effect. The resonance starts in the case of finned cylinder I before the bare cylinder II although its effective diameter is smaller than the diameter of the bare cylinder II. This confirms the fact that the effect of the fins is not solely due to an increase in the effective diameter. This early onset of resonance can be explained by the higher sound pressure which is more capable to entrain the vortex shedding at lower reduced velocities.

At resonance, it is observed that the lock-in is stronger for the bare cylinders. The lock-in gets weaker as the fin density increases. At the beginning of the lock-in, the sound pressure is the same for the bare cylinders and the finned cylinders I. However, the sound pressure starts to drop earlier in case of the finned cylinders

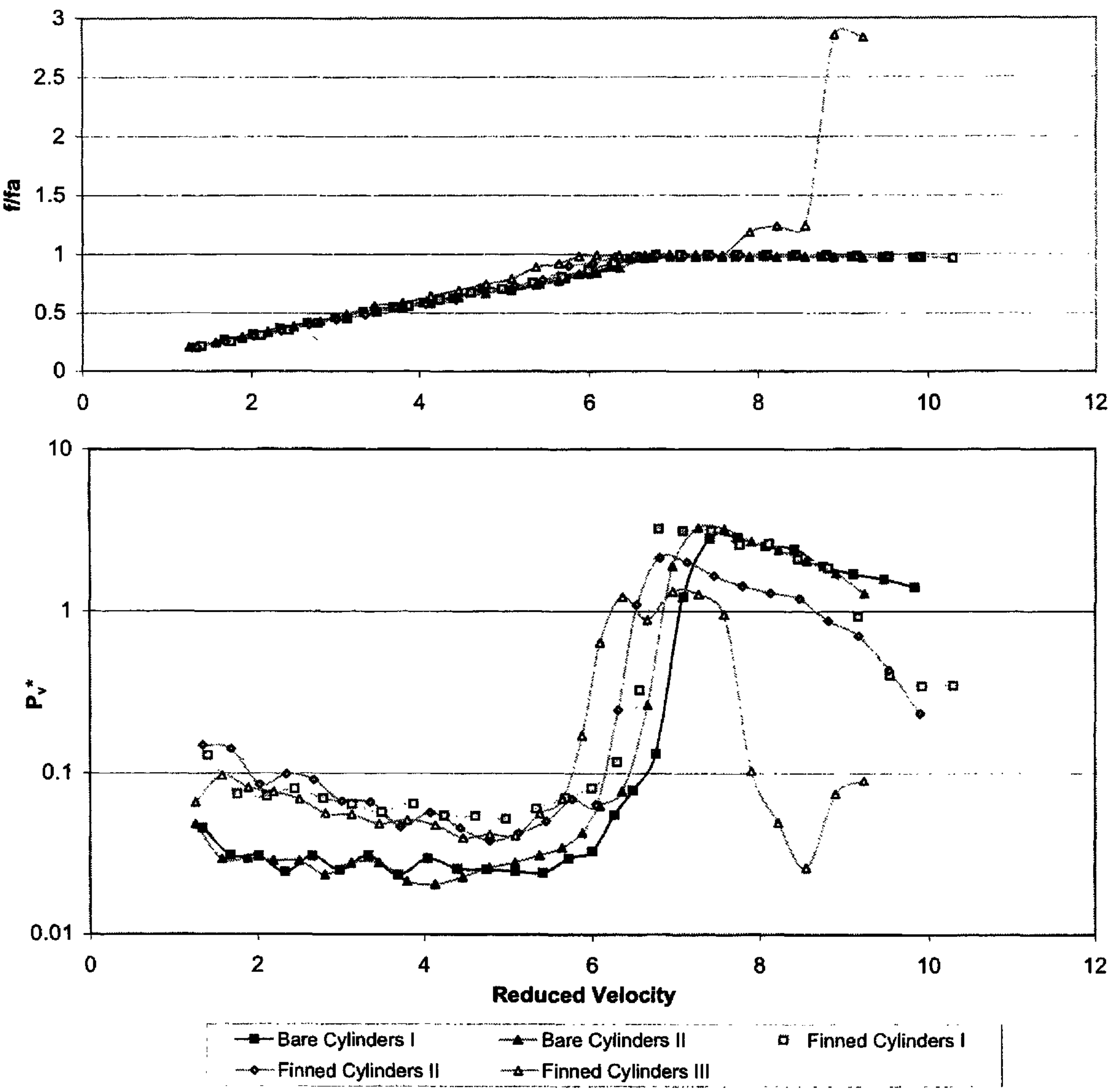

Figure 4.30: Variations of f_v/f_a and P^* with V_r for tandem cylinders with a spacing ratio $S/D_e = 1.5$.

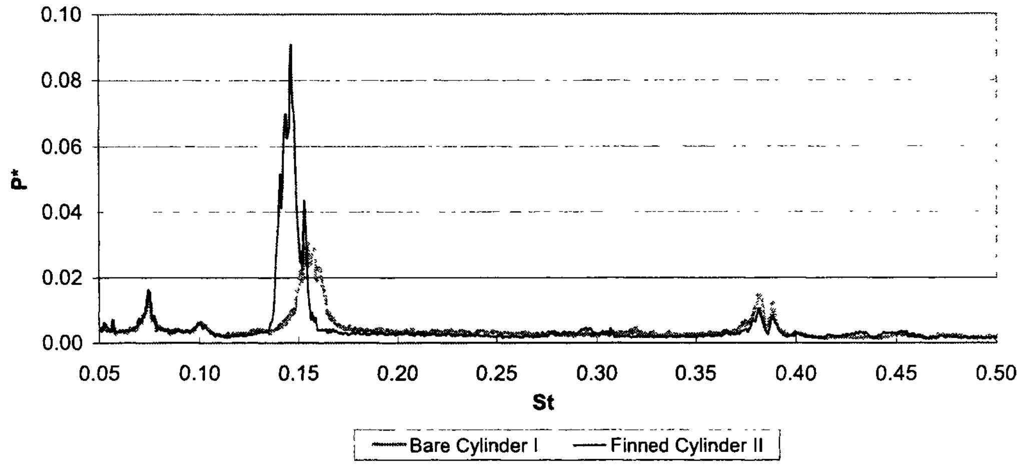

Figure 4.31: Dimensionless pressure spectra for tandem bare cylinders I and finned Cylinders II before resonance with $S/D_e = 1.5$ at $V_r = 2.66$.

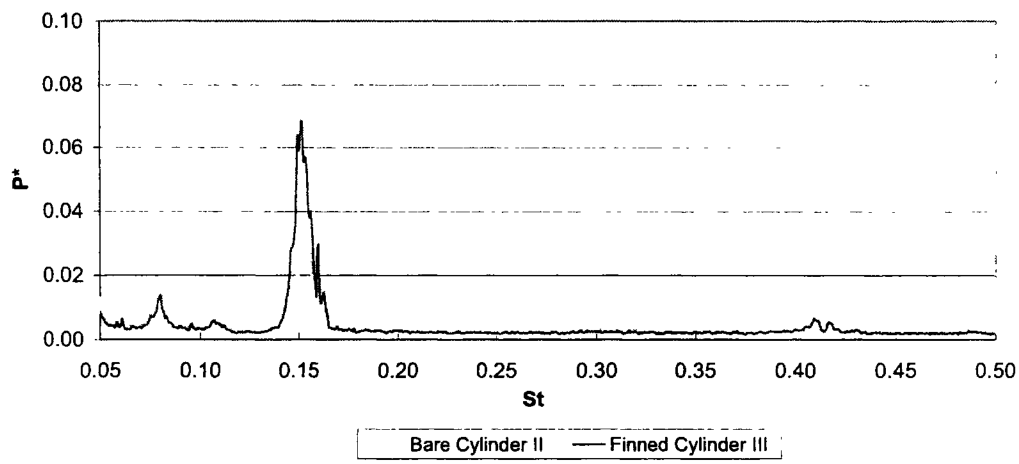

Figure 4.32: Dimensionless pressure spectra for tandem bare cylinders type II and finned Cylinders type III before resonance with $S/D_e = 1.5$ at $V_r = 2.5$.

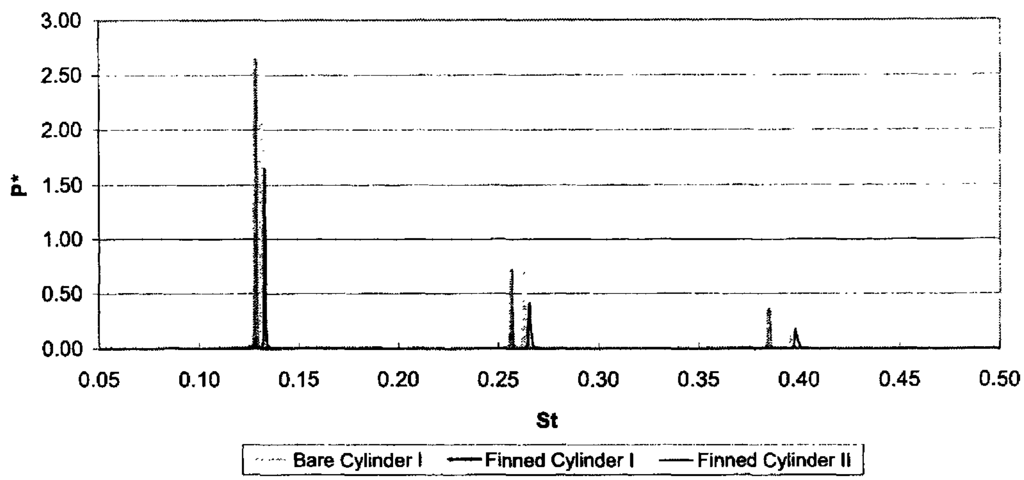

Figure 4.33: Dimensionless pressure spectra for the tandem cylinders with $S/D_e = 1.5$ at resonance ($V_r = 7.73$).

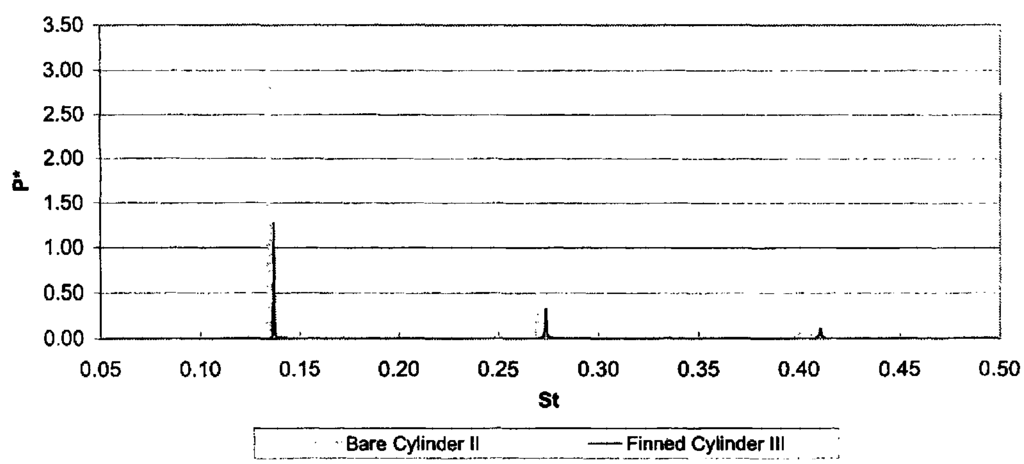

Figure 4.34: Dimensionless pressure spectra for the tandem bare cylinders with $S/D_e = 1.5$ at resonance ($V_r = 7.57$).

I at $V_r = 9.5$ which indicates that the lock-in is weaker.

Generally, it is observed that increasing the fin density weakens significantly the lock-in of the vortex shedding process with the acoustic natural frequency of the test section.

The third mode started to be excited for finned cylinder III at $V_r = 8.9$ (figure 4.35). All other tandem cylinders (bare and finned) were not able to excite the third mode. This is likely due to the higher turbulence intensity generated by the high density fins which promote the excitation of the third mode. This turbulence intensity was not enough for the other cases to excite the third mode. Also, the lock in with the first mode is stronger for the other cases which makes it more difficult for the vortex shedding to couple with the third mode.

Velocity Measurement

It is of interest to get more insight into the process of vortex shedding in the range before resonance. The sound pressure at the vortex shedding frequency was higher in the case of finned cylinders than it is in the case of bare cylinders. Velocity measurements may give more information about the differences between the finned and the bare cylinder flow. Measurements were performed on the bare cylinders I and the finned cylinders II at $Re = 3.7 \times 10^4$, which corresponds to $V_r = 3.2$, at downstream distance $x/D_e = 2.5$ from the downstream cylinder centerline.

Figure (4.36) shows the mean velocity profiles for the bare and finned cylinders. It is observed that the wake of the finned cylinders is wider than that of the bare cylinders. The deficit in the mean velocity profile for the tandem finned

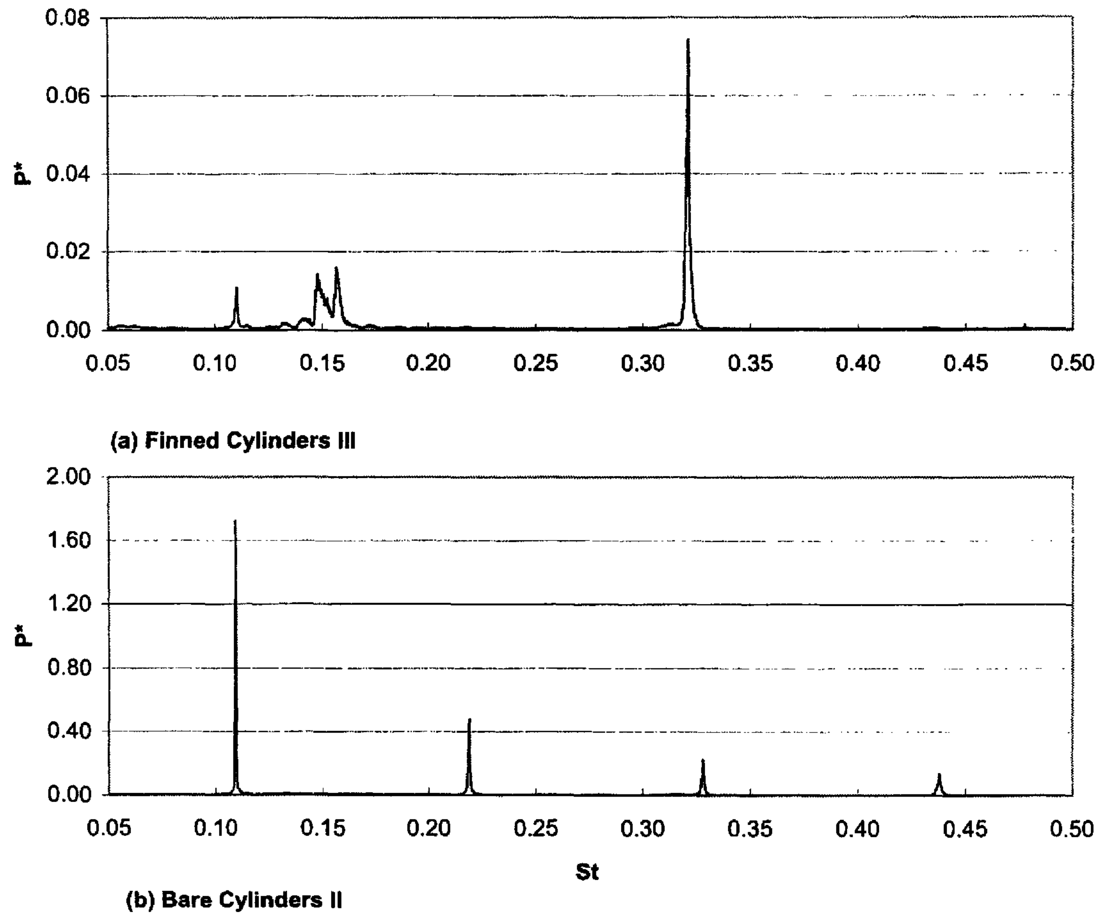

Figure 4.35: Dimensionless pressure spectra for tandem cylinders with $S/D_e = 1.5$ at $V_r = 7.57$.

cylinders is less than that in case of single finned cylinder at the same Reynolds number as shown in figure (4.37). The deficit in the mean velocity is also less than that for the all cases of the single cylinders, wether finned or bare, that have been investigated in this study. The wake is wider also than all of the other cases which shows the significant change in the flow characteristics in this case. The mean velocity is nearly constant over a very wide range from $+0.8$ to -0.8.

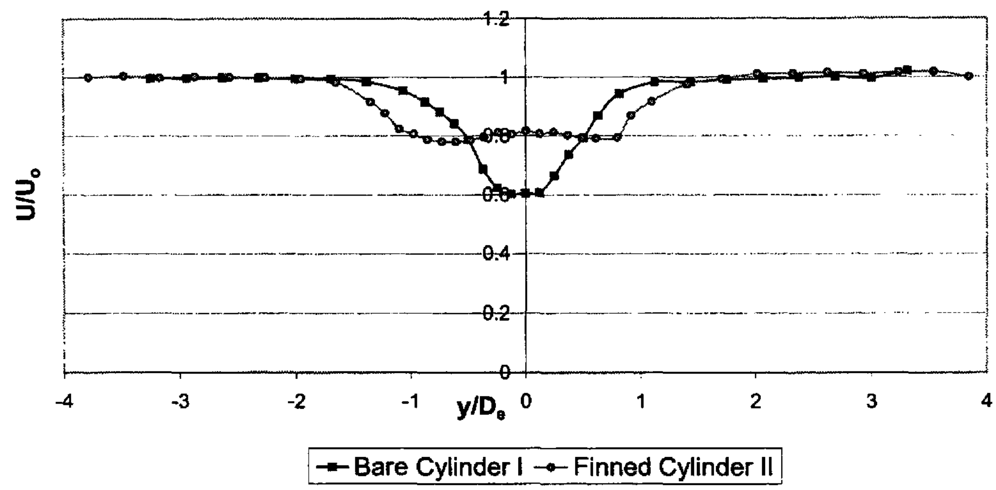

Figure 4.36: Dimensionless mean velocity profiles for two cylinders in tandem with $S/D_e = 1.5$ at $x/D_e = 2.5$ for $Re = 3.7 \times 10^4$, $V_r = 3.34$.

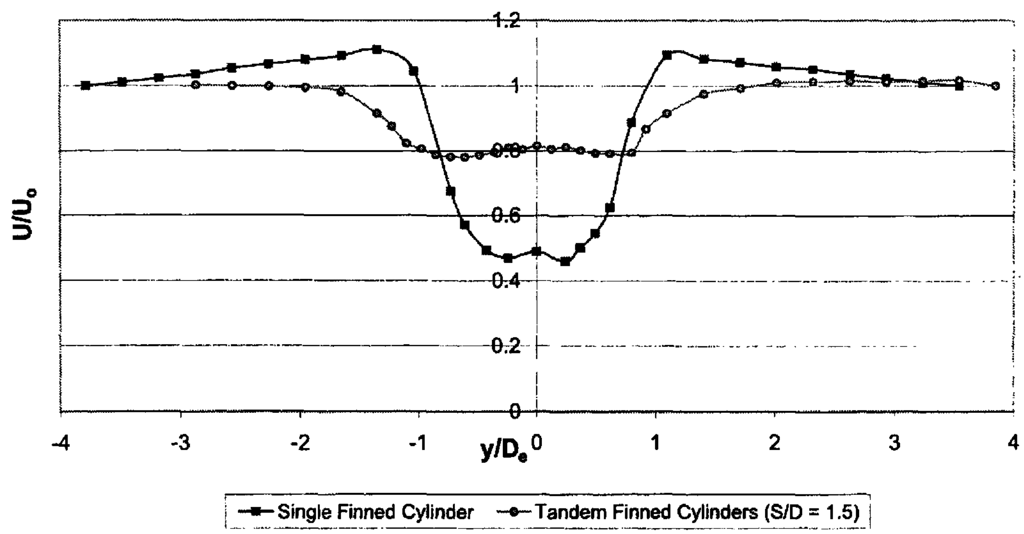

Figure 4.37: Dimensionless mean velocity profiles for finned cylinders II at $x/D_e = 2.5$ and $Re = 3.7 \times 10^4$, $V_r = 3.34$.

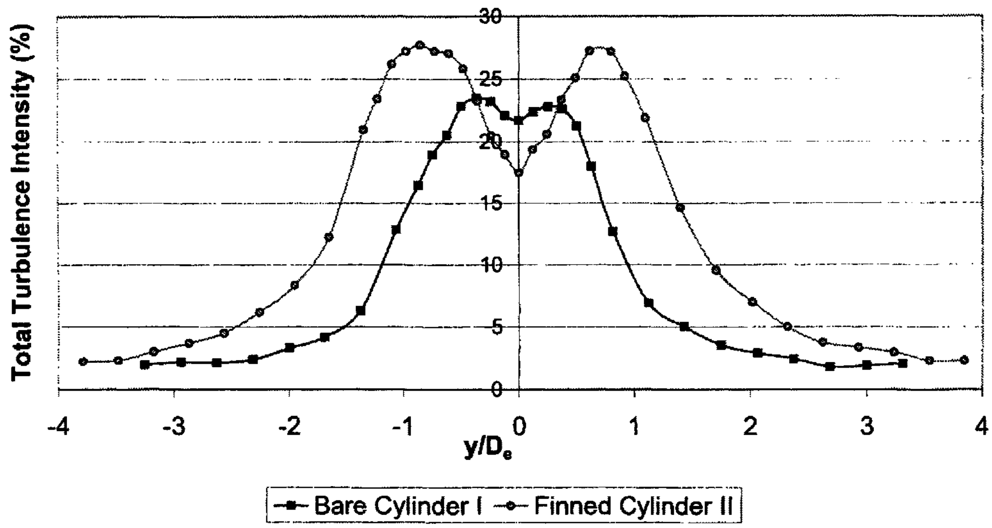

Figure 4.38: Turbulence intensity profiles for two cylinders in tandem at $x/D_e = 2.5$ for $Re = 3.7 \times 10^4$, $V_r = 3.34$.

The total turbulence intensity was higher in case of the finned cylinder and the profile shows a wider wake than the case of the bare cylinder (figure 4.38). A reduced turbulence level at the wake center is still observed.

The total turbulence intensity profile is wider in this case than in the wake of the single finned cylinder case. This is due to the increase in the across stream turbulent stresses relative to the case of the single finned cylinder. Also, the maximum turbulence intensity in case of the single finned cylinder is higher than the tandem finned cylinders (figure 4.39).

Turbulence intensity at the fundamental vortex shedding component for the tandem finned cylinders is substantially higher than that for the tandem bare cylinders (figure 4.40) which agrees with the microphone measurements. As shown in figure (4.41), Tu_f is also higher for the tandem finned cylinders than in the case

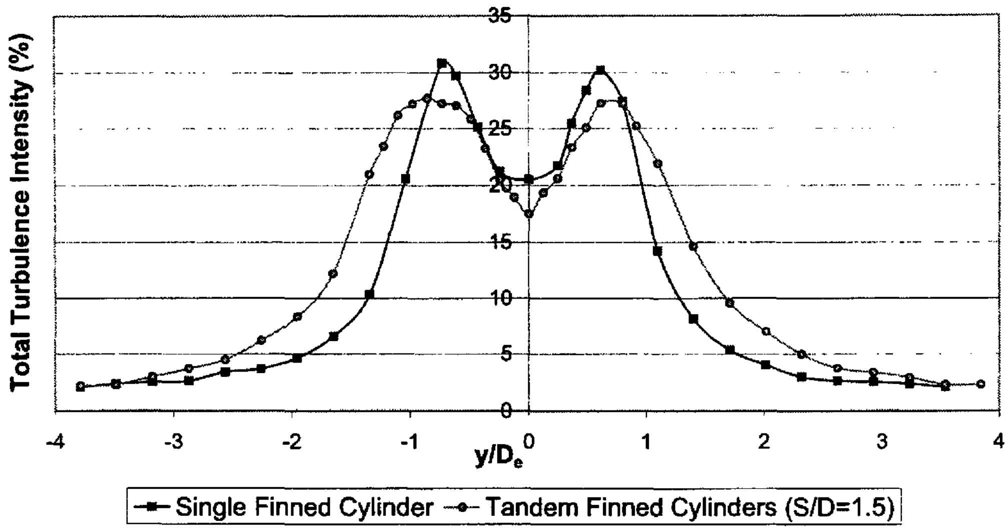

Figure 4.39: Total turbulence intensity profiles for finned cylinders of type II at $x/D_e = 2.5$ for $Re = 3.7 \times 10^4$, $V_r = 3.34$.

of the single finned cylinder at the same Reynolds number which means that the vortex shedding process has been enhanced by adding another finned cylinder at $S/D_e = 1.5$ upstream of the single finned cylinder. This is in contrast with the case of bare cylinders where the addition of a downstream cylinder weakened the vortex shedding process.

Typical velocity spectra at the maximum turbulence intensity are compared in figure (4.42). It is observed that the the vortex shedding peak is not only stronger, but also sharper and more concentrated in case of finned cylinders than in the case of the bare cylinders.

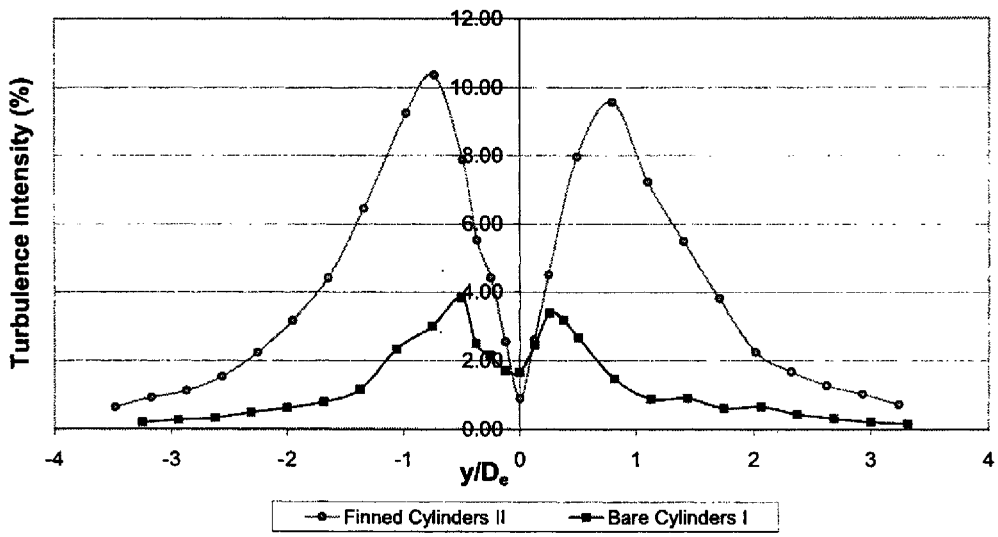

Figure 4.40: Turbulence intensity profiles at the fundamental vortex shedding component for tandem cylinders with $S/D_e = 1.5$ at $x/D_e = 2.5$ for $Re = 3.7 \times 10^4$, $V_r = 3.34$.

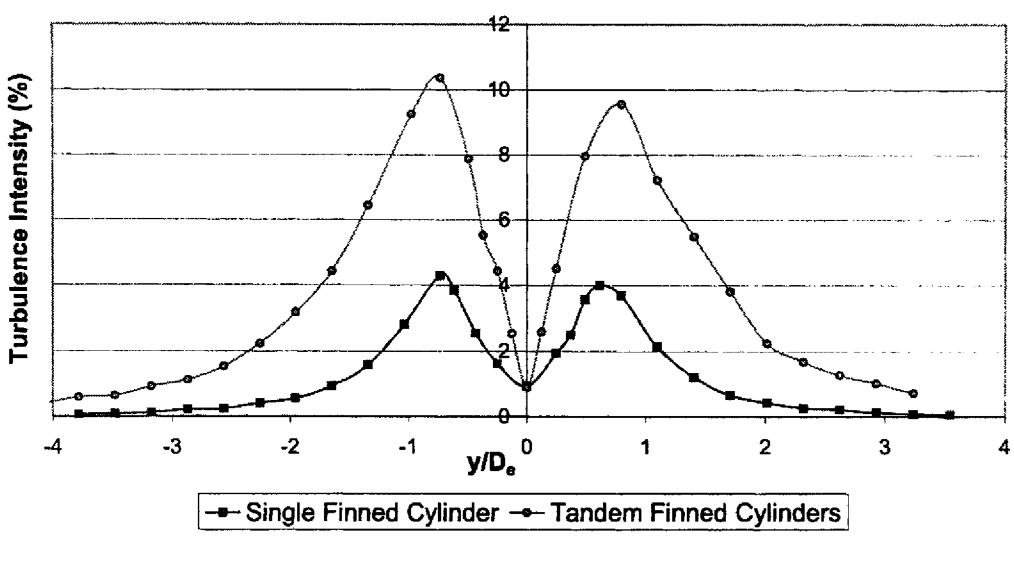

Figure 4.41: Turbulence intensity profiles due to fundamental vortex shedding component for finned cylinders of type II at $x/D_e = 2.5$ and $Re = 3.7 \times 10^4$, $V_r = 3.34$.

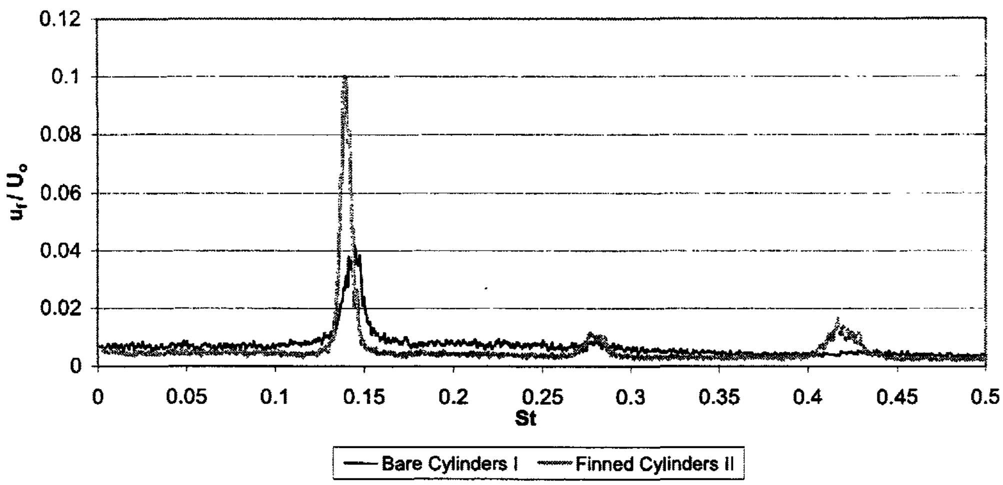

Figure 4.42: Dimensionless velocity spectra at the maximum turbulence intensity point at $x/D_e = 2.5$ for the tandem bare and finned cylinders with $S/D_e = 1.5$ at $Re = 3.7 \times 10^4$, $V_r = 3.34$.

4.2.2.2 Tandem Finned Cylinders With $\mathbf{S/D_e = 2}$

The flow pattern for the tandem bare cylinders with a spacing ratio $S/D_e = 2$ is a quasi-stationary vortex shedding with reattachment as has been explained earlier.

Figure (4.43) shows the change in the dimensionless frequency and the dimensionless sound pressure at vortex shedding frequency with the reduced velocity. It is observed for this case, as in the previous cases, that the vortex shedding frequency is changing linearly with the velocity before the onset of resonance, which suggests that the flow pattern remains the same for the finned cylinders as with all cases of the bare cylinders. The sound pressure at vortex shedding frequency before the resonance range is higher for the finned cylinders than for the bare cylinders, which again is different from the single cylinders case (figures 4.44 and

4.45).

The first mode is strongly excited earlier in the case of bare cylinders as explained before and the vortex shedding locks in with the first mode acoustic natural frequency. In the case of finned cylinders, the first mode was excited as well but the resonance was much weaker than the case of bare cylinders. In particular, resonance did not occur at the lower reduced velocity range ($V_r = 3.5 - 5$). The sound produced at resonance frequency in this range was not sufficiently high to entrain all the vortex shedding so that the vortex shedding peak was still clear and distinguished.

Figure (4.46) shows the difference in magnitude of the non-dimensionalized sound pressure at the first mode frequency (P_r^*) for the different cases of tandem cylinders with $S/D_e = 2$. Figure (4.47) and figure (4.48) show the difference between the bare and the finned cylinders sound pressure spectra at the first resonance range of the bare cylinders. It is observed that the magnitude of the first mode sound pressure for the bare cylinders is more than ten times higher than that in the case of finned cylinders.

It is observed that increasing the fin density promotes the onset of resonance. However, the lock-in becomes significantly weaker, in terms of pressure levels at vortex shedding frequency and the lock-in velocity range. Figures (4.49) and (4.50) show the spectra of the non-dimensionalized sound pressure at the post-coincidence resonance. The lock-in for the bare cylinders was so strong that it continued until the maximum attainable flow velocity.

In the case of bare cylinders, the vortex shedding frequency gets out of

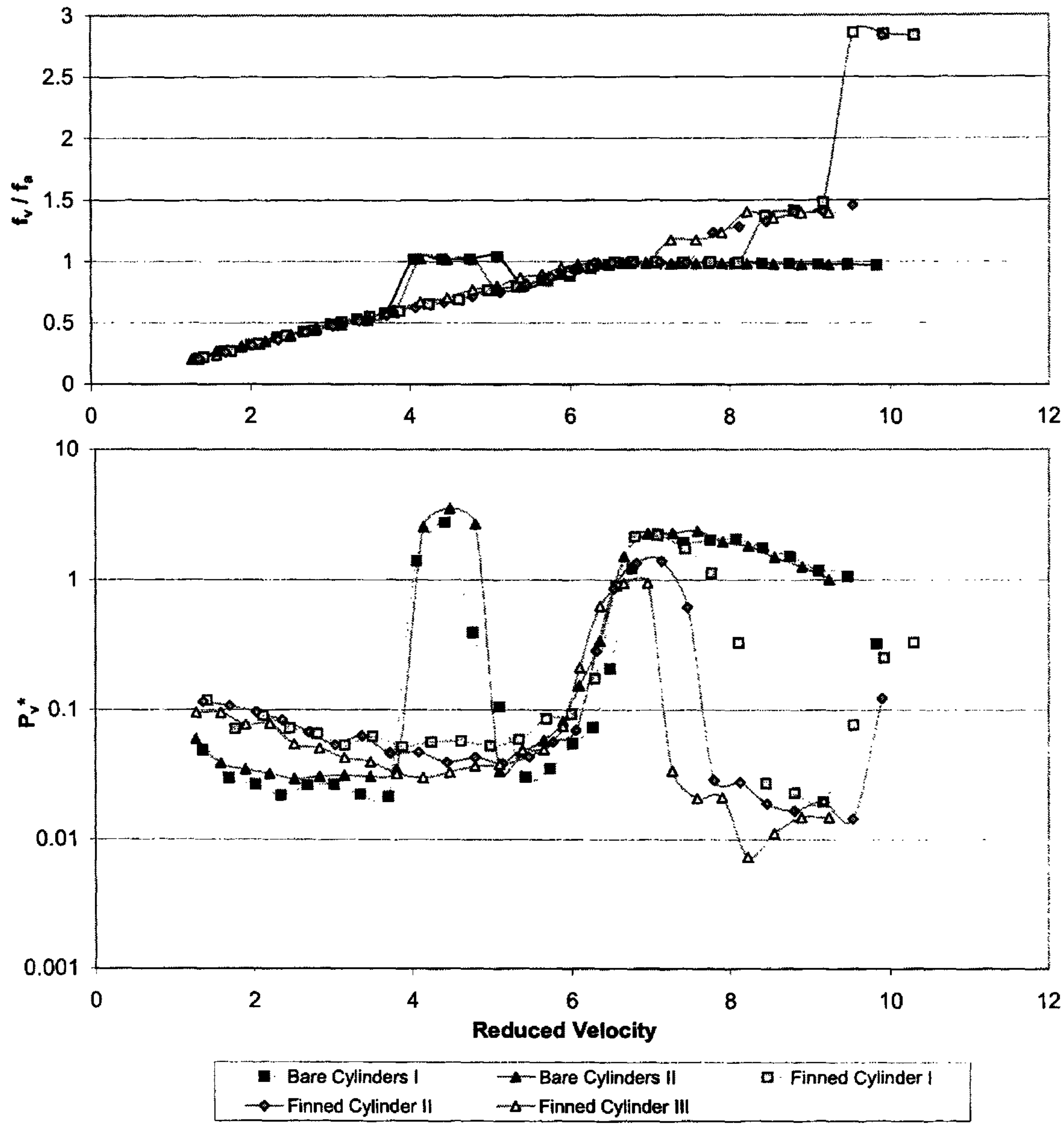

Figure 4.43: Variations in f_v/f_a and P^* with V_r for tandem cylinders with a spacing ratio $S/D_e = 2$.

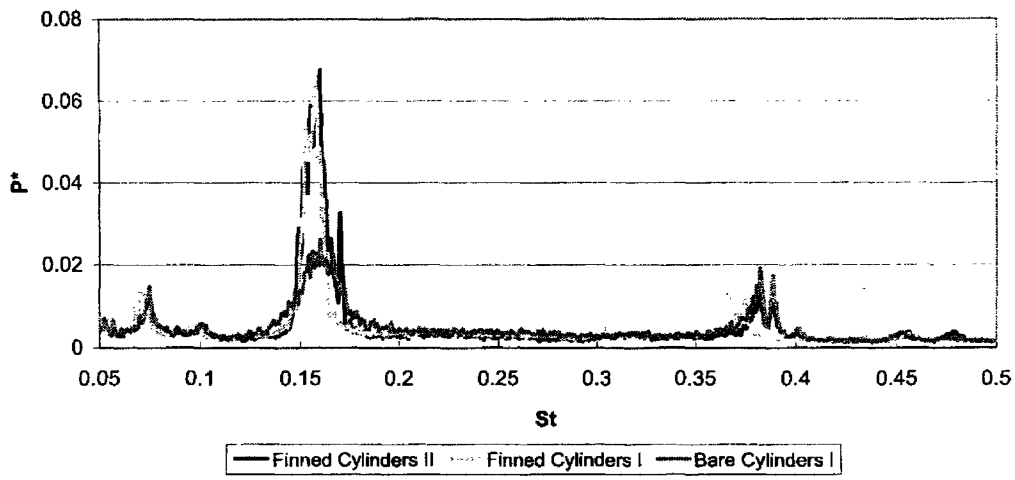

Figure 4.44: Dimensionless pressure spectra for the tandem cylinders with $S/D_e = 2$ before resonance ($V_r = 2.68$).

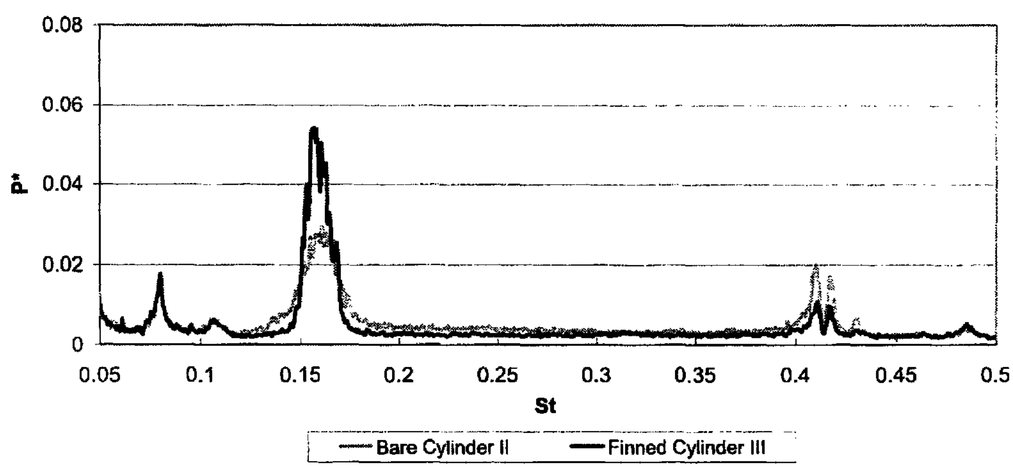

Figure 4.45: Dimensionless pressure spectra for the tandem cylinders with $S/D_e = 2$ before resonance ($V_r = 2.5$).

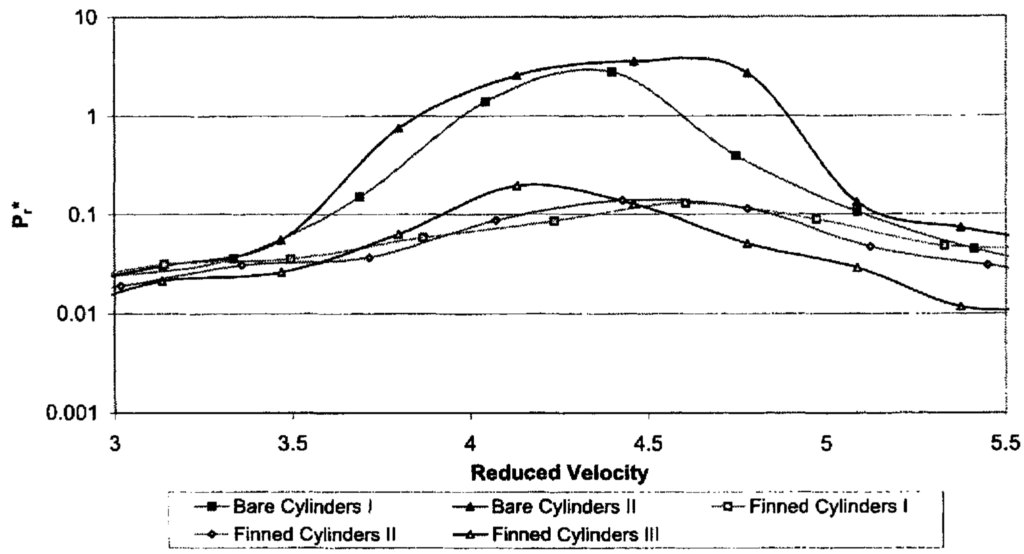

Figure 4.46: Variations in P_r^* with V_r for tandem cylinders with a spacing ratio $S/D = 2$.

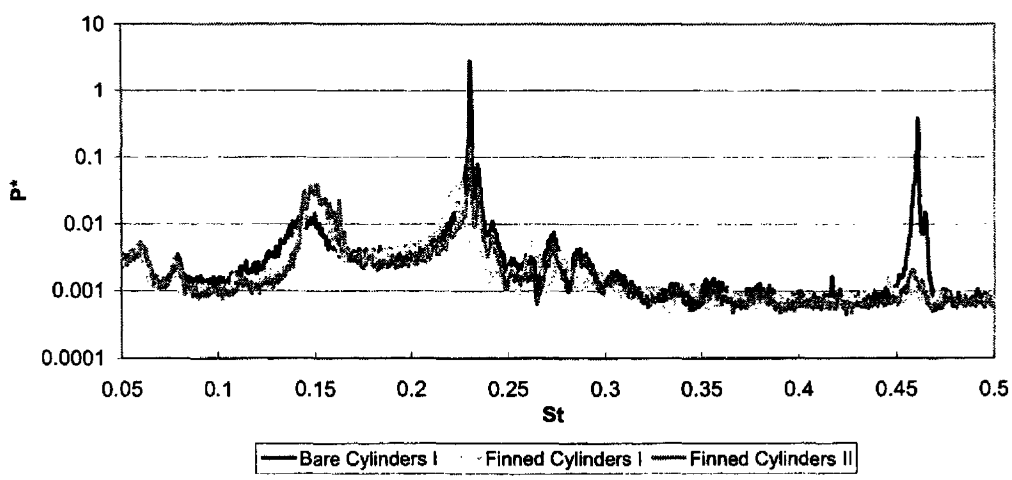

Figure 4.47: Dimensionless pressure spectra for the tandem cylinders with $S/D_e = 2$ at the first resonance range ($V_r \simeq 4.5$).

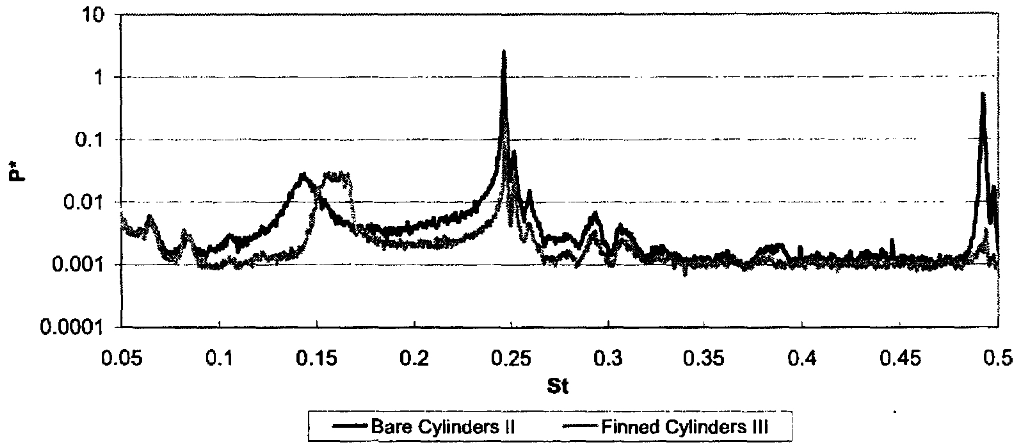

Figure 4.48: Dimensionless pressure spectra for the tandem cylinders with $S/D_e = 2$ at the early resonance ($V_r = 4.13$).

the lock-in after the first mode excitation. This vortex shedding frequency then changed linearly with the velocity in this range as well.

The finned cylinders of type I and type II were able to excite the third mode at the end of the velocity range while the finned cylinders of type III were not able to excite the third mode within the range of the attainable velocity. Figure(4.51) shows the non-dimensionalized pressure spectra for the finned cylinders of types I and II.

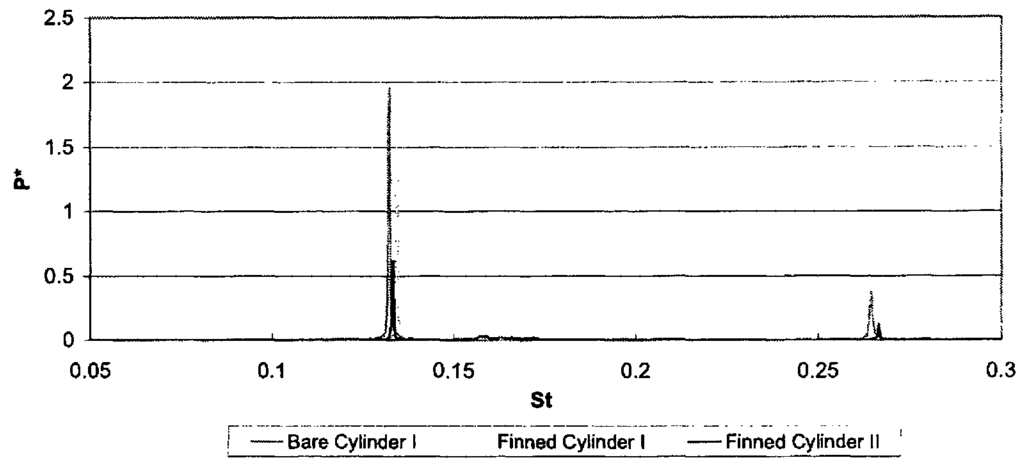

Figure 4.49: Dimensionless pressure spectra for the tandem cylinders with $S/D_e = 2$ at the post-coincidence resonance ($V_r \simeq 7.4$).

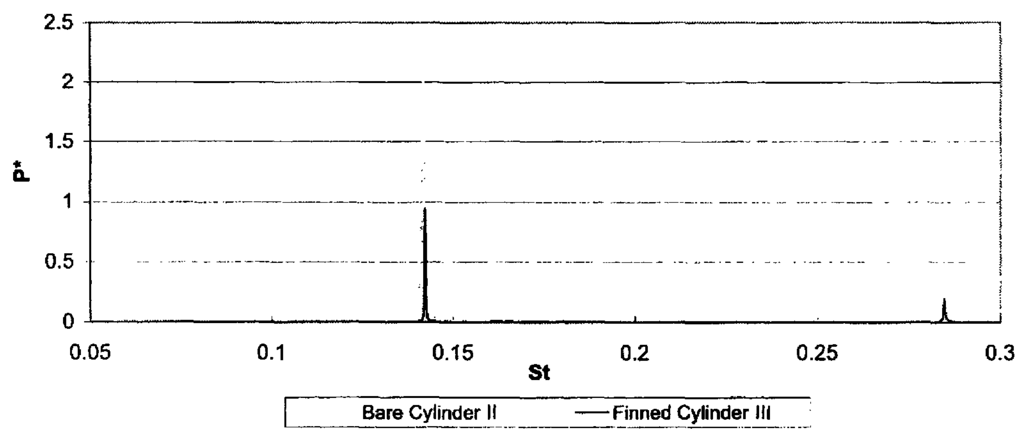

Figure 4.50: Dimensionless pressure spectra for the tandem cylinders with $S/D_e = 2$ at the post-coincidence resonance ($V_r = 6.95$).

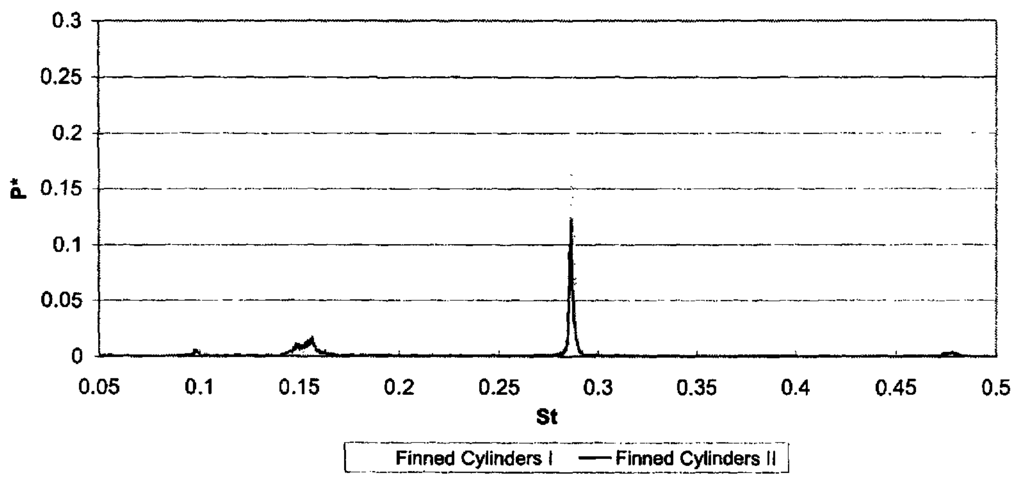

Figure 4.51: Dimensionless pressure spectra for the tandem cylinders with $S/D_e = 2$ at $V_r = 9.9$.

4.2.2.3 Tandem Cylinders With a Spacing Ratio $S/D_e = 3$

For this spacing ratio, vortex shedding is expected to occur in the gap between the cylinders. The interaction between the relatively larger vortices and the downstream cylinder seems to have a strong effect on the flow in this case.

The sound pressure at the vortex shedding frequency before resonance was virtually the same for all the cylinders (figure 4.52). At higher velocities, just before the lock-in, P_v^* for the bare cylinders was higher than P_v^* for the finned cylinders. The finned cylinders of type III has the minimum sound pressure level at vortex shedding frequency in the range of velocity from $V_r = 2.8$ until the resonance. Another feature observed for this spacing is that the first mode response before resonance in the case of bare cylinders was stronger than that of the finned cylinders. Figures (4.53) and figure (4.54) show the difference in P_v^* as well as in the first mode response at a velocity just before the onset of the first mode range.

In the case of finned cylinders, the first mode excitation at the pre-coincidence lock-in range was very strong . The measurements show, contrary to the case of $S/D_e = 2$, that the sound pressure was higher in case of the finned cylinders (figure 4.55 and 4.56). The first mode excitation was strong enough to entrain the vortex shedding and to have a strong lock-in between the vortex shedding frequency and the first acoustic mode frequency.

Despite the higher sound pressure levels in the case of finned cylinders at the pre-coincide resonance range, P_v^* for the finned cylinders was significantly lower than that of the bare cylinders in the post-coincidence resonance range. This fact is clearly depicted in figure (4.52) and figures (4.57 and 4.58).

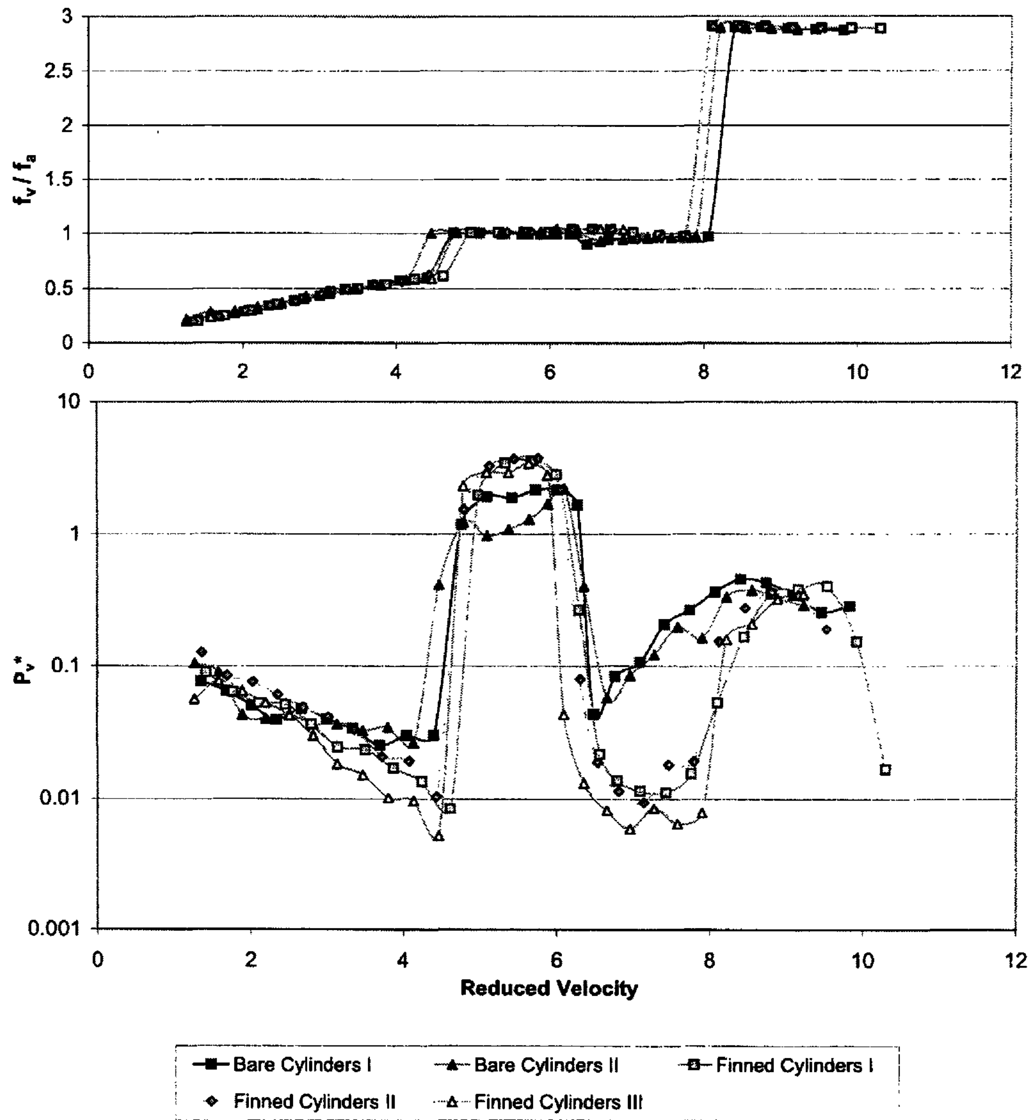

Figure 4.52: Variations in f_v/f_a and P_v^* with V_r for tandem cylinders with a spacing ratio $S/D_e = 3$.

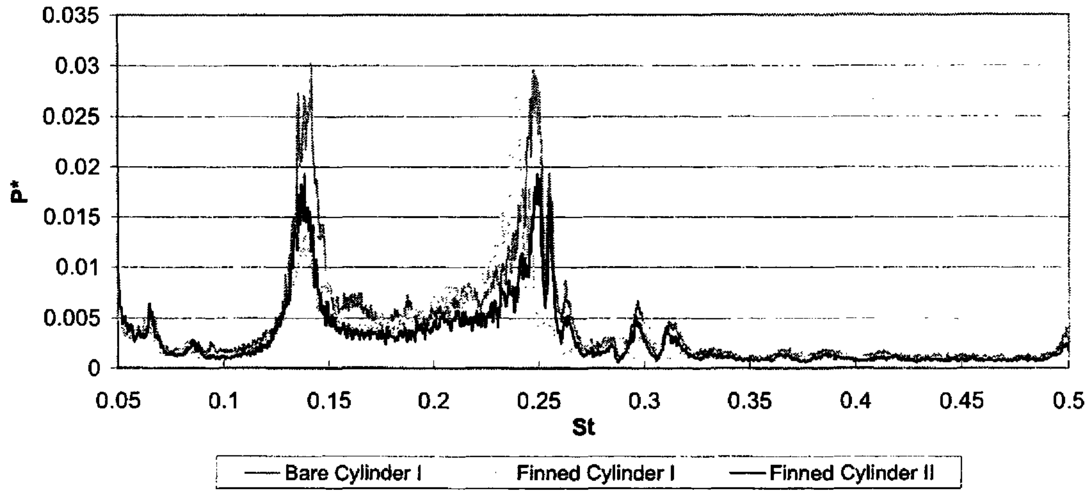

Figure 4.53: Dimensionless pressure spectra for the tandem cylinders with $S/D_e = 3$ before the onset of the post-coincidence resonance ($V_r \simeq 4.1$).

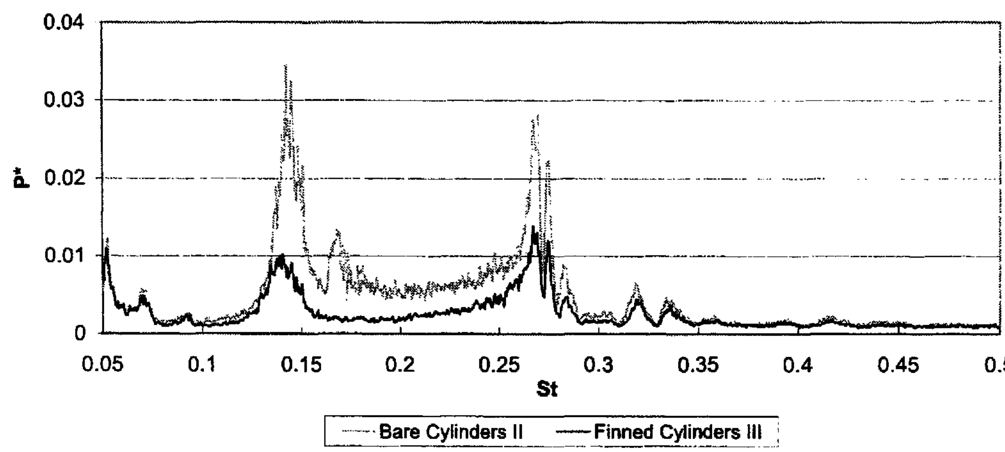

Figure 4.54: Dimensionless pressure spectra for the tandem cylinders with $S/D_e = 3$ before the onset of the post-coincidence resonance ($V_r = 3.8$).

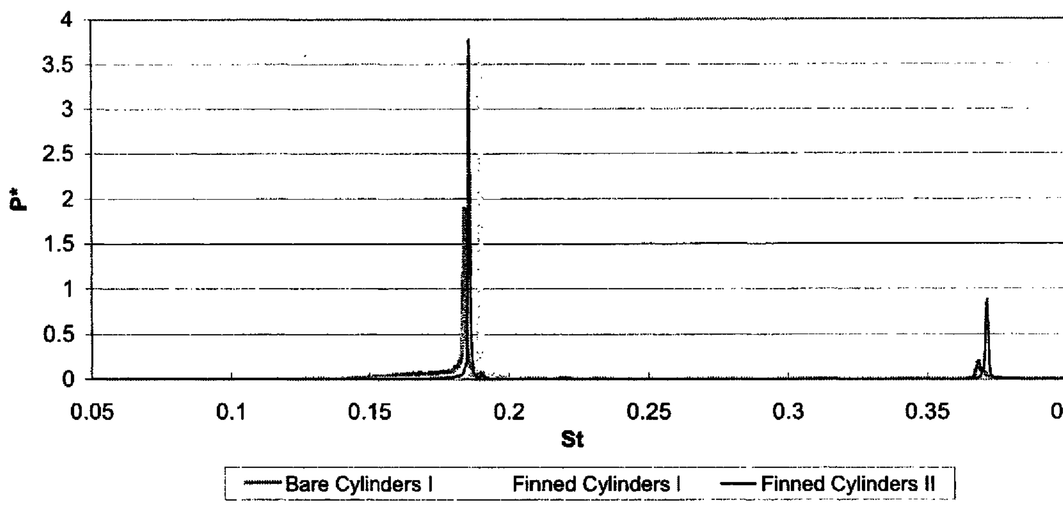

Figure 4.55: Dimensionless pressure spectra for the tandem cylinders with $S/D_e = 3$ at the pre-coincidence resonance ($V_r \simeq 5.4$).

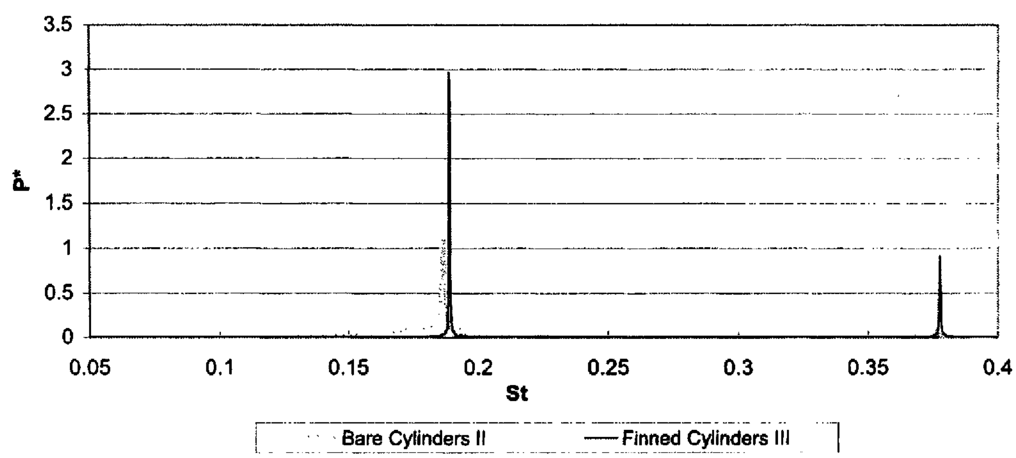

Figure 4.56: Dimensionless pressure spectra for the tandem cylinders with $S/D_e = 3$ at the pre-coincidence resonance ($V_r = 5.7$).

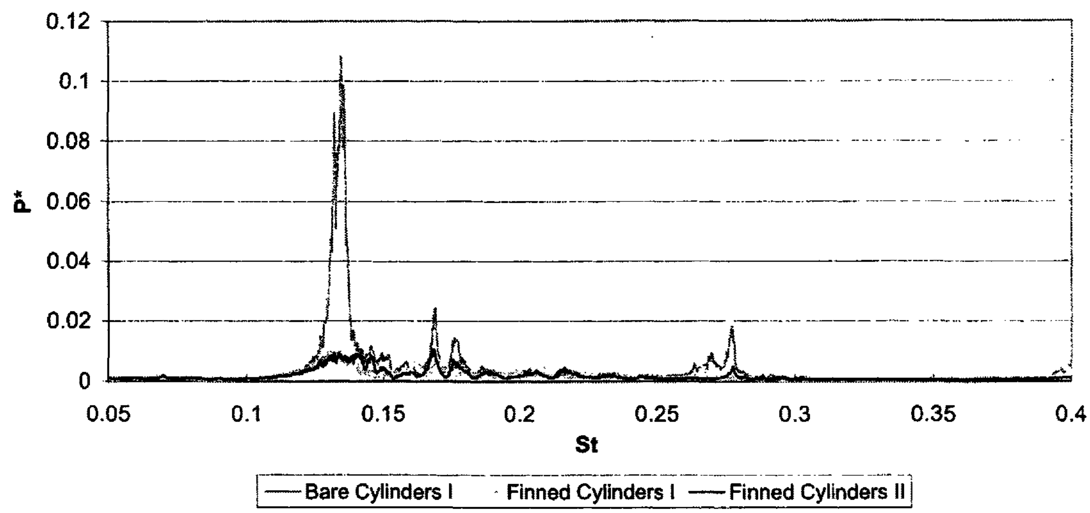

Figure 4.57: Dimensionless pressure spectra for the tandem cylinders with $S/D_e = 3$ at the post-coincidence resonance of the first acoustic mode ($V_r \simeq 7.08$).

The third mode was strongly excited for the finned and the tandem bare cylinders as well. As can be seen in figures (4.59 and 4.60), there is no significant difference between P_v^* for the finned and the bare cylinders.

Velocity Measurements

In the post-coincidence resonance, there is a quite significant difference in the sound pressure level at the vortex shedding frequency between the bare and the finned tandem cylinders at this spacing ratio. Hotwire measurements were therefore performed to understand the cause of this difference. The finned cylinders II and the bare cylinders I were selected for these measurements.

Figure (4.61) shows the difference between the mean velocity profiles at the downstream position $x/D_e = 2.5$ for the tandem bare cylinder of type I and the tandem finned cylinders of type II with a spacing ratio $S/D_e = 3$ at $V_r = 8.2$. It is

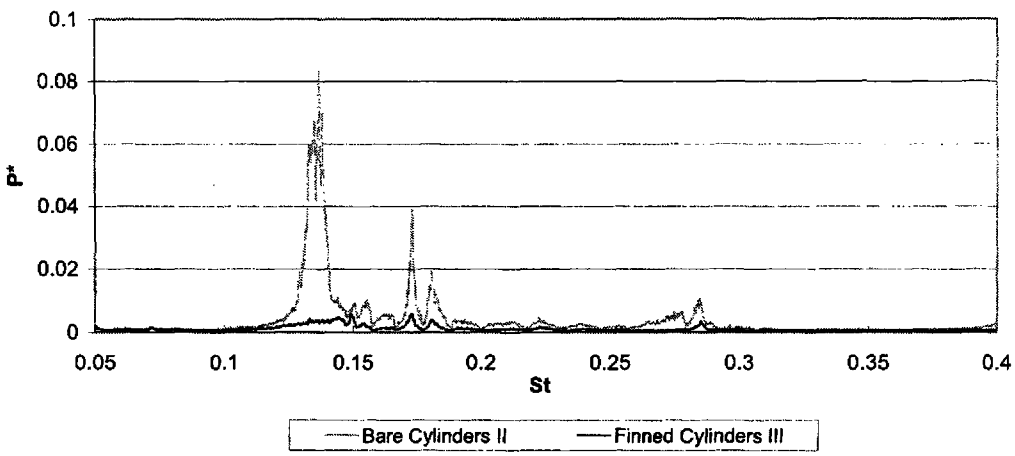

Figure 4.58: Dimensionless pressure spectra for the tandem cylinders with $S/D_e = 3$ at the post-coincidence resonance of the first acoustic mode ($V_r = 6.95$).

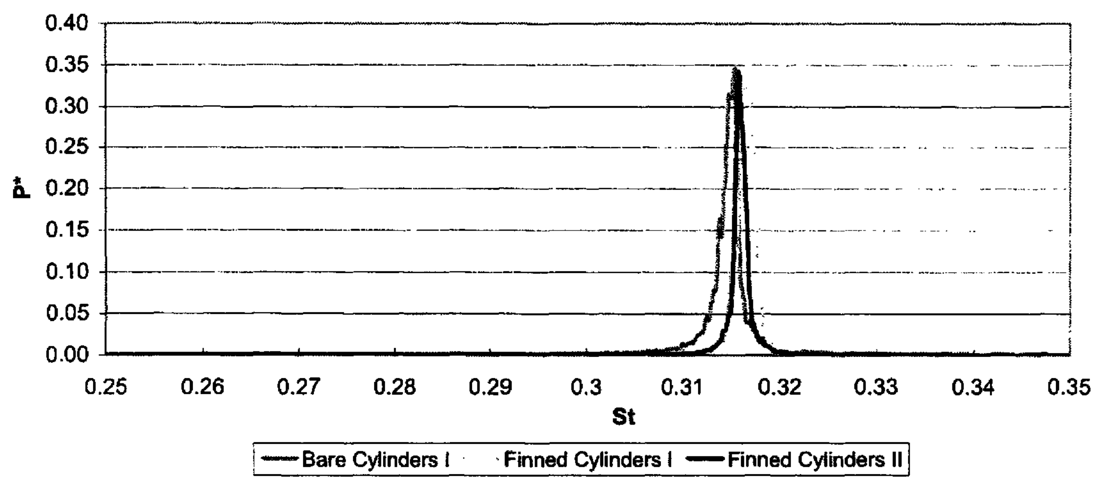

Figure 4.59: Dimensionless pressure spectra for the tandem cylinders with $S/D_e = 3$ at the third acoustic mode resonance, $V_r \simeq 9.1$.

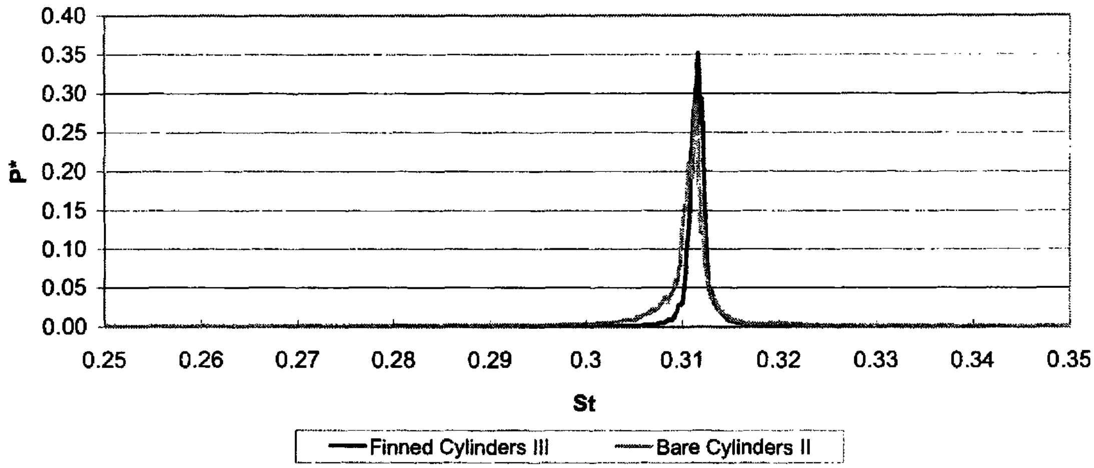

Figure 4.60: The dimensionless pressure spectra for the tandem cylinders with $S/D_e = 3$ at the third acoustic mode resonance, ($V_r = 9.23$)

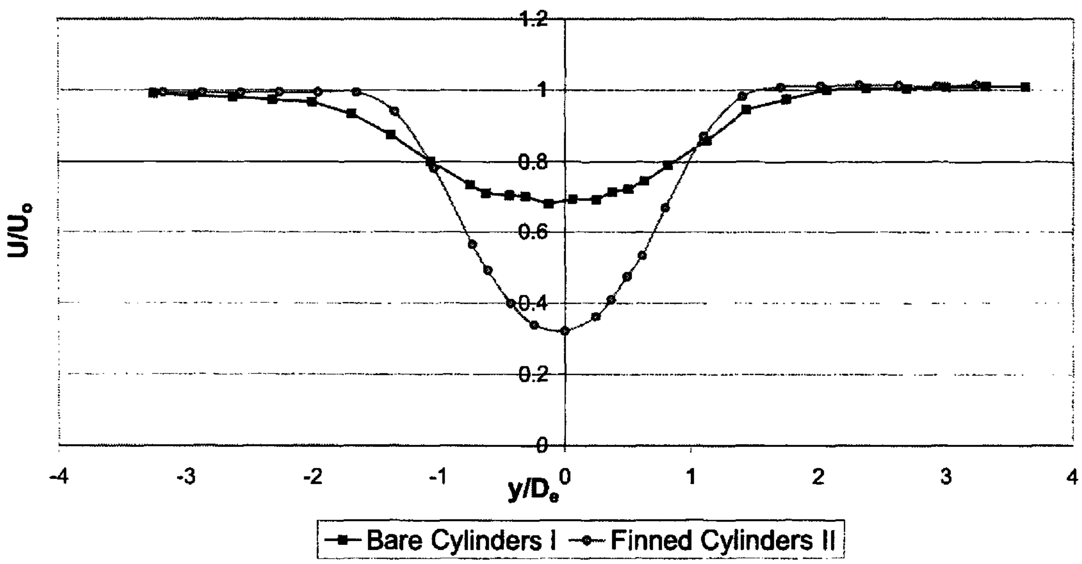

Figure 4.61: Dimensionless velocity profiles for two cylinders in tandem with $S/D_e = 3$ at $x/D_e = 2.5$ for $Re = 9.49 \times 10^4$, $V_r = 8.2$.

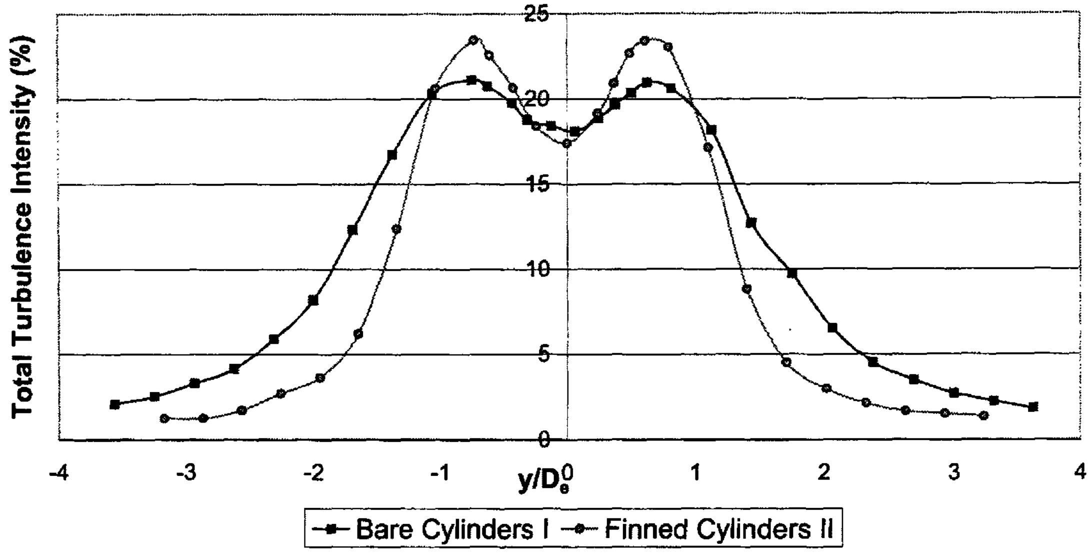

Figure 4.62: Total turbulence intensity profiles for two cylinders in tandem at $x/D_e = 2.5$ for $Re = 9.49 \times 10^4$, $V_r = 8.2$.

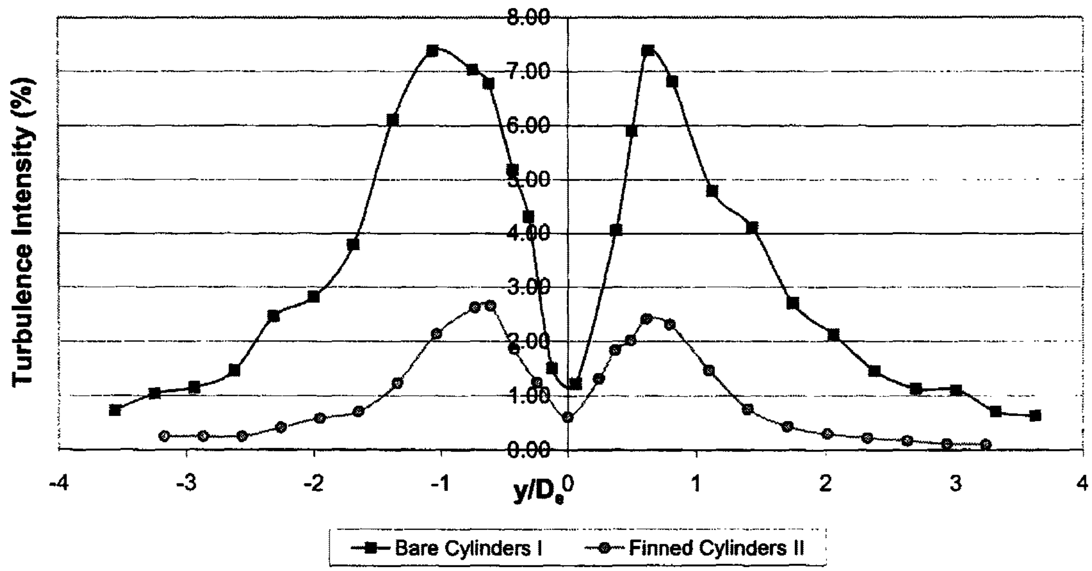

Figure 4.63: The turbulence intensity profiles due to fundamental vortex shedding component at $x/D = 2.5$ for $Re = 9.49 \times 10^4$, $V_r = 8.2$.

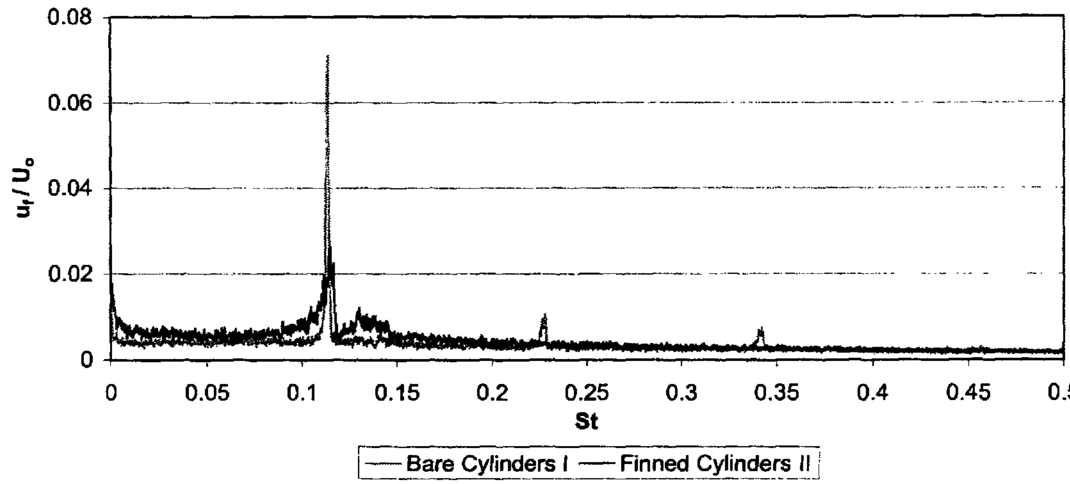

Figure 4.64: The dimensionless velocity spectra at the maximum turbulence intensity point at $x/D_e = 2.5$ for the tandem bare and finned cylinders of $S/D_e = 3$

observed that the deficit in the mean velocity profile in the case of finned cylinders is larger than that for the bare cylinders. The hump that has been observed for the single cylinder no longer exists. The portion with nearly constant velocity that has been observed in some of the previous cases of finned cylinder doesn't exist. The velocity is decreasing smoothly to the minimum at $y/D_e = 0$.

The total turbulence intensity profiles are similar with a somewhat higher peak value for the finned cylinders (figure 4.62). The turbulence intensity profile for the bare cylinders is wider which indicates a wider wake.

The turbulence intensity at the fundamental vortex shedding frequency, Tu_f, is much higher for the bare cylinders than the finned cylinders (figure 4.63). This again agrees with the measurements done by the microphone. Figure (4.64) shows typical velocity spectra at maximum turbulence intensity point. The figure shows the stronger resonance and the existence of higher harmonics in the case of bare

Table 4.2: Strouhal numbers for the single and the tandem finned cylinders

	Single Cylinder	Tandem Cylinders		
		$S/D_e = 1.5$	$S/D_e = 2$	$S/D_e = 3$
Finned Cylinder Type I	0.194	0.145	0.154	0.143
Finned Cylinder Type II	0.19	0.143	0.151	0.147
Finned Cylinder Type III	0.194	0.158	0.16	0.145

cylinders where the vortex shedding process occurs at resonance frequency. In the case of the finned cylinders, the vortex shedding was not fully entrained by the resonance frequency and there are no higher harmonics as in the case of bare tandem cylinders.

4.2.3 Strouhal Number for Finned Cylinders

The Strouhal numbers for finned cylinders have been determined from the spectra of the sound pressure measured by the microphone before the onset of lock-in with the acoustic natural frequency of the test section. As has been shown, the relation between f_v/f_a and V_r is linear for the finned cylinders which means that the Strouhal number is constant at all the velocities before the onset of resonance.

The Strouhal numbers have been calculated for the all cases based on the effective diameter as explained in section (3.1). The use of the effective diameter is generally observed to collapse the values of the Strouhal number for single and tandem finned cylinders which agrees with the observation of Mair (1974) for single finned cylinders.

Table (4.2) shows the values of the Strouhal number for the finned cylinders. It is observed that the value of Strouhal number for single finned cylinders doesn't change significantly with the change in the fin density. It is observed also that the Strouhal number values for the single finned cylinders are generally less than that of the single bare cylinder (Table 4.1) which agrees with the results of Mair (1974).

The high fin density is observed to affect the Strouhal number in the case of $S/D_e = 1.5$. Although the Strouhal number is virtually the same for finned cylinders I and II with $S/D_e = 1.5$, it is observed to be higher for the finned cylinders III, which have the highest fin density, as shown in table (4.2). The same is also observed in the case of finned cylinders with $S/D_e = 2$. However, the difference between the Strouhal number of finned cylinders III and that of finned cylinders I and II for this case is smaller than the case of $S/D_e = 1.5$.

For the case of $S/D_e = 3$, the values of Strouhal number for all types of finned cylinders are observed to be very close. The Strouhal number values for the finned cylinders at this spacing are generally observed to be very close to that of the bare cylinders (Table 4.1).

4.3 Overview of The Flow Over Finned Cylinders

Cross-flow over finned cylinders has shown a different behavior from that of bare cylinders. It turned out that the flow pattern changes significantly by the introduction of the fins into the cylinders. The flow physics seems to be quite complicated especially at the lock-in range.

The introduction of the fins into the single cylinders caused a significant disruption to the flow. This disruption increased with the increase in the flow velocity. The resonance was very weak in the case of the finned cylinders compared to the bare cylinders. Increasing the fin density, increased the disruption. The wake characteristics also change significantly. The wake becomes wider with higher turbulence intensities and the vortex shedding becomes weaker.

The fins have changed the flow behavior in the case of tandem cylinders as well. The effect of the fins was not just to disrupt the flow and weaken the vortex shedding. In fact, the introduction of the fins enhanced the vortex shedding in some cases compared to the corresponding tandem bare cylinders.

For the tandem cylinders with a spacing ratio $S/D_e = 2$, the introduction of the fins enhanced the vortex shedding significantly before the onset of resonance. However, the fins seem to cause the resonance to be weaker for this spacing. The resonance in the case of finned cylinders at the pre-coincidence resonance range was not strong enough to entrain the vortex shedding. The post-coincidence resonance was weaker as well. The vortex shedding frequency emerges from the lock-in and was able to excite the third mode for the finned cylinders of types II and III.

When the spacing ratio is decreased to $S/D_e = 1.5$, the pre-coincidence resonance disappears from the bare and the finned cylinders as well. The fins at this spacing cause the sound pressure to decrease at resonance. The resonance becomes weaker as the fin density increases. For the high fin density of type III, the lock-in with the first mode was so weak that the vortex shedding was able to emerge out of the lock-in and excites the third mode. However, the fins enhance the vortex shedding before resonance, as in the case of $S/D_e = 2$.

When the spacing ratio is increased to $S/D_e = 3$, the vortex shedding process becomes significantly weaker than the other spacing ratios before the onset of resonance. The first and the third modes are excited. The level of the first mode resonance at the pre-coincidence range becomes stronger in the case of finned cylinders. However, it is much weaker at the post-coincidence resonance. The third mode is excited for the finned and the bare cylinders. The lock-in with the third mode in the case of finned cylinders is as strong as in the case of bare cylinders.

It is observed generally that the post-coincidence resonance becomes significantly weaker as the spacing ratio is increased from $S/D_e = 2$ to $S/D_e = 3$ while the third mode excitation becomes stronger.

CHAPTER 5
Conclusions

The effect of fins on vortex shedding and acoustic resonance for single and two tandem cylinders with spacing ratios $S/D_e = 1.5$, 2, and 3 have been investigated for the range of Reynolds number from 1.56×10^4 to 1.13×10^5. The main conclusions obtained from this study are summarized in the following.

1. The introduction of fins reduces the strength of vortex shedding from single cylinders. This effect becomes more apparent with the increase in Reynolds number. Moreover, the fins in the case of single cylinders increase the broadband turbulence. The increase in the broadband turbulence becomes more significant with the increase in the fin density.

2. The fins in the case of single cylinders cause the sound pressure to decrease at resonance. Increasing the fin density beyond a certain limit causes the sound pressure at acoustic resonance to drop significantly and it becomes very weak.

3. The single finned cylinders have a larger mean velocity deficit than single bare cylinders. Larger velocity gradients have been observed in the wake of single finned cylinders.

4. For tandem cylinders with $S/D_e = 1.5$, the fins cause the sound pressure before the onset of resonance to increase which is the opposite of the effect of

fins in the case of single cylinders. The fins promote the onset of resonance as well.

5. The resonance is weaker for the tandem finned cylinders with $S/D_e = 1.5$ than for the tandem bare cylinders with the same spacing ratio. The sound pressure levels are lower and the vortex shedding emerges earlier from lock-in range in comparison with the tandem bare cylinders. Generally, increasing the fin density at this spacing weakens the resonance. Increasing the fin density beyond a certain limit may cause the vortex shedding to emerge earlier from the lock-in with the first mode and to excite the third resonance mode.

6. For tandem cylinders with $S/D_e = 2$, the fins produce higher sound pressure level before resonance than that of the bare cylinders. However, the fins significantly weaken the pre-coincidence resonance. The excitation becomes so weak that the produced sound is not sufficiently high to entrain the vortex shedding and produce resonance. In the case of bare cylinders at similar conditions, vortex shedding produced very strong resonance.

7. The fins weaken the post-coincidence resonance for the finned cylinders with $S/D_e = 2$, but this effect is less pronounced than that observed during the pre-coincidence resonance. Increasing the fin density causes the sound pressure levels at resonance to decrease and causes the vortex shedding to emerge earlier from resonance. The finned cylinders at this spacing are capable of exciting the third mode at a lower reduced velocity than the bare cylinders.

8. For tandem cylinders with $S/D_e = 3$, the fins resulted in a very strong pre-coincidence resonance. This resonance is stronger for the finned cylinders than for the bare cylinders at the same velocity range. However, the fins weaken the post-coincidence resonance. The finned cylinders at this spacing were able to excite the third mode with no significant difference in the sound pressure levels between the bare and the finned cylinders.

9. Generally, it is observed that increasing the spacing ratio results in decreasing the strength of the post-coincidence resonance while increasing the strength of pre-coincidence resonance. It was observed also that the third mode excitation becomes stronger with the increase in the spacing ratio.

10. The lock-in range for tandem bare and finned cylinders are generally broader than that for the case of single cylinders. The sound pressure levels at resonance are generally higher for the tandem cylinders.

A lot of work is still needed in order to improve our understanding of this subject. Some of the main aspects that are in need to further study are summarized in the following:

1. The effect of fin height on vortex shedding and acoustic resonance need to be investigated. It is suggested that the measurements made in this study be repeated for finned cylinders with different fin heights.

2. The mechanism of first mode excitation in the case of tandem cylinders need to be understood. It has been shown in this study that the behavior

of the acoustic response in the pre-coincidence resonance range is different from that in the post-coincidence resonance range. It is suggested to investigate the flow behavior at resonance in the gap between the cylinders as well as downstream of the cylinders using flow visualization techniques complemented with measurements of pressure fluctuation at the surface of the tandem cylinders at resonance.

3. The velocity measurements performed in this study using hotwire anemometer show very interesting results for the tandem cylinders. The mean velocity deficit in the wake of the finned cylinders was less than that in the case of the bare cylinders for $S/D_e = 1.5$. However, the mean velocity deficit was larger for the tandem finned cylinders with $S/D_e = 3$. This difference may be due to a fundamental difference in the wake behavior in these cases. More hotwire measurements in the wake of the bare and the finned cylinders are needed in order to investigate the wake behavior of the finned and the bare cylinders at these two spacing ratios and to determine the reasons for the difference.

BIBLIOGRAPHY

Achenbach, E. & Heinecke, E. (1981), 'On vortex shedding from smooth and rough cylinders in the range of reynold numbers 6×10^3 to 5×10^6', *Journal of Fluid Mechanics* **109**, 239–251.

Alam, M. M., Moriya, M., Takai, K. & Sakamoto, H. (2003), 'Fluctuating fluid forces acting on two circular cylinders in a tandem arrangement at a subcritical Reynolds number', *Journal of Wind Engineering and Industrial Aerodynamics* **91**, 139–154.

Arie, M., Kiya, M., Moriya, M. & Mori, H. (1983), 'Pressure fluctuations on the surface of two circular cylinders in tandem arrangement', *Journal of Fluids Engineering* **105**, 161–167.

Baird, R. C. (1954), 'Pulsation-induces vibration in utility steam generation units', *Combustion* **25**(10), 38–44.

Blevins, R. D. (1985), 'The effect of sound on vortex shedding from circular cylinders', *Journal of Fluid Mechanics* **161**, 217–237.

Blevins, R. D. (1990), *Flow-induced Vibration*, second edn, Von Nostrad Reinhold, New York.

Bloor, M. S. & Gerrard, J. H. (1966), 'Measurements on turbulent vortices in a cylinder wake', *Proceedings of the Royal Society of London. Series A, Mathematical and Physical Sciences* **294**, 319–342.

Brevoort, M. J. & Rollin, V. G. (1937), Air flow around finned cylinders, Report 555, NASA.

Carvajal-Mariscal, I., Sanchez-Silva, F. & Quinto-Diez, P. (2001), 'Flow dynamics between the inclined fins of a finned tube', *International journal of heat and fluid flow* **22**, 519–524.

Drescher, H. (1956), 'Messung der auf querongestromte zylinder ausgeubten seitlich veranderten drucke', *Zeitschrift für Flugwissensschaft* **4**, 17–21.

Eisinger, F. L. & Sullivan, R. E. (1993), 'Unusual acoustic vibration in heat exchanger and steam generator tube banks possibly caused by fluid-acoustic instability', *Journal of Engineering for Gas turbines and power* **115**, 411–417.

Fan, H. (2002), Vortex shedding and acoustic resonance of an array of tubes with twisted serrated fins, Master's thesis, McMaster University.

Feng, C. (1968), The measurement of vortex-induced effects in flow past stationary and oscillating circular and d-section cylinder, Master's thesis, University of British Columbia.

Friehe, C. A. (1980), 'Vortex shedding from cylinders at low Reynolds numbers', *Journal of Fluid Mechanics* **100**, 237–241.

Griffen, O. M. (1982), 'Some recent studies of vortex shedding with applications to marine tubular and risers', *Journal of Energy Resources Technology* **104**, 2–13.

Hamakawa, H., Fukano, T., Nishida, E. & Aragaki, M. (2001), Vortex shedding from a circular cylinder with fin, AIAA, Maastricht, Netherlands.

Igarashi, T. (1981), 'Characteristics of the flow around two circular cylinders arranged in tandem (1st report)', *Bulletin of the JSME* **24**(188), 323–331.

Igarashi, T. (1984), 'Characteristics of the flow around two circular cylinders arranged in tandem (2nd report, unique phenomenon at small spacing)', *Bulletin of the JSME* **27**(233), 2380–2387.

Jebodhsingh, D. (2002), The effect of fins on vortex shedding, Master's thesis, McMaster University.

King, R. (1977), 'Vortex excited oscillations of yawed circular cylinders', *Journal of Fluids Engineering* **99**, 495–502.

Kouba, J. (1986), Vortex shedding and acoustic emission in finned tube banks exposed to cross flow, Vol. 104 of *PVP Symposium on Flow-Induced Vibration*, ASME, pp. 213 – 217.

Lee, T. & Basu., S. (1997), 'Nonintrusive measurements of the boundary layer developing on a single and two circular cylinders', *Experiments in Fluids* **23**, 187–192.

Lee, T. & Panagakos, A. (1997), Investigation of boundary layer behavior on single and tandem cylinders, *in* 'Fluid-Structure Interaction, Aeroelasticity, Flow-Induced Vibration and Noise', Vol. AD-53-1, ASME.

Lienhard, J. (1966), 'Synopsis of lift, drag and vortex frequency data for rigid circular cylinders', *Washington state university, College of engineering, Resarch division bulletin* **300**.

Lin, J. C., Yang, Y. & Rockwell, D. (2002), 'Flow past two cylinders in tandem: Instantaneous and avaraged flow structure', *Journal of Fluids and Stuctures* **16**(8), 1059–1071.

Ljungkrona, L., Norberg, C. & Sunden, B. (1991), 'Free-stream turbulence and tube spacing effects on surface pressure fluctuations for two tubes in an in-line arrangement', *Journal of Fluids and Structures* (5), 701–727.

Macleod, G. O. (1995), Side branch inlet rounding effects on flow excited acoustic resonance, Master's thesis, McMaster University.

Mair, W. A., Jones, P. D. F. & Palmer, R. K. W. (1975), 'Vortex shedding from finned tubes', *Journal of Sound and Vibration* **39**(3), 293–296.

Nemoto, A., Takakuwa, A. & Tsutsui, M. (1997), Flow-induced acoustic resonance caused by fin-tube bundles, Vol. 53-2 of *Fluid-Structure Interaction, Aeroelasticity, Flow-Induced Vibration and Noise Symposium*, ASME, pp. 311–320.

Nemoto, A. & Yamada, M. (1992), Flow-induced acoustic resonance caused by fin-tube bundles, Vol. 243-4 of *PVP Symposium on Flow-Induced Vibration and Noise*, ASME, pp. 137 – 151.

Nemoto, A. & Yamada, M. (1994), Flow-induced acoustic resonance in staggered tube banks, Vol. 273 of *PVP Symposium on Flow-Induced Vibration*, ASME, pp. 273 – 282.

Norberg, C. & Sunden, B. (1987), 'Turbulence and Reynolds number effects on the flow and fluid forces on a single cylinder in cross flow', *Journal of Fluids and Structures* (1), 337–357.

Oengören, A. & Ziada, S. (1992), 'Vorticity shedding and acoustic resonance in an in-line tube bundle part ii: Acoustic resonance', *Journal of Fluids and Structures* **6**, 239–309.

Oengören, A. & Ziada, S. (1998), 'An in-depth study of vortex shedding, acoustic resonance and turbulent forces in normal triangle tube arrays', *Journal of Fluids and Structures* **12**, 717–758.

Pettigrew, M. J., Taylor, C. E., Fisher, N. J., Yetisir, M. & Smith, B. A. W. (1998), 'Flow-induced vibration: recent findings and open questions', *Nuclear Engineering and Design* **185**, 249–276.

Prandtl, L. (1927), 'The generation of vortices in fluids of small viscosity', *Journal of the Royal Aeronautical Society* **31**, 720–741.

Rayleigh, J. W. S. (1915), 'Aeoline tones', *Philosophical Magazine* **29**.

Reid, D. R. & Taborek, J. (1994), 'Selection criteria for plain and segmented finned tubes for heat recovery systems', *Journal of Engineering for Gas Turbines and Power* **116**(2), 406–410.

Rockwell, D. (1998), 'Vortex body interactions', *Annual Review of Fluid Mechanics* **30**, 199–229.

Ryu, B.-N., Kim, K.-C. & Boo, J.-S. (2003), 'The effect of serratefd fins on the flow around a circular cylinder', *KSME International Journal* **17**(6), 925–934.

She, H. N. H. (2000), Acoustic resonance of confined shallow cavity in low mach number flow, Master of engineering thesis, McMaster University.

Stoneman, S. A. T., Hourigan, K., Stokes, A. N. & Welsh, M. C. (1988), 'Resonant sound caused by flow past two plates in tandem in a duct.', *Journal of Fluid Mechanics* **192**, 455–484.

Stowell, E. Z. & Deming, A. F. (1936), 'Vortex noise from rotating cylinderical rods', *Journal of Acoustical Society of America* **7**.

Sviadosch, V., Katinas, V. & Perednis, E. (1990), Vibrations of smooth and finned tubes in a cross flow of viscous fluid at different turbulence levels, Vol. 202 of *PVP conference on Vibration Control of Mechanical, Structural, and Fluid-Structural Systems*, ASME, pp. 69–74.

Tanaka, H., Imayama, Z., Koga, K. & Katayama, K. (1998), Acoustic resonant vibration and its exciting force by tube bundle, Vol. 154 of *PVP Symposium on Flow-Induced Vibration*, ASME, pp. 123 – 130.

von Karman, T. & Rubach, H. (1912), 'Uber den mechanismus des flussigkeits und luftwiderstandes', *Physikalische Zeitschrift* **13**.

von Kruger, F. & Lauth, A. (1914), 'Theorie der hiebtone', *Annalen der Physik* **44**, 801–812.

Weaver, D. S., Ziada, S., Au-Yang, M., Chen, S. S., Païdoussis, M. P. & Pettigrew, M. J. (2000), 'Flow-induced vibrations in power and process plant components – progress and prospects', *Journal of Pressure Vessel Technology* **122**, 122–348.

Zdravkovich, M. M. (1981), 'Review and classification of various aerodynamics and hydrodynamic means for suppressing vortex shedding', *Journal of Wind Engineering and Industrial Aerodynamics* (7), 145–189.

Zdravkovich, M. M. (1984), Classification of flow-induced oscillations of two parallel circular cylinders in various arrangements, *in* 'Symposium on Flow-Induced Vibrations, Volume 2: Vibration of Arrays of Cylinders in Cross Flow'.

Zdravkovich, M. M. (1985), 'Flow induced oscillations of two interfering circular cylinders', *Journal of Sound and Vibration* **101**, 511–521.

Zdravkovich, M. M. (1988), 'Review of interference-induced oscillations in flow past two parallel circular cylinders in various arrangements', *Journal of Wind Engineering and Industrial Aerodynamics* **28**(1), 183–200.

Zdravkovich, M. M. (1997), *Flow Around Circular Cylinders*, Vol. 1, Oxford University Press.

Zdravkovich, M. M. (2003), *Flow Around Circular Cylinders*, Vol. 2, Oxford University Press.

Ziada, S. & Oengören, A. (1990), 'Flow-induced acoustical resonances of in-line tube bundles', *Sulzer Technical Review* **72**(1), 45–47.

Ziada, S. & Oengören, A. (2000), 'Flow periodicity and acoustic resonance in parallel triangle tube bundles', *Journal of Fluids and Structures* **14**, 197–219.

Ziada, S., Oengören, A. & Bühlmann, E. T. (1989), 'On acoustical resonance in tube arrays - part I: Experiments', *Journal of Fluids and Structures* **3**, 293–314.